12.006J/18.353J
Nonlinear Dynamics I: Chaos

Daniel H. Rothman
Massachusetts Institute of Technology

Contents

0   Acknowledgements and references

Since 1989 I have taught a one-semester course on nonlinear dynamics and chaos to MIT undergraduates. Students come from thoughout the institute, but predominantly from mathematics, physics, and my own department (Earth, Atmospheric, and Planetary Sciences). Since 1998 the course has been jointly sponsored by the Department of Mathematics.

The lecture notes that follow have undergone frequent revisions, but perhaps never more so than in 2004, when they were (finally) converted to LaTeX. The conversion followed from LaTeX notes prepared by Kurt Steinkraus, a student in 2003.

Advice and assistance from my TA's has not only been much appreciated, but frequently resulted in new ideas for the course. The TA's included, in rough order of appearance, Andrew Gunstensen, John Olson, Olav van Genabeek, Kelvin Chan, Davide Stelitano, Joshua Weitz, Alison Cohen, Greg Lawson, and David Forney. Thanks are of course also due to the students themselves.

The construction of the course has been influenced heavily by the book by Bergé, Pomeau, and Vidal [1]. Although some sections of the notes, particularly in the first half of the course, derive directly from their book, a greater debt manifests itself in a shared "philosophy" and organization: the introduction by way of oscillators, the emphasis on data analysis, the extensive comparison between theory and experiment, and, perhaps most importantly, the progression, in the second half of the course, from partial differential equations to ordinary differential equations to maps.

There are many other sources of inspiration. Occasionally these are listed explicitly in the notes, or references to figures contained within them are made. Particular lectures and references used to construct the notes (aside from Bergé, Pomeau, and Vidal [1]) include the following:

- Systems of ODE's: Strogatz [2] and Beltrami [3].

- Liouville's theorem: Tolman [4].

- Van der Pol equation: Strogatz [2].

- Floquet theory: Bender and Orszag [5].

- Mathieu equation: Landau and Lifshitz [6].

- Fluid dynamics: Tritton [7], Landau and Lifshitz [8], and Palm [9].

- Strange attractors: Abraham and Shaw [10].

- Lorenz equations: Lorenz [11] and Tritton [7].

- Hénon attrator: Hénon [12].

- Fractals: Barnsley [13] and Grassberger and Procaccia [14].

- Period doubling: Feigenbaum [15], Schuster [16], and Kadanoff [17].

References

[1] Bergé, P., Pomeau, Y., and Vidal, C. *Order Within Chaos: Toward a Deterministic Approach to Turbulence.* John Wiley & Sons, New York, (1984).

[2] Strogatz, S. *Nonlinear dynamics and Chaos.* Addison-Wesley, New York, (1994).

[3] Beltrami, E. *Mathematics for Dynamic Modeling.* Academic Press, San Diego, (1987).

[4] Tolman, R. C. *The Principles of Statistical Mechanics.* Dover, New York, (1979).

[5] Bender, C. M. and Orszag, S. A. *Advanced Mathematical Methods for Scientists and Engineers.* McGraw Hill, New York, (1978).

[6] Landau, L. D. and Lifshitz, E. M. *Mechanics.* Pergamon Press, Oxford, England, (1976).

[7] Tritton, D. J. *Physical Fluid Dynamics, 2nd edition.* Clarendon Press, Oxford, (1988).

[8] Landau, L. D. and Lifshitz, E. M. *Fluid Mechanics.* Pergamon Press, New York, (1959).

[9] Palm, E. Nonlinear thermal convection. *Annual Review of Fluid Mechanics* **7**, 39–61 (1975).

[10] Abraham, R. H. and Shaw, C. D. *Dynamics–The Geometry of Behavior.* Aerial Press, Santa Cruz, CA, (1982).

[11] Lorenz, E. N. Deterministic aperiodic flow. *J. Atmos. Sci.* **20**, 130–141 (1963).

[12] Hénon, M. A two-dimensional mapping with a strange attractor. *Commun. Math. Phys.* **50**, 69–77 (1976).

[13] Barnsley, M. *Fractals Everywhere.* Academic Press, San Diego, (1988).

[14] Grassberger, P. and Procaccia, I. Measuring the strangeness of strange attractors. *Physica D* **9**, 189–208 (1983).

[15] Feigenbaum, M. Universal behavior in nonlinear systems. *Los Alamos Science* **1**, 4–27 (1980).

[16] Schuster, H. G. *Deterministic Chaos: An Introduction.* VCH, Weinheim, Germany, (1988).

[17] Kadanoff, L. P. Roads to chaos. *Physics Today* , December (1983).

1 Pendulum

1.1 Free oscillator

To introduce dynamical systems, we begin with one of the simplest: a *free oscillator.* Specifically, we consider an unforced, undamped pendulum.
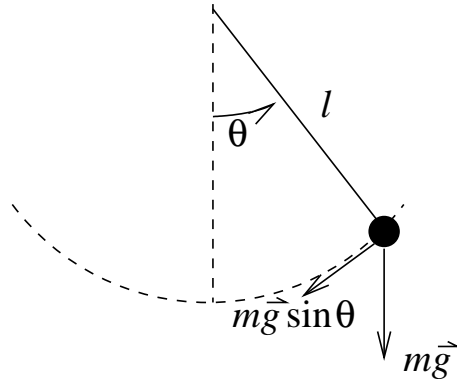
The arc length (displacement) between the pendulum's current position and rest position ($\theta = 0$) is

$$s = l\theta$$

Therefore

$$
\begin{aligned}
\dot{s} &= l\dot{\theta} \\
\ddot{s} &= l\ddot{\theta}
\end{aligned}
$$

From Newton's 2nd law,

$$F = ml\ddot{\theta}$$

The restoring force is given by $-mg\sin\theta$. (It acts in the direction opposite to $\text{sgn}(\theta)$). Thus

$$F = ml\ddot{\theta} = -mg\sin\theta$$

or

$$\frac{\mathrm{d}^2\theta}{\mathrm{d}t^2} + \frac{g}{l}\sin\theta = 0.$$

Our pendulum equation is idealized: it assumes, e.g., a point mass, a rigid geometry, and most importantly, **no friction**.

The equation is nonlinear, because of the $\sin\theta$ term. Thus the equation is not easily solved.

However for small $\theta \ll 1$ we have $\sin\theta \simeq \theta$. Then
$$\frac{\mathrm{d}^2\theta}{\mathrm{d}t^2} = -\frac{g}{l}\theta$$
whose solution is
$$\theta = \theta_0 \cos\left(\sqrt{\frac{g}{l}}t + \phi\right)$$
or
$$\theta = \theta_0 \cos(\omega t + \phi)$$
where the angular frequency is
$$\omega = \sqrt{\frac{g}{l}},$$
the period is
$$T = 2\pi\sqrt{\frac{l}{g}},$$
and θ_0 and ϕ come from the initial conditions.

Note that the motion is exactly periodic.
Furthermore, the period T is independent of the amplitude θ_0.
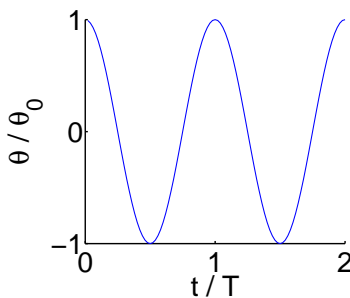
1.2   Global view of dynamics

What do we need to know to completely describe the instantaneous state of the pendulum?
$$\text{The position } \theta \text{ and the velocity } \frac{\mathrm{d}\theta}{\mathrm{d}t} = \dot{\theta}.$$

Instead of integrating our o.d.e. for the pendulum, we seek a representation of the solution in the plane of θ and $\dot{\theta}$.

Because the solution is periodic, we know that the resulting trajectory must be closed:
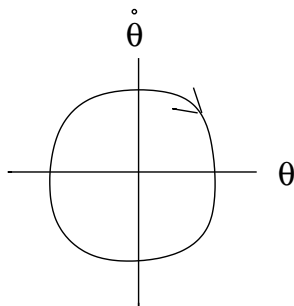
In which direction is the flow?
What shape does the curve take?

To calculate the curve, we note that it should be characterized by constant energy, since no energy is input to the system (it is not driven) and none is dissipated (there is no friction).

Therefore we compute the energy $E(\theta, \dot{\theta})$, and expect the trajectories to be curves of $E(\theta, \dot{\theta}) = $ const.

1.3   Energy in the plane pendulum
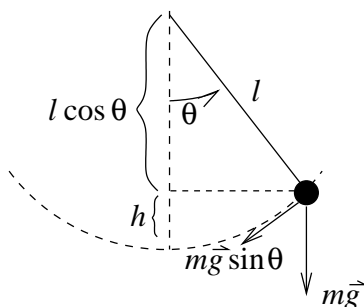
The pendulum's height above its rest position is $h = l - l\cos\theta$.
As before, $s = $ arc length $= l\theta$.

The kinetic energy T is

$$T = \frac{1}{2}m\dot{s}^2 = \frac{1}{2}m(l\dot{\theta})^2 = \frac{1}{2}ml^2\dot{\theta}^2$$

The potential energy U is

$$\begin{aligned} U = mgh &= mg(l - l\cos\theta) \\ &= mgl(1 - \cos\theta) \end{aligned}$$

Therefore the energy $E(\theta, \dot{\theta})$ is

$$E(\theta, \dot{\theta}) = \frac{1}{2}ml^2\dot{\theta}^2 + mgl(1 - \cos\theta)$$

We check that $E(\theta, \dot{\theta})$ is a constant of motion by calculating its time derivative:

$$\begin{aligned} \frac{\mathrm{d}E}{\mathrm{d}t} &= \frac{1}{2}ml^2(2\dot{\theta}\ddot{\theta}) + mgl\dot{\theta}\sin\theta \\ &= ml^2\dot{\theta}\left(\ddot{\theta} + \frac{g}{l}\sin\theta\right) \\ &= 0 \quad \text{(since the pend. eqn. } \ddot{\theta} = -\frac{g}{l}\sin\theta) \end{aligned}$$

So what do these curves look like?
Take θ_0 to be the highest point of motion.
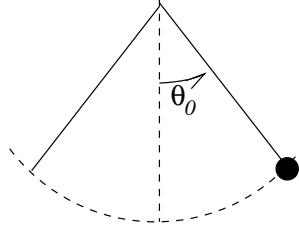
Then

$$\dot{\theta}(\theta_0) = 0$$

and

$$E(\theta_0, \dot{\theta}\,|_{\theta_0}) = mgl(1 - \cos\theta_0)$$

Since $\cos\theta = 1 - 2\sin^2(\theta/2)$,

$$\begin{aligned} E(\theta_0, \dot{\theta}\,|_{\theta_0}) &= 2mgl\sin^2\left(\frac{\theta_0}{2}\right) \\ &= E(\theta, \dot{\theta}) \text{ in general, since } E \text{ is conserved} \end{aligned}$$

10

Now write $T = E - U$:

$$\frac{1}{2}ml^2\dot{\theta}^2 = 2mgl\left(\sin^2\frac{\theta_0}{2} - \sin^2\frac{\theta}{2}\right) \tag{1}$$

$$\dot{\theta}^2 = 4\frac{g}{l}\left(\sin^2\frac{\theta_0}{2} - \sin^2\frac{\theta}{2}\right) \tag{2}$$

For small θ_0 such that $\theta \ll 1$,

$$\dot{\theta}^2 \simeq 4\frac{g}{l}\left(\frac{\theta_0^2}{4} - \frac{\theta^2}{4}\right)$$

or

$$\left(\frac{\dot{\theta}}{\sqrt{g/l}}\right)^2 + \theta^2 \simeq \theta_0^2$$

Thus for small θ the curves are circles of radius θ_0 in the plane of θ and $\dot{\theta}/\sqrt{g/l}$.
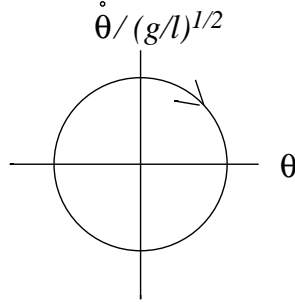
What about θ_0 large?

Consider the case $\theta_0 = \pi$.

For $\theta_0 = \pi$, $E = 2mgl$, and equation (2) gives

$$\dot{\theta}^2 = 4\frac{g}{l}\left[\sin^2\left(\frac{\pi}{2}\right) - \sin^2\left(\frac{\theta}{2}\right)\right]$$

$$= 4\frac{g}{l}\cos^2\left(\frac{\theta}{2}\right)$$

Thus for $\theta_0 = \pi$, the curves are the cosines

$$\dot{\theta} = \pm 2\sqrt{\frac{g}{l}}\cos\left(\frac{\theta}{2}\right).$$
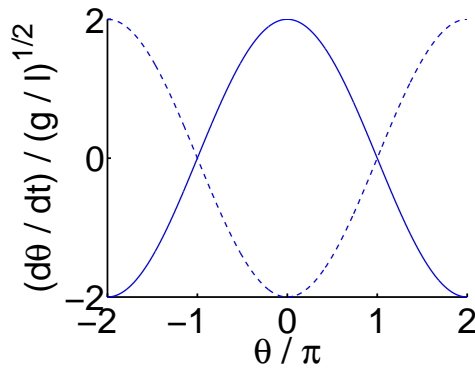
Intuitively, we recognize that this curve separates
oscillatory motion ($E < 2mgl$) from rotary motion ($E > 2mgl$).

Thus for undampled, nonlinear pendulum we can construct the following
phase portrait:
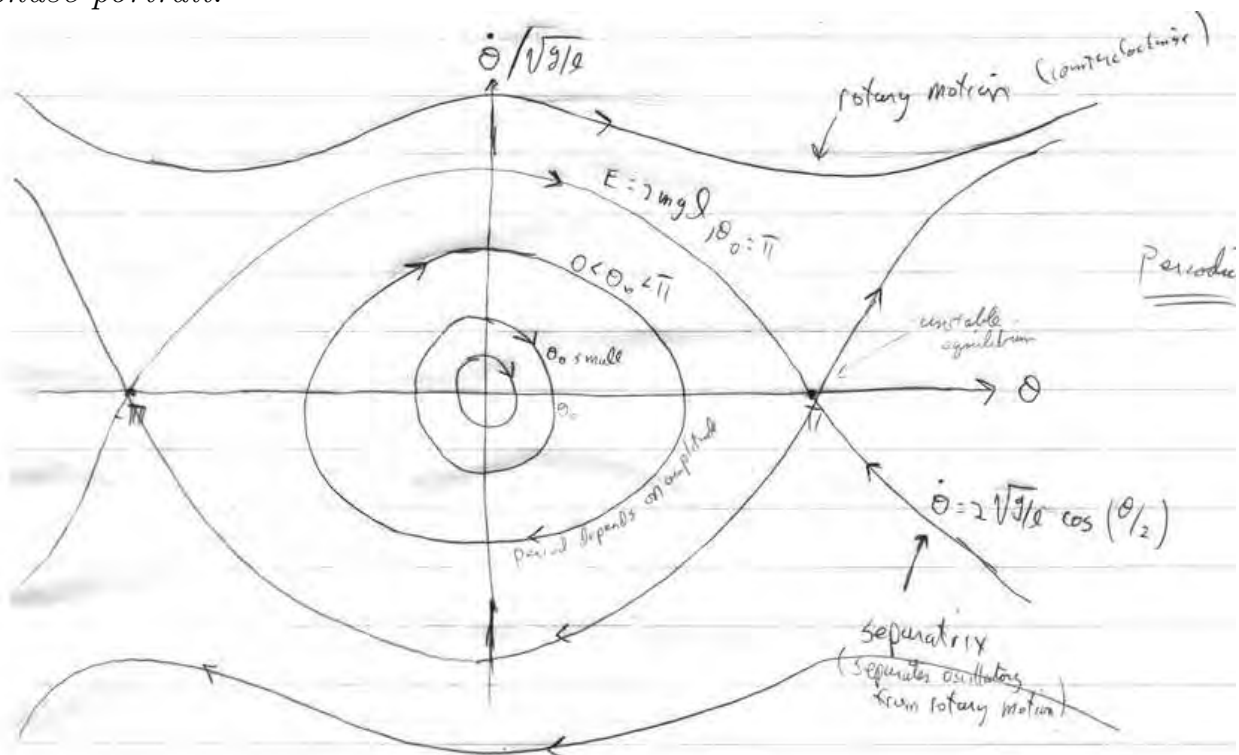
The portrait is periodic.

The points $\dot{\theta} = 0$, $\theta = \ldots, -2\pi, 0, 2\pi, \ldots$ are *stable* equilibrium, or fixed,
points (actually, *marginally stable*).

The points $\dot{\theta} = 0$, $\theta = \ldots, -3\pi, -\pi, \pi, 3\pi \ldots$ are *unstable* fixed points.

The trajectories appear to cross, but they do not. *Why not?*
(Deterministic trajectories.)

If the trajectories actually arrive to these crossing points, then what happens?
(The motion stops, awaiting instability. But we shall see that it would take
infinite time to arrive at these points.)

2 Stability of solutions to ODEs

How can we address the question of stability in general?

We proceed from the example of the pendulum equation. We reduce this second order ODE,

$$\ddot{\theta} + \frac{g}{l}\sin\theta = 0,$$

to two first order ODE's.

Write $x_1 = \theta$, $x_2 = \dot{\theta}$. Then

$$\dot{x}_1 = x_2$$
$$\dot{x}_2 = -\frac{g}{l}\sin x_1$$

The equilibrium points, or *fixed points*, are where the trajectories in phase space *stop*, i.e. where

$$\dot{\vec{x}} = \begin{pmatrix} \dot{x}_1 \\ \dot{x}_2 \end{pmatrix} = \vec{0}$$

For the pendulum, this requires

$$x_2 = 0$$
$$x_1 = \pm n\pi, \quad n = 0, 1, 2, \ldots$$

Since $\sin x_1$ is periodic, the only distinct fixed points are

$$\begin{pmatrix} \theta \\ \dot{\theta} \end{pmatrix} = \begin{pmatrix} 0 \\ 0 \end{pmatrix} \qquad \text{and} \qquad \begin{pmatrix} \theta \\ \dot{\theta} \end{pmatrix} = \begin{pmatrix} \pi \\ 0 \end{pmatrix}$$

Intuitively, the first is stable and the second is not.
How may we be more precise?

2.1 Linear systems

Consider the problem in general. First, assume that we have the linear system

$$\dot{u}_1 = a_{11}u_1 + a_{12}u_2$$
$$\dot{u}_2 = a_{21}u_1 + a_{22}u_2$$

or

$$\dot{\vec{u}} = A\vec{u}$$

with

$$\vec{u}(t) = \begin{pmatrix} u_1(t) \\ u_2(t) \end{pmatrix} \qquad \text{and} \qquad A = \begin{pmatrix} a_{11} & a_{12} \\ a_{21} & a_{22} \end{pmatrix}$$

Assume A has an inverse and that its eigenvalues are distinct. Then the only fixed point (where $\dot{\vec{u}} = 0$) is $\vec{u} = 0$.

The solution, in general, is

$$\vec{u}(t) = \alpha_1 e^{\lambda_1 t} \vec{c_1} + \alpha_2 e^{\lambda_2 t} \vec{c_2}$$

where

- λ_1, λ_2 are eigenvalues of A.

- $\vec{c_1}$, $\vec{c_2}$ are eigenvectors of A.

- α_1 and α_2 are constants (deriving from initial conditions).

What are the possibilities for stability?

1. λ_1 and λ_2 are both real.

    (a) If $\lambda_1 < 0$ and $\lambda_2 < 0$, then $u(t) \to 0$ as $t \to \infty$.
        $\Rightarrow$ **stable**.
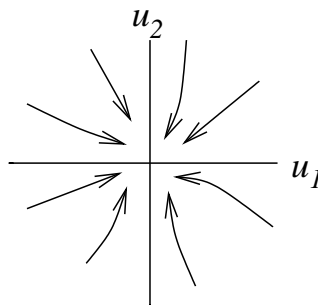
(b) If $\lambda_1 > 0$ and $\lambda_2 > 0$, then $u(t) \to \infty$ as $t \to \infty$.
$\Rightarrow$ **unstable**.
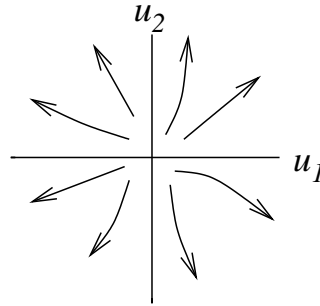
(c) If $\lambda_1 < 0 < \lambda_2$,

- If $\vec{u}(0)$ is a multiple of $\vec{c_1}$, then $u(t) \to 0$ as $t \to \infty$.
- If $\vec{u}(0)$ is a multiple of $\vec{c_2}$, then $u(t) \to \infty$ as $t \to \infty$.

$\Rightarrow$ **unstable saddle**.
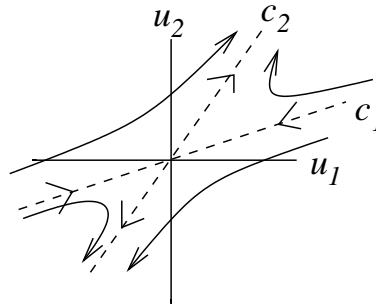
2. λ_1, λ_2 are both complex. Then

$$\lambda = \sigma \pm iq.$$

Assuming $\vec{u}(t)$ is real,

$$\vec{u}(t) = e^{\sigma t}(\vec{\beta_1} \cos qt + \vec{\beta_2} \sin qt)$$

($\vec{\beta_1}, \vec{\beta_2}$ are formed from a linear combination of of A's eigenvectors and the initial conditions).

There are three possibilities:

(a) $\text{Re}\{\lambda\} = \sigma > 0 \implies$ **unstable**.

16
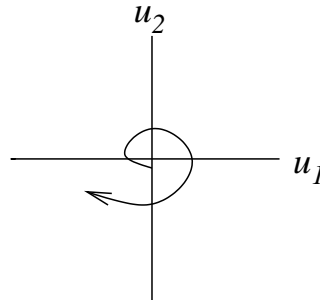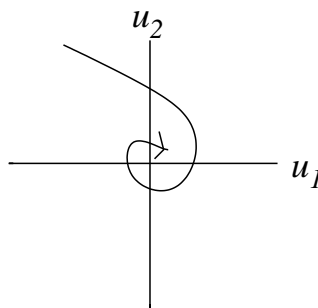
(b) $\sigma < 0 \implies$ **stable**.

(c) $\sigma = 0 \implies$ **marginally stable**.
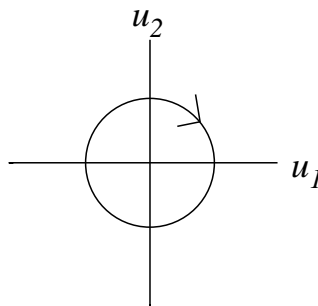
We leave the case of repeated eigenvalues to Strogatz (pp. 135-6).

2.2 Nonlinear systems

We are interested in the qualitative behavior of systems like

$$\begin{aligned} \dot{x}_1 &= f_1(x_1, x_2) \\ \dot{x}_2 &= f_2(x_1, x_2) \end{aligned}$$

where f_1 and f_2 are nonlinear functions of x_1 and x_2.

Suppose $\begin{pmatrix} x_1^* \\ x_2^* \end{pmatrix}$ is a fixed point. Is it stable?

Define $u_i = x_i - x_i^*$ to be a small departure from the fixed point.

Perform a Taylor expansion around the fixed point.

For a one dimensional function $g(x)$ we would have

$$g(x^* + u) \simeq g(x^*) + g'(x^*) \cdot u$$

17

Here we obtain

$$f_i(x_1, x_2) = \underbrace{f_i(x_1^*, x_2^*)}_{=0 \text{ since fixed pt}} + \frac{\partial f_i}{\partial x_1}(x_1^*, x_2^*)\, u_1 + \frac{\partial f_i}{\partial x_2}(x_1^*, x_2^*)\, u_2 + O(u^2)$$

The first term vanishes since it is evaluated at the fixed point.

Also, since

$$u_i = x_i - x_i^*$$

we have

$$\dot{u}_i = \dot{x}_i = f_i(x_1, x_2)$$

Substituting $\dot{u}_i = f_i(x_1, x_2)$ above, we obtain

$$\dot{\vec{u}} \simeq A\vec{u}$$

where

$$A = \left(\begin{array}{cc} \frac{\partial f_1}{\partial x_1} & \frac{\partial f_1}{\partial x_2} \\[2ex] \frac{\partial f_2}{\partial x_1} & \frac{\partial f_2}{\partial x_2} \end{array} \right)\Bigg|_{\vec{x}=\vec{x}^*}$$

A is called the **Jacobian** matrix of f at $\vec{x}^*$.

We now apply these results to the pendulum. We have

$$\begin{aligned} \dot{x}_1 &= f_1(x_1, x_2) = x_2 \\ \dot{x}_2 &= f_2(x_1, x_2) = -\frac{g}{l}\sin x_1 \end{aligned}$$

and

$$A = \left(\begin{array}{cc} 0 & 1 \\ -g/l & 0 \end{array} \right) \qquad \text{for } \left(\begin{array}{c} x_1^* \\ x_2^* \end{array} \right) = \left(\begin{array}{c} 0 \\ 0 \end{array} \right)$$

There is a different A for the case $\left(\begin{array}{c} x_1^* \\ x_2^* \end{array} \right) = \left(\begin{array}{c} \pi \\ 0 \end{array} \right)$. (The sign of g/l changes.)

The question of stability is then addressed just as in the linear case, via calculation of the eigenvalues and eigenvectors.

3   Conservation of volume in phase space

We show (via the example of the pendulum) that frictionless systems *conserve* volumes (or areas) in phase space.

Conversely, we shall see, dissipative systems *contract* volumes.

Suppose we have a 3-D phase space, such that

$$
\begin{aligned}
\dot{x}_1 &= f_1(x_1, x_2, x_3) \\
\dot{x}_2 &= f_2(x_1, x_2, x_3) \\
\dot{x}_3 &= f_3(x_1, x_2, x_3)
\end{aligned}
$$

or

$$
\frac{\mathrm{d}\vec{x}}{\mathrm{d}t} = \vec{f}(\vec{x})
$$

The equations describe a "flow," where $\mathrm{d}\vec{x}/\mathrm{d}t$ is the velocity.

A set of initial conditions enclosed in a volume V flows to another position in phase space, where it occupies a volume V', neither necessarily the same shape nor size:
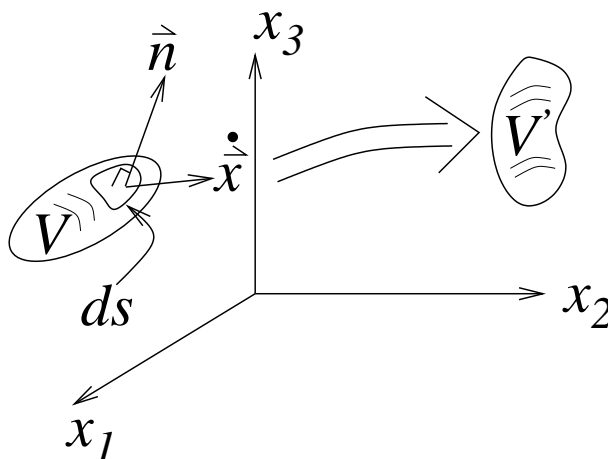
Assume the volume V has surface S.

Let

- ρ = density of initial conditions in V;

- $\rho \vec{f}$ = rate of flow of points (trajectories emanating from initial conditions) through unit area perpendicular to the direction of flow;

- ds = a small region of S; and

- $\vec{n}$ = the unit normal (outward) to ds.

Then
$$\text{net flux of points out of } S = \int_S (\rho \vec{f} \cdot \vec{n})ds$$
or
$$\int_V \frac{\partial \rho}{\partial t}dV = -\int_S (\rho \vec{f} \cdot \vec{n})ds$$
i.e., a positive flux $\implies$ a loss of "mass."

Now we apply the divergence theorem to convert the integral of the vector field $\rho \vec{f}$ on the surface S to a volume integral:
$$\int_V \frac{\partial \rho}{\partial t}dV = -\int_V [\vec{\nabla} \cdot (\rho \vec{f})]dV$$
Letting the volume V shrink, we have
$$\frac{\partial \rho}{\partial t} = -\vec{\nabla} \cdot (\rho \vec{f})$$
Now follow the motion of V to V' in time δt:
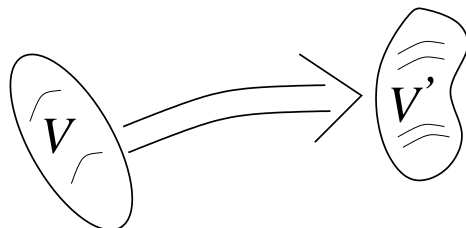
The boundary deforms, but it always contains the same points.

We wish to calculate $d\rho/dt$, which is the rate of change of ρ **as the volume moves**:

$$\frac{d\rho}{dt} = \frac{\partial\rho}{\partial t} + \frac{\partial\rho}{\partial x_1}\frac{dx_1}{dt} + \frac{\partial\rho}{\partial x_2}\frac{dx_2}{dt} + \frac{\partial\rho}{\partial x_3}\frac{dx_3}{dt}$$

$$= -\vec{\nabla}\cdot(\rho\vec{f}) + (\vec{\nabla}\rho)\cdot\vec{f}$$

$$= -(\vec{\nabla}\rho)\cdot\vec{f} - \rho\vec{\nabla}\cdot f + (\vec{\nabla}\rho)\cdot\vec{f}$$

$$= -\rho\vec{\nabla}\cdot\vec{f}$$

Note that the number of points in V is

$$N = \rho V$$

Since points are neither created nor destroyed we must have

$$\frac{dN}{dt} = V\frac{d\rho}{dt} + \rho\frac{dV}{dt} = 0.$$

Thus, by our previous result,

$$-\rho V\vec{\nabla}\cdot\vec{f} = -\rho\frac{dV}{dt}$$

or

$$\frac{1}{V}\frac{dV}{dt} = \vec{\nabla}\cdot\vec{f}$$

This is called the *Lie derivative.*

We shall next arrive at the following main results by example:

- $\vec{\nabla}\cdot\vec{f} = 0 \Rightarrow$ volumes in phase space are conserved. Characteristic of conservative or Hamiltonian systems.

- $\vec{\nabla}\cdot\vec{f} < 0 \Rightarrow dV/dt < 0 \Rightarrow$ volumes in phase space contract. Characteristic of dissipative systems.

We use the example of the pendulum:

$$\dot{x}_1 = x_2 = f_1(x_1, x_2)$$
$$\dot{x}_2 = -\frac{g}{l}\sin x_1 = f_2(x_1, x_2)$$

Calculate

$$\vec{\nabla} \cdot \vec{f} \;=\; \frac{\partial \dot{x}_1}{\partial x_1} + \frac{\partial \dot{x}_2}{\partial x_2} \;=\; 0 + 0$$

Pictorially
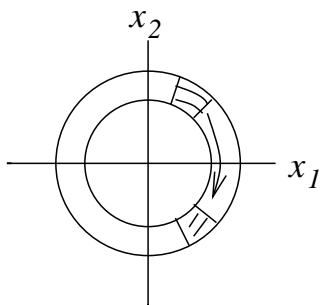
Note that the area is conserved.

Conservation of areas holds for *all* conserved systems. This is conventionally derived from Hamiltonian mechanics and the canonical form of equations of motion.

In conservative systems, the conservation of volumes in phase space is known as *Liouville's theorem.*

4 Damped oscillators and dissipative systems

4.1 General remarks

We have seen how conservative systems behave in phase space.
What about dissipative systems?

What is a fundamental difference between dissipative systems and conservative systems, aside from volume contraction and energy dissipation?

- Conservative systems are invariant under time reversal.

- Dissipative systems are not; they are *irreversible.*

Consider again the undamped pendulum:

$$\frac{\mathrm{d}^2\theta}{\mathrm{d}t^2} + \omega^2 \sin\theta = 0.$$

Let $t \to -t$ and thus $\partial/\partial t \to -\partial/\partial t$.
There is no change—the equation is *invariant* under the transformation.

The fact that most systems are dissipative is obvious if we run a movie backwards (ink drop, car crash, cigarette smoke...)

Formally, how may dissipation be represented? **Include terms proportional to odd time derivatives.**, i.e., break time-reversal invariance.

In the linear approximation, the damped pendulum equation is

$$\frac{\mathrm{d}^2\theta}{\mathrm{d}t^2} + \gamma\frac{\mathrm{d}\theta}{\mathrm{d}t} + \omega^2\theta = 0$$

where

$$\omega^2 = g/l$$
$$\gamma = \text{damping coefficient}$$

The sign of γ is chosen so that positive damping is opposite the direction of motion.

How does the energy evolve over time? As before, we calculate

$$\text{kinetic energy} = \frac{1}{2}ml^2\dot\theta^2$$
$$\text{potential energy} = mlg(1 - \cos\theta) \simeq mlg\left(\frac{\theta^2}{2}\right)$$

where we have assumed $\theta \ll 1$ in the approximation.

Summing the kinetic and potential energies, we have

$$E(\theta, \dot\theta) = \frac{1}{2}ml^2\left(\dot\theta^2 + \frac{g}{l}\theta^2\right)$$
$$= \frac{1}{2}ml^2(\dot\theta^2 + \omega^2\theta^2)$$

Taking the time derivative,

$$\frac{\mathrm{d}E}{\mathrm{d}t} = \frac{1}{2}ml^2(2\dot{\theta}\ddot{\theta} + 2\omega^2\dot{\theta}\theta)$$

Substituting the damped pendulum equation for $\ddot{\theta}$,

$$\frac{\mathrm{d}E}{\mathrm{d}t} = ml^2[\dot{\theta}(-\gamma\dot{\theta} - \omega^2\theta) + \omega^2\dot{\theta}\theta]$$

$$= -ml^2\gamma\dot{\theta}^2$$

Take $ml^2 = 1$. Then

$$\frac{\mathrm{d}E}{\mathrm{d}t} = -\gamma\dot{\theta}^2$$

Conclusion:

$$\begin{aligned}
\gamma = 0 &\Rightarrow \text{ Energy conserved (no friction)} \\
\gamma > 0 &\Rightarrow \text{ friction (energy is dissipated)} \\
\gamma < 0 &\Rightarrow \text{ energy increases without bound}
\end{aligned}$$

4.2   Phase portrait of damped pendulum

Let $x = \theta$, $y = \dot{\theta}$.
Then

$$\begin{aligned}
\dot{x} &= \dot{\theta} = y \\
\dot{y} &= \ddot{\theta} = -\gamma\dot{\theta} - \omega^2\theta = -\gamma y - \omega^2 x
\end{aligned}$$

or

$$\begin{pmatrix} \dot{x} \\ \dot{y} \end{pmatrix} = \begin{pmatrix} 0 & 1 \\ -\omega^2 & -\gamma \end{pmatrix} \begin{pmatrix} x \\ y \end{pmatrix}$$

The eigenvalues of the system are solutions of

$$(-\lambda)(-\gamma - \lambda) + \omega^2 = 0$$

Thus

$$\lambda = -\frac{\gamma}{2} \pm \frac{1}{2}\sqrt{\gamma^2 - 4\omega^2}$$

Assume $\gamma^2 \ll \omega^2$ (i.e., weak damping, small enough to allow oscillations). Then the square root is complex, and we may approximate λ as

$$\lambda = -\frac{\gamma}{2} \pm i\omega$$

The solutions are therefore exponentially damped oscillations of frequency ω:

$$\theta(t) = \theta_0 e^{-\gamma t/2} \cos(\omega t + \phi)$$

θ_0 and ϕ derive from the initial conditions.

There are three generic cases:

- for $\gamma > 0$, trajectories spiral inwards and are **stable**.
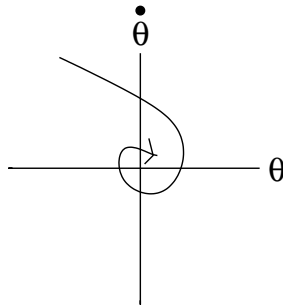
- for $\gamma = 0$, trajectories are **marginally stable** periodic oscillations.
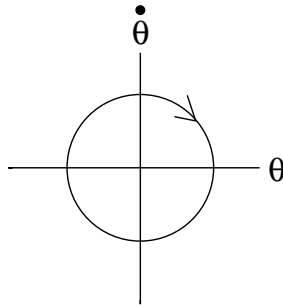
- for $\gamma > 0$, trajectories spiral outwards and are **unstable**.
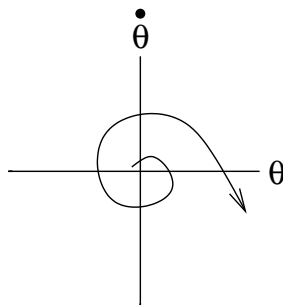
It is obvious from the phase portraits that the damped pendulum contracts areas in phase space:
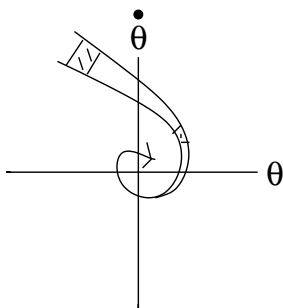
We quantify it using the Lie derivative,

$$\frac{1}{V}\frac{\mathrm{d}V}{\mathrm{d}t} = \vec{\nabla} \cdot \vec{f}$$

which yields

$$\frac{\partial \dot{x}}{\partial x} + \frac{\partial \dot{y}}{\partial y} \;=\; 0 - \gamma \;=\; -\gamma \;<\; 0$$

The inequality not only establishes area contraction, but γ gives the rate.

4.3   Summary

Finally, we summarize the characteristics of dissipative systems:

- Energy not conserved.

- Irreversible.

- Contraction of areas (volumes) in phase space.

Note that the contraction of areas is not necessarily simple.

In a 2-D phase space one might expect

$\dot{\theta}$ (vertical axis), θ (horizontal axis), time
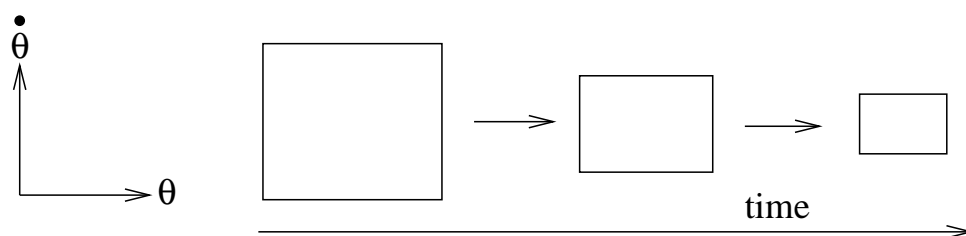
However, we can also have

time
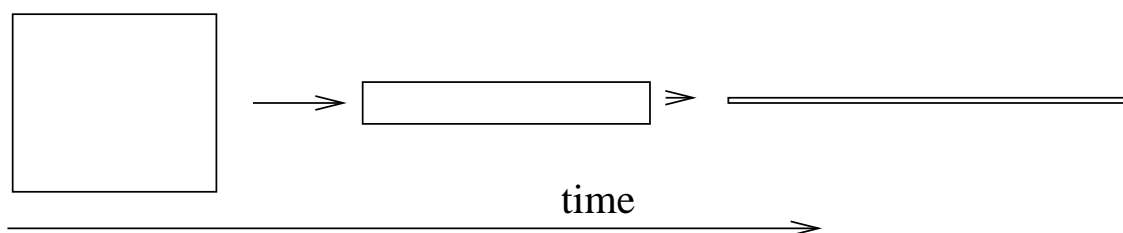
i.e., we can have expansion in one dimension and (a greater) contraction in the other.

In 3-D the stretching and thinning can be even stranger!

5 Forced oscillators and limit cycles

5.1 General remarks

How may we describe a forced oscillator?
The linear equation

$$\ddot{\theta} + \gamma\dot{\theta} + \omega^2\theta = 0 \tag{3}$$

is in general inadequate. Why?

Linearity $\Rightarrow$ if $\theta(t)$ is a solution, then so is $\alpha\theta(t)$, α real. This is incompatible with bounded oscillations (i.e., $\theta_{\max} < \pi$).

We therefore introduce an equation with

- a nonlinearity; and

- an energy source that compensates viscous damping.

5.2 Van der Pol equation

Consider a damping coefficient $\gamma(\theta)$ such that

$$\gamma(\theta) > 0 \qquad \text{for } |\theta| \text{ large}$$

$$\gamma(\theta) < 0 \qquad \text{for } |\theta| \text{ small}$$

Express this in terms of θ^2:

$$\gamma(\theta) = \gamma_0 \left(\frac{\theta^2}{\theta_0^2} - 1 \right)$$

where $\gamma_0 > 0$ and θ_0 is some reference amplitude.

Now, obviously,

$$\gamma > 0 \qquad \text{for } \theta^2 > \theta_0^2$$
$$\gamma < 0 \qquad \text{for } \theta^2 < \theta_0^2$$

28

Substituting γ into (3), we get

$$\frac{d^2\theta}{dt^2} + \gamma_0 \left(\frac{\theta^2}{\theta_0^2} - 1 \right) \frac{d\theta}{dt} + \omega^2\theta = 0$$

This equation is known as the *van der Pol equation.* It was introduced in the 1920's as a model of nonlinear electric circuits used in the first radios.

In van der Pol's (vaccum tube) circuits,

- high current $\implies$ positive (ordinary) resistance; and

- low current $\implies$ negative resistance.

The basic behavior: large oscillations decay and small oscillations grow.

We shall examine this system in some detail. First, we write it in *non-dimensional* form.

We define new units of time and amplitude:

- unit of time $= 1/\omega$

- unit of amplitude $= \theta_0$.

We transform

$$\begin{aligned} t &\rightarrow t'/\omega \\ \theta &\rightarrow \theta'\theta_0 \end{aligned}$$

where θ' and t' are non-dimensional.

Substituting above, we obtain

$$\omega^2 \frac{d^2\theta'}{dt'^2}\theta_0 + \gamma_0 \left[\left(\frac{\theta'\theta_0}{\theta_0} \right)^2 - 1 \right] \frac{d\theta'}{dt'}\omega\theta_0 + \omega^2\theta'\theta_0 = 0$$

Divide by $\omega^2\theta_0$:

$$\frac{d^2\theta'}{dt'^2} + \frac{\gamma_0}{\omega} \left(\theta'^2 - 1 \right) \frac{d\theta'}{dt'} + \theta' = 0$$

29

Now define the dimensionless control parameter

$$\varepsilon = \frac{\gamma_0}{\omega} > 0.$$

Finally, drop primes to obtain

$$\frac{\mathrm{d}^2\theta}{\mathrm{d}t^2} + \varepsilon(\theta^2 - 1)\frac{\mathrm{d}\theta}{\mathrm{d}t} + \theta = 0. \tag{4}$$

What can we say about the phase portraits?

- When the amplitude of oscillations is small $(\theta_{\max} < 1)$, we have

$$\varepsilon(\theta_{\max}^2 - 1) < 0 \Rightarrow \text{negative damping}$$

Thus trajectories spiral outward:
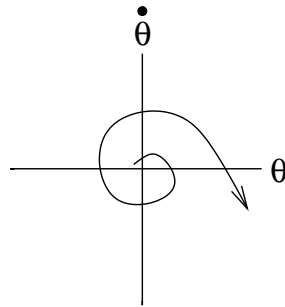
- But when the amplitude of oscillations is large $(\theta_{\max} > 1)$,

$$\varepsilon(\theta_{\max}^2 - 1) > 0 \Rightarrow \text{positive damping}$$

The trajectories spiral inward:
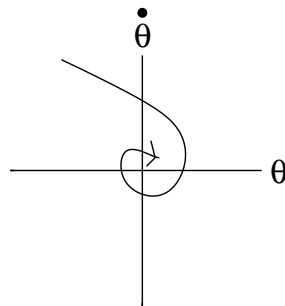
Intuitively, we expect a closed trajectory between these two extreme cases:
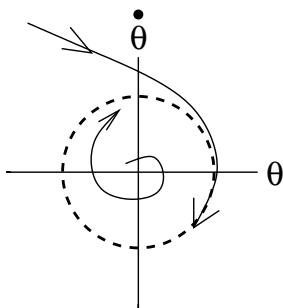
This closed trajectory is called a **limit cycle**.

For $\varepsilon > 0$, the limit cycle is an *attractor* (and is stable).

This is a new kind of attractor. Instead of representing a single fixed point, it represents stable oscillations.

Examples of such stable oscilations abound in nature: heartbeats (**see Figure from Glass**); circadian (daily) cycles in body temperature, etc. Small perturbations always return to the standard cycle.

What can we say about the limit cycle of the van der Pol equation?

With the help of various theorems (see Strogatz, Ch. 7) one can prove the existence and stability of the limit cycle.

We may, however, make substantial progress with a simple energy balance argument.

5.3   Energy balance for small ε

Let $\varepsilon \to 0$, and take θ small. Using our previous expression for energy in the pendulum, the non-dimensional energy is

$$E(\theta, \dot{\theta}) = \frac{1}{2}(\dot{\theta}^2 + \theta^2)$$

The time variation of energy is

$$\frac{\mathrm{d}E}{\mathrm{d}t} = \frac{1}{2}(2\dot{\theta}\ddot{\theta} + 2\dot{\theta}\theta)$$

From the van der Pol equation (4), we have

$$\ddot{\theta} = -\varepsilon(\theta^2 - 1)\dot{\theta} - \theta.$$

Substituting this into the expression for $\mathrm{d}E/\mathrm{d}t$, we obtain

$$\frac{\mathrm{d}E}{\mathrm{d}t} = \varepsilon\dot{\theta}^2(1 - \theta^2) - \theta\dot{\theta} + \theta\dot{\theta} \tag{5}$$

$$= \varepsilon\dot{\theta}^2(1 - \theta^2) \tag{6}$$

Now define the average of a function $f(t)$ over one period of the oscillation:

$$\overline{f} \equiv \frac{1}{2\pi} \int_{t_0}^{t_O+2\pi} f(t)\mathrm{d}t.$$

Then the average energy variation over one period is

$$\overline{\frac{\mathrm{d}E}{\mathrm{d}t}} = \frac{1}{2\pi} \int_{t_0}^{t_0+2\pi} \frac{\mathrm{d}E}{\mathrm{d}t}\mathrm{d}t.$$

Substituting equation (6) for $\mathrm{d}E/\mathrm{d}t$, we obtain

$$\overline{\frac{\mathrm{d}E}{\mathrm{d}t}} = \varepsilon\overline{\dot{\theta}^2} - \varepsilon\overline{\dot{\theta}^2\theta^2}.$$

In steady state, the production of energy, $\varepsilon\overline{\dot{\theta}^2}$, is exactly compensated by the dissipation of energy, $\varepsilon\overline{\dot{\theta}^2\theta^2}$. Thus

$$\varepsilon\overline{\dot{\theta}^2} = \varepsilon\overline{\dot{\theta}^2\theta^2}$$

or

$$\overline{\dot{\theta}^2} = \overline{\dot{\theta}^2\theta^2}.$$

Now consider the limit $\varepsilon \to 0$ (from above).
We know the approximate solution:

$$\theta(t) = \rho\sin t,$$

i.e., simple sinusoidal oscillation of unknown amplitude ρ.

We proceed to calculate ρ from the energy balance.

The average rate of energy production is

$$\overline{\dot{\theta}^2} \simeq \frac{1}{2\pi} \int_{t_0}^{t_0+2\pi} \rho^2 \cos^2 t \, \mathrm{d}t = \frac{1}{2}\rho^2.$$

The average rate of energy dissipation is

$$\overline{\dot{\theta}^2 \theta^2} \simeq \frac{1}{2\pi} \int_{t_0}^{t_0+2\pi} \rho^4 \sin^2 t \cos^2 t \, \mathrm{d}t = \frac{1}{8}\rho^4.$$

The energy balance argument gives

$$\frac{1}{2}\rho^2 = \frac{1}{8}\rho^4.$$

Therefore

$$\rho = 2.$$

We thus find that, independent of $\varepsilon = \gamma_0/\omega$, we have the following approximate solution for $\varepsilon \ll 1$:

$$\theta(t) \simeq 2\sin t.$$

That is, we have a limit cycle with an amplitude of 2 dimensionless units. Graphically,
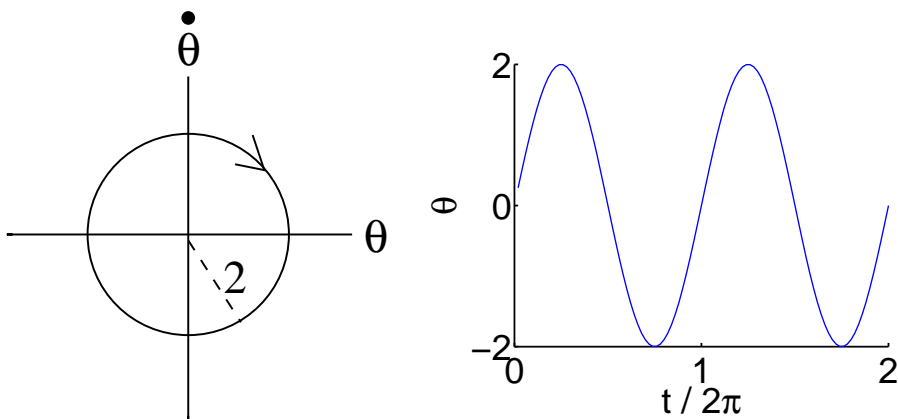
Further work (see, e.g., Strogatz) shows that this limit cycle is stable.

5.4 Limit cycle for ε large

The case of ε large requires a different analysis. We follow the argument given in Strogatz (p. 212).

First, we introduce an unconventional set of phase plane variables (not $\dot{x} = y, \dot{y} = \ldots$). That is, the phase plane coordinates will not be θ and $\dot{\theta}$.

Recall the van der Pol equation (4), but write in terms of $x = \theta$:

$$\ddot{x} + \varepsilon(x^2 - 1)\dot{x} + x = 0. \tag{7}$$

Notice that

$$\ddot{x} + \varepsilon\dot{x}(x^2 - 1) = \frac{\mathrm{d}}{\mathrm{d}t}\left[\dot{x} + \varepsilon\left(\frac{1}{3}x^3 - x\right)\right].$$

Let

$$F(x) = \frac{1}{3}x^3 - x \tag{8}$$

and

$$w = \dot{x} + \varepsilon F(x). \tag{9}$$

Then, using (8) and (9), we have

$$\dot{w} = \ddot{x} + \varepsilon\dot{x}(x^2 - 1).$$

Substituting the van der Pol equation (7), this gives

$$\dot{w} = -x \tag{10}$$

Now rearrange equation (9) to obtain

$$\dot{x} = w - \varepsilon F(x) \tag{11}$$

We have thus parameterized the system by x and w. However we make one more change of variable. Write

$$y = w/\varepsilon.$$

Then (10) and (11) become

$$\dot{x} = \varepsilon[y - F(x)] \tag{12}$$

$$\dot{y} = -\frac{1}{\varepsilon}x \tag{13}$$

Now consider a trajectory in the x-y plane.

First, draw the *nullcline* for x, that is, the curve showing where $\dot{x} = 0$. This is the cubic curve $y = F(x)$.
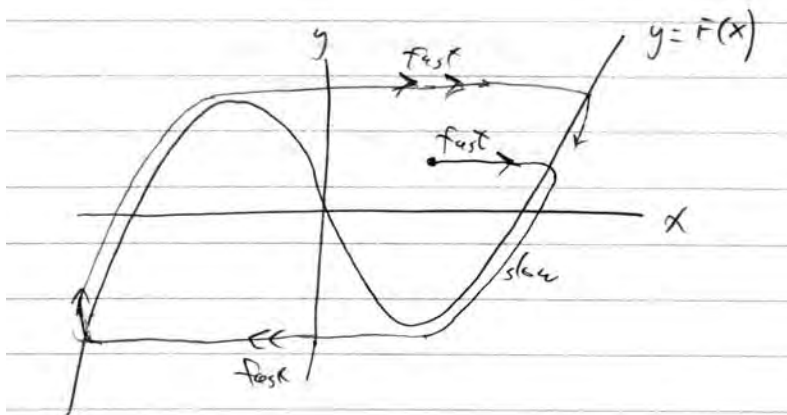
Now imagine a trajectory starting not too close to $y = F(x)$, i.e.. suppose

$$y - F(x) \sim 1.$$

Then from the equations of motion (12) and (13),

$$\dot{x} \ \sim \ \varepsilon \gg 1$$
$$\dot{y} \ \sim \ 1/\varepsilon \ll 1 \qquad \text{assuming } x \sim 1.$$

Thus the horizontal velocity is large and the vertical velocity is small. $\Rightarrow$ trajectories move horizontally.

The y-nullcline shows that the vertical velocity vanishes for $x = 0$.)

Eventually the trajectory is so close to $y = F(x)$ such that

$$y - F(x) \sim \frac{1}{\varepsilon^2}$$

implying that

$$\dot{x} \sim \dot{y} \sim \frac{1}{\varepsilon}.$$

Thus the trajectory crosses the nullcline (vertically, since $\dot{x} = 0$ on the null-cline).

Then $\dot{x}$ changes sign, we still have $\dot{x} \sim \dot{y} \sim 1/\varepsilon$, and the trajectories crawl slowly along the nullcline.

What happens at the knee (the minimum of $F(x)$)?
The trajectories jump sideways again, as may be inferred from the symmetry
$x \to -x, \ y \to -y$.

The trajectory closes to form the limit cycle.

Summary: The dynamics has two widely separated time scales:

- The crawls: $\Delta t \sim \varepsilon \qquad (\dot{x} \sim 1/\varepsilon)$

- The jumps: $\Delta t \sim 1/\varepsilon \qquad (\dot{x} \sim \varepsilon)$

A time series of $x(t) = \theta(t)$ shows a classic **relaxation oscillation**:
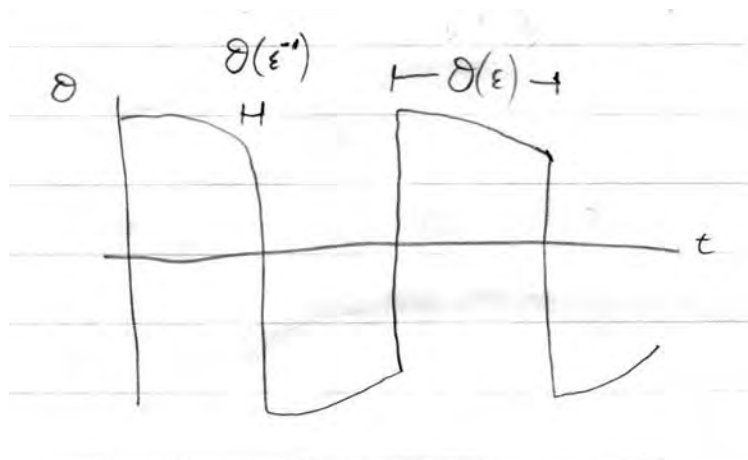
Relaxation oscillations are periodic processes with two time scales: a slow
buildup is followed by a fast discharge.

Examples include

- stick-slip friction (earthquakes, avalanches, bowed violin strings, etc.)

- nerve cells, heart beats (large literature in mathematical biology...)

5.5   A final note

Limit cycles exist only in nonlinear systems. Why?

A linear system $\dot{\vec{x}} = A\vec{x}$ can have closed periodic orbits, but not an *isolated* orbit.

That is, linearity requires that if $\vec{x}(t)$ is a solution, so is $\alpha\vec{x}(t)$, $\alpha \neq 0$.

Thus the amplitude of a periodic cycle in a linear system depends on the initial conditions.

The amplitude of a limit cycle, however, is independent of the initial conditions.

6 Parametric oscillator

6.1 Mathieu equation

We now study a different kind of forced pendulum.

Specifically, imagine subjecting the pivot of a simple frictionless pendulum to an alternating vertical motion:
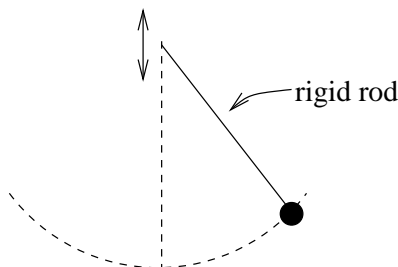
This is called a "parametric pendulum," because the motion depends on a time-dependent parameter.

Consider the parametric forcing to be a time-dependent gravitational field:

$$g(t) = g_0 + \beta(t)$$

The linearized equation of motion is then (in the undamped case)

$$\frac{\mathrm{d}^2\theta}{\mathrm{d}t^2} + \frac{g(t)}{l}\theta = 0.$$

The time-dependence of $g(t)$ makes the equation hard to solve. We know, however, that the rest state

$$\theta = \dot{\theta} = 0$$

is a solution. But is the rest state stable?

We investigate the stability of the rest state for a special case: $g(t)$ periodic and sinusoidal:

$$g(t) = g_0 + g_1 \cos(2\omega t)$$

Substituting into the equation of motion then gives

$$\frac{\mathrm{d}^2\theta}{\mathrm{d}t^2} + \omega_0^2 \left[1 + h\cos(2\omega t)\right]\theta = 0 \tag{14}$$

where
$$\omega_0^2 = g_0/l \qquad \text{and} \qquad h = g_1/g_0 \gg 0.$$
Equation (14) is called the *Mathieu equation.*

The excitation (forcing) term has amplitude h and period
$$T_{\text{exc}} = \frac{2\pi}{2\omega} = \frac{\pi}{\omega}$$
On the other hand, the natural, unexcited period of the pendulum is
$$T_{\text{nat}} = \frac{2\pi}{\omega_0}$$

We wish to characterize the stability of the rest state. Our previous methods are unapplicable, however, because of the time-dependent parametric forcing.

We pause, therefore, to consider the theory of linear ODE's with periodic coefficients, known as *Floquet theory.*

6.2   Elements of Floquet Theory

Reference: Bender and Orszag, p. 560.

We consider the general case of a second-order linear ODE with periodic coefficients. We seek to determine the conditions for stability.

We begin with two observations:

1. If the coefficients are periodic with period T, then if $\theta(t)$ is a solution, so is $\theta(t + T)$.

2. Any solution $\theta(t)$ is a linear combination of two linearly independent solutions $\theta_1(t)$ and $\theta_2(t)$:
$$\theta(t) = A\theta_1(t) + B\theta_2(t) \tag{15}$$
   where A and B come from initial conditions. (Reason: the system is linear and second-order.)

Since $\theta_1(t)$ and $\theta_2(t)$ are solutions, periodicity $\Rightarrow \theta_1(t+T)$ and $\theta_2(t+T)$ are also solutions.

Then $\theta_1(t+T)$ and $\theta_2(t+T)$ may themselves be represented as linear combinations of $\theta_1(t)$ and $\theta_2(t)$:

$$\theta_1(t+T) = \alpha\theta_1(t) + \beta\theta_2(t)$$

$$\theta_2(t+T) = \gamma\theta_1(t) + \delta\theta_2(t)$$

Thus

$$\theta(t+T) = A\left[\alpha\theta_1(t) + \beta\theta_2(t)\right] + B\left[\gamma\theta_1(t) + \delta\theta_2(t)\right]$$

$$= (A\alpha + B\gamma)\theta_1(t) + (A\beta + B\delta)\theta_2(t)$$

We rewrite the latter expression as

$$\theta(t+T) = A'\theta_1(t) + B'\theta_2(t) \tag{16}$$

where

$$\begin{pmatrix} A' \\ B' \end{pmatrix} = \begin{pmatrix} \alpha & \gamma \\ \beta & \delta \end{pmatrix} \begin{pmatrix} A \\ B \end{pmatrix}$$

or

$$\vec{a}' = M\vec{a}, \qquad \vec{a} = \begin{pmatrix} A \\ B \end{pmatrix}.$$

Now choose $\begin{pmatrix} A \\ B \end{pmatrix}$ to be an eigenvector of M, with λ the associated eigenvalue. Any other $\vec{a}$ would have a projection onto one of the eigenvectors.

Then

$$A' = \lambda A \qquad \text{and} \qquad B' = \lambda B.$$

Using (16) and (15), we find that

$$\theta(t+T) = \lambda\theta(t).$$

Thus $\theta(t)$ is periodic within a scale factor λ. The question of stability then hinges on the magnitude of λ.

Define
$$\mu = \frac{\ln |\lambda|}{T} \qquad \Rightarrow \qquad \lambda = e^{\mu T}.$$
(We are interested only in growth or decay, not oscillations due to the exponential multiplier.)
Then
$$\theta(t + T) = e^{\mu T}\theta(t).$$
Here θ is rescaled by $e^{\mu T}$ each period.

Finally, define $P(t)$ to be periodic such that $P(t + T) = P(t)$. The rescaling may now be expressed continuously as
$$\theta(t) = e^{\mu t}P(t).$$

[The above $\Rightarrow \theta(t+T) = e^{\mu(t+T)}P(t+T) = e^{\mu T}e^{\mu t}P(t) = e^{\mu T}\theta(t)$.]

Stability thus rests on the sign of μ.

Thus we find that the solution to a linear second-order ODE with periodic coefficient—e.g., the Mathieu equation—is of the form

(exponential growth or decay) $*$ (periodic function of time)

6.3 Stability of the parametric pendulum

We proceed to determine under what conditions the rest state of the Mathieu equation is unstable, leading to exponentially growing oscillations.

We expect the tendency toward instability to be strongest when the excitation frequency is twice the natural frequency, ω_0, of the pendulum.
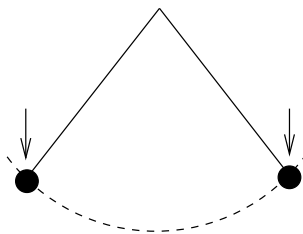
This is called *parametric resonance.*

The Mathieu equation (for $\theta \ll 1$) is

$$\frac{\mathrm{d}^2\theta}{\mathrm{d}t^2} + \omega_0^2 \left[1 + h\cos(2\omega t)\right]\theta = 0.$$

We take the forcing frequency to be $2\omega_0 + \varepsilon$, $\varepsilon \ll 1$:

$$\ddot{\theta} + \omega_0^2 \left[1 + h\cos(2\omega_0 + \varepsilon)t\right]\theta = 0. \tag{17}$$

We assume that the excitation amplitude $h \ll 1$, and seek solutions of the general form

$$\theta(t) = a(t)\cos\left(\omega_0 + \frac{1}{2}\varepsilon\right)t + b(t)\sin\left(\omega_0 + \frac{1}{2}\varepsilon\right)t.$$

The frequency $\omega_0 + \frac{1}{2}\varepsilon$ is motivated by our resonance argument. Stability will depend on whether $a(t)$ and $b(t)$ exponentially grow or decay.

We begin by substituting $\theta(t)$ into the equation of motion. We will then retain terms that are linear in ε and first-order in h.

The calculation is messy but is aided by recalling trig identities like[*]

$$\cos\left[\left(\omega_0 + \frac{1}{2}\varepsilon\right)t\right]\cos\left[(2\omega_0 + \varepsilon)t\right] = \frac{1}{2}\cos\underbrace{\left[3\left(\omega_0 + \frac{1}{2}\varepsilon\right)t\right]}_{\text{higher freq term}} + \frac{1}{2}\cos\left[\left(\omega_0 + \frac{1}{2}\varepsilon\right)t\right].$$

The term with frequency $3(\omega_0 + \frac{1}{2}\varepsilon)$ may be shown to be higher order with respect to h. Such higher frequency terms create small amplitude perturbations of the solution and are neglected. (You shall see on a problem set how such terms arise from nonlinearities.)

Also, we shall retain only those terms that are first-order in ε. Thus we neglect the $\mathcal{O}(\varepsilon^2)$ associated with accelerations $\ddot{\theta}$. We also assume

$$\dot{a} \sim \varepsilon a, \qquad \dot{b} \sim \varepsilon b,$$

and thereby neglect $\ddot{a}$, $\ddot{b}$. These assumptions are validated by the final result.

---

[*]That is, we use $\cos A\cos B = \frac{1}{2}[\cos(A+B) + \cos(A-B)]$ and $\sin A\sin B = \frac{1}{2}[\sin(A+B) + \sin(A-B)]$.

The result of the substitution is

$$
- \left(2\dot{a} + b\varepsilon + \frac{1}{2}h\omega_0 b \right) \omega_0 \sin \left[\left(\omega_0 + \frac{1}{2}\varepsilon \right) t \right]
$$

$$
+ \left(2\dot{b} - a\varepsilon + \frac{1}{2}h\omega_0 a \right) \omega_0 \cos \left[\left(\omega_0 + \frac{1}{2}\varepsilon \right) t \right] = 0
$$

For this expression to be true for all t, the coefficients of both cos and sin must equal zero, i.e,

$$
2\dot{a} + b\varepsilon + \frac{1}{2}h\omega_0 b = 0
$$

$$
2\dot{b} - a\varepsilon + \frac{1}{2}h\omega_0 a = 0
$$

We seek solutions $a(t) \propto e^{\mu t}$ and $b(t) \propto e^{\mu t}$.
Thus, substitute $\dot{a} = \mu a$, $\dot{b} = \mu b$:

$$
\mu a + \frac{1}{2}b \left(\varepsilon + \frac{1}{2}h\omega_0 \right) = 0
$$

$$
\frac{1}{2}a \left(\varepsilon - \frac{1}{2}h\omega_0 \right) - \mu b = 0
$$

These equations have a solution when the determinant of the coefficients of a and b vanishes. Thus

$$
-\mu^2 - \frac{1}{4}\left[\varepsilon^2 - \left(\frac{1}{2}h\omega_0 \right)^2 \right] = 0
$$

or

$$
\text{or } \mu^2 = \frac{1}{4}\left[\left(\frac{1}{2}h\omega_0 \right)^2 - \varepsilon^2 \right] \tag{18}
$$

Instability (parametric resonance) occurs when μ is real and positive. This will occur when $\mu^2 > 0$, or

$$
-\frac{1}{2}h\omega_0 < \varepsilon < \frac{1}{2}h\omega_0.
$$

43

This result is summarized in the following *phase diagram*:
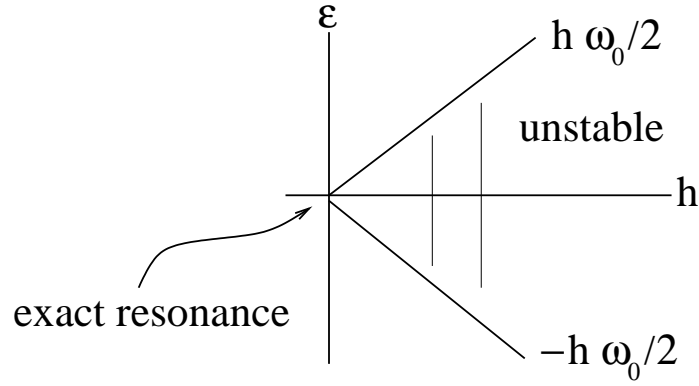
Thus we see that resonance occurs not only for $\varepsilon = 0$, but for a range of ε within the lines $\pm h\omega_0/2$.

The larger the forcing amplitude, the less necessary it is for the force to be exactly resonant $(\omega = 0)$.

Conversely, infinitesimal forcing (i.e., h) is sufficient for instability so long as $\varepsilon \to 0$.

6.4   Damping

The damped parametric pendulum is

$$\ddot{\theta} + 2\gamma\dot{\theta} + \omega_0^2 \left[1 + h\cos((2\omega_0 + \varepsilon)t)\right]\theta = 0$$

For unforced oscillations $(h = 0)$, damping produces solutions like

$$\theta(t) \simeq e^{-\gamma t} \times (\text{oscillation}).$$

For $h > 0$, we expect

$$\theta(t) \sim e^{(\mu - \gamma)t} \times (\text{oscillation})$$

where the factor $e^{\mu t}$ results from the periodic forcing.

The instability boundary is therefore no longer given by $\mu = 0$ (i.e., equation (18)), but by

$$\mu - \gamma = 0.$$

Instability thus occurs for $\mu^2 > \gamma^2$. Using equation (18), we obtain

$$\mu^2 = \frac{1}{4}\left[\left(\frac{1}{2}h\omega_0\right)^2 - \varepsilon^2\right] > \gamma^2$$

or

$$-\left[\left(\frac{1}{2}h\omega_0\right)^2 - 4\gamma^2\right]^{1/2} < \varepsilon < \left[\left(\frac{1}{2}h\omega_0\right)^2 - 4\gamma^2\right]^{1/2}$$

Setting $\varepsilon = 0$ (exact resonance) shows that instability is only possible when the quantity in the brackets is positive. Thus we require $h > h_c$, where

$$h_c = \frac{4\gamma}{\omega_0}$$

The phase diagram is therefore modified accordingly:
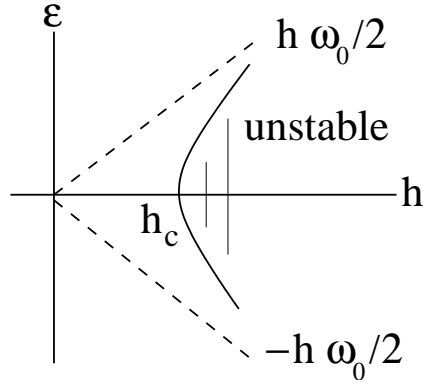
6.5   Further physical insight

We have seen that the instability is strongest at exact resonance.

That is, if the natural period of the pendulum is T_{nat}, the most unstable excitation has period

$$T_{\mathrm{exc}} = \frac{1}{2}T_{\mathrm{nat}}$$

corresponding to angular frequencies

$$\omega_{\mathrm{exc}} = 2\omega_0$$

This is called a *subharmonic* instability, because instability results at half the frequency of the excitation (i.e., $\omega_0 = \omega_{\mathrm{exc}}/2$).

What other periods of excitation would be expected to lead to instability for small h?

Any integer multiple of T_{nat} suffices. Why? Because this would correspond roughly to, say, pushing a child on a swing every nth time he/she arrives at maximum height.

Therefore (weaker) instabilities will occur for

$$T_{\mathrm{exc}} = \text{integer} \times \left(\frac{1}{2} T_{\mathrm{nat}} \right).$$

7 Fourier transforms

Except in special, idealized cases (such as the linear pendulum), the precise oscillatory nature of an observed time series $x(t)$ may not be identified from $x(t)$ alone.

We may ask

- How well-defined is the the dominant frequency of oscillation?

- How many frequencies of oscillation are present?

- What are the relative contributions of all frequencies?

The analytic tool for answering these and myriad related questions is the *Fourier transform*.

7.1 Continuous Fourier transform

We first state the Fourier transform for functions that are continuous with time.

The Fourier transform of some function $f(t)$ is

$$F(\omega) = \frac{1}{\sqrt{2\pi}} \int_{-\infty}^{\infty} f(t) e^{-i\omega t} \mathrm{d}t$$

Similarly, the inverse Fourier transform is

$$f(t) = \frac{1}{\sqrt{2\pi}} \int_{-\infty}^{\infty} F(\omega) e^{i\omega t} \mathrm{d}\omega.$$

That the second relation is the inverse of the first may be proven, but we save that calculation for the discrete transform, below.

7.2 Discrete Fourier transform

We are interested in the analysis of experimental (or numerical) data, which is almost always discrete. Thus we specialize to *discrete Fourier transforms.*

In modern data, one almost always observes a discretized signal

$$x_j, \qquad j = \{0, 1, 2, \ldots, n-1\}$$

We take the *sampling interval*—the time between samples—to be Δt. Then

$$x_j = x(j\Delta t).$$

The discretization process is pictured as
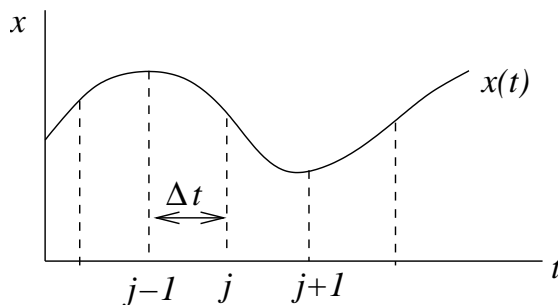
A practical question concerns the choice of Δt. To choose it, we must know the highest frequency, f_{max}, contained in $x(t)$.

The shortest period of oscillation is

$$T_{\min} = 1/f_{\max}$$

Pictorially,
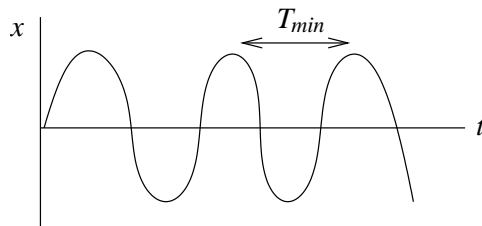
We require at least two samples per period. Therefore

$$\Delta t \le \frac{T_{\min}}{2} = \frac{1}{2f_{\max}}.$$

The discrete Fourier transform (DFT) of a time series $x_j, j = 0, 1, \ldots, n-1$ is

$$\hat{x}_k = \frac{1}{\sqrt{n}} \sum_{j=0}^{n-1} x_j \exp\left(-i\frac{2\pi jk}{n}\right) \qquad k = 0, 1, \ldots, n-1$$

To gain some intuitive understanding, consider the range of the exponential multiplier.

- $k = 0 \Rightarrow \exp(-i2\pi jk/n) = 1$. Then

$$\hat{x}_0 = \frac{1}{\sqrt{n}} \sum_j x_j$$

  Thus $\hat{x}_0$ is, within a factor of $1/\sqrt{n}$, equal to the mean of the x_j's.

  This is the "DC" component of the transform.

  Question: Suppose a seismometer measures ground motion. What would $\hat{x}_0 \neq 0$ mean?

- $k = n/2 \Rightarrow \exp(-i2\pi jk/n) = \exp(-i\pi j)$. Then

$$\hat{x}_{n/2} = \frac{1}{\sqrt{n}} \sum_j x_j(-1)^j \qquad (19)$$

$$= x_0 - x_1 + x_2 - x_3 \ldots \qquad (20)$$

  Frequency index $n/2$ is clearly the highest accessible frequency.

- The frequency indices $k = 0, 1, \ldots, n/2$ correspond to frequencies

$$f_k = k/t_{\max},$$

  i.e., k oscillations per $t_{\max}$, the period of observation.
  Index $k = n/2$ then corresponds to

$$f_{\max} = \left(\frac{n}{2}\right)\left(\frac{1}{n\Delta t}\right) = \frac{1}{2\Delta t}$$

But if $n/2$ is the highest frequency that the signal can carry, what is the significance of $\hat{x}_k$ for $k > n/2$?

For real x_j, frequency indicies $k > n/2$ are *redundant*, being related by

$$\hat{x}_k = \hat{x}^*_{n-k}$$

where z^* is the complex conjugate of z (i.e., if $z = a + ib$, $z^* = a - ib$).

We derive this relation as follows. From the definition of the DFT, we have

$$
\begin{aligned}
\hat{x}^*_{n-k} &= \frac{1}{\sqrt{n}} \sum_{j=0}^{n-1} x_j \exp\left(+i\frac{2\pi j(n-k)}{n}\right) \\
&= \frac{1}{\sqrt{n}} \sum_{j=0}^{n-1} x_j \underbrace{\exp\left(i2\pi j\right)}_{1} \exp\left(\frac{-i2\pi jk}{n}\right) \\
&= \frac{1}{\sqrt{n}} \sum_{j=0}^{n-1} x_j \exp\left(\frac{-i2\pi jk}{n}\right) \\
&= \hat{x}_k
\end{aligned}
$$

where the $+$ in the first equation derives from the complex conjugation, and the last line again employs the definition of the DFT.

Note that we also have the relation

$$\hat{x}^*_{-k} = \hat{x}^*_{n-k} = \hat{x}_k.$$

The frequency indicies $k > n/2$ are therefore sometimes referred to as *negative frequencies*

7.3 Inverse DFT

The inverse DFT is given by

$$x_j = \frac{1}{\sqrt{n}} \sum_{k=0}^{n-1} \hat{x}_k \exp\left(+i\frac{2\pi jk}{n}\right) \qquad j = 0, 1, \ldots, n-1$$

We proceed to demonstrate this inverse relation. We begin by substituting the DFT for $\hat{x}_k$, using dummy variable j':

$$
\begin{aligned}
x_j &= \frac{1}{\sqrt{n}} \sum_{k=0}^{n-1} \frac{1}{\sqrt{n}} \left[\sum_{j'=0}^{n-1} x_{j'} \exp\left(-i\frac{2\pi j'k}{n}\right) \right] \exp\left(+i\frac{2\pi kj}{n}\right) \\
&= \frac{1}{n} \sum_{j'=0}^{n-1} x_{j'} \sum_{k=0}^{n-1} \exp\left(-i\frac{2\pi k(j'-j)}{n}\right) \\
&= \frac{1}{n} \sum_{j'=0}^{n-1} x_{j'} \times \left\{ \begin{array}{ll} n, & j'=j \\ 0, & j' \neq j \end{array} \right. \\
&= \frac{1}{n}(nx_j) \\
\\
&= x_j
\end{aligned}
$$

The third relation derives from the fact that the previous $\sum_k$ amounts to a sum over the unit circle in the complex plane, except when $j' = j$. The sum over the circle always sums to zero. For example, consider $j' - j = 1, n = 4$. The elements of the sum are then just the four points on the unit circle that intersect the real and imaginary axes, i.e., the

$$
\begin{aligned}
\sum_{k=0}^{n-1} \exp\left(-i\frac{2\pi k(j'-j)}{n}\right) &= e^0 + e^{-i\pi/2} + e^{-i\pi} + e^{-i3\pi/2} \\
&= 1 + i - 1 - i \\
&= 0.
\end{aligned}
$$

Finally, note that the DFT relations imply that x_j is periodic in n, so that $x_{j+n} = x_j$. This means that a finite time series is treated precisely as if it were recurring, as illustrated below:
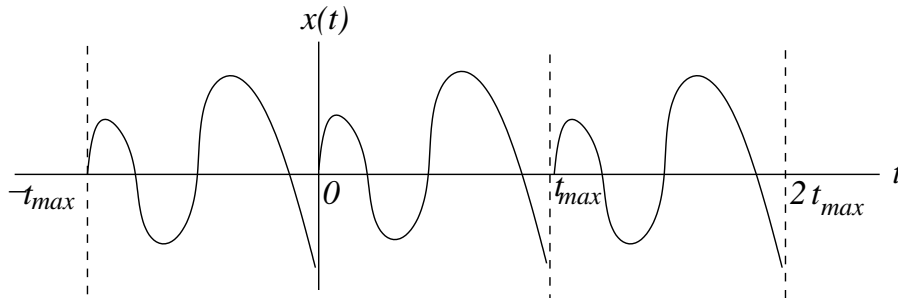
7.4 Autocorrelations, power spectra, and the Wiener-Khintchine theorem

Assume that the time series x_j has zero mean and that it is periodic, i.e., $x_{j+n} = x_j$.

Define the **autocorrelation function** ψ:

$$\psi_m = \frac{1}{n} \sum_{j=0}^{n-1} x_j x_{j+m}$$

where

$$\psi_m = \psi(m\Delta t)$$

The autocorrelation function measures the degree to which a signal resembles itself over time. Thus it measures the predictability of the future from the past. Some intuition may be gained as follows:

- Consider, for example, $m = 0$. Then

$$\psi_0 = \frac{1}{n} \sum_{j=0}^{n-1} x_j^2,$$

  which is the mean squared value of x_j (i.e., its variance).

- Alternatively, if $m\Delta t$ is much less than the dominant period of the data, ψ_m should not be too much less than ψ_0.

- Last, if $m\Delta_t$ is much greater than the dominant period of the data, $|\psi_m|$ is relatively small.

A typical ψ_m looks like
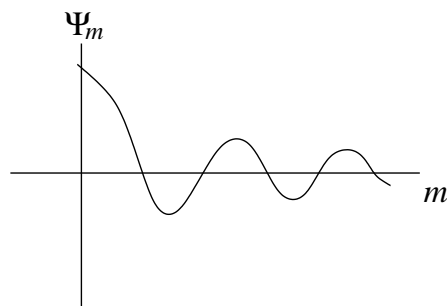
Define the **power spectrum** to be the magnitude squared of the Fourier transform; i.e.,

$$|\hat{x}_k|^2 = \frac{1}{n} \left| \sum_{j=0}^{n-1} x_j \exp\left(-i\frac{2\pi jk}{n}\right) \right|^2.$$

We proceed to show that for real time series x_j,

$$\text{autocorrelation} \propto \text{Fourier transform of the power spectrum.}$$

This is called the the *Wiener-Khintchine theorem.* We proceed to derive this relation.

Substitute the inverse DFT for x_j in ψ_m:

$$\psi_m = \frac{1}{n} \sum_{j=0}^{n-1} \left[\frac{1}{\sqrt{n}} \sum_{k=0}^{n-1} \hat{x}_k \exp\left(i\frac{2\pi kj}{n}\right) \right] \left[\frac{1}{\sqrt{n}} \sum_{k'=0}^{n-1} \hat{x}_{k'} \exp\left(i\frac{2\pi k'(j+m)}{n}\right) \right]$$

$$= \frac{1}{n^2} \sum_{k=0}^{n-1} \sum_{k'=0}^{n-1} \hat{x}_k \hat{x}_{k'} \exp\left(i\frac{2\pi mk'}{n}\right) \underbrace{\sum_{j=0}^{n-1} \exp\left(i\frac{2\pi j(k+k')}{n}\right)}_{\substack{= n, \quad k' = n - k \\ = 0, \quad k' \neq n - k}}$$

$$= \frac{1}{n} \sum_{k=0}^{n-1} \hat{x}_k \hat{x}_{n-k} \exp\left(i\frac{2\pi m(n-k)}{n}\right)$$

$$= \frac{1}{n} \sum_{k=0}^{n-1} \hat{x}_k \hat{x}_k^* \exp\left(-i\frac{2\pi mk}{n}\right)$$

In the last line we have used the redundancy relation $\hat{x}_k^* = \hat{x}_{n-k}$.

We thus find that

$$\psi_m \propto \text{Fourier transform of the power spectrum } \hat{x}_k \hat{x}_k^* = |\hat{x}_k|^2$$

Of course the inverse relation holds also.

For real time series $\{x_j\}$, the power spectrum contains redundant information that is similar to that of the Fourier transform but more severe:

$$|\hat{x}_k|^2 = \hat{x}_k \hat{x}_k^* = \hat{x}_k \hat{x}_{n-k} = \hat{x}_{n-k}^* \hat{x}_{n-k} = |\hat{x}_{n-k}|^2.$$

This redundancy results from the fact that neither the autocorrelation nor the power spectra contain information on any "phase lags" in either x_j or its individual frequency components.

Thus while the DFT of an n-point time series results in n independent quantities ($2 \times n/2$ complex numbers), the power spectrum yields only $n/2$ independent quantities.

One may therefore show that there are an infinite number of time series that have the same power spectrum, but that each time series uniquely defines its Fourier transform, and vice-versa.

Consequently a time series cannot be reconstructed from its power spectrum or autocorrelation function.

7.5   Power spectrum of a periodic signal

Consider a periodic signal

$$x(t) = x(t + T) = x \left(t + \frac{2\pi}{\omega} \right)$$

Consider the extreme case where the period T is equal to the duration of the signal:

$$T = t_{\max} = n \triangle t$$

The Fourier components are separated by

$$\Delta f = \frac{1}{t_{\max}}$$

i.e. at frequencies

$$0, \ 1/T, \ 2/T, \ldots, (n-1)/T.$$

7.5.1   Sinusoidal signal

In the simplest case, $x(t)$ is a sine or cosine, i.e.,

$$x(t) = \sin \left(\frac{2\pi t}{t_{\max}} \right).$$

What is the Fourier tranform? Pictorially, we expect
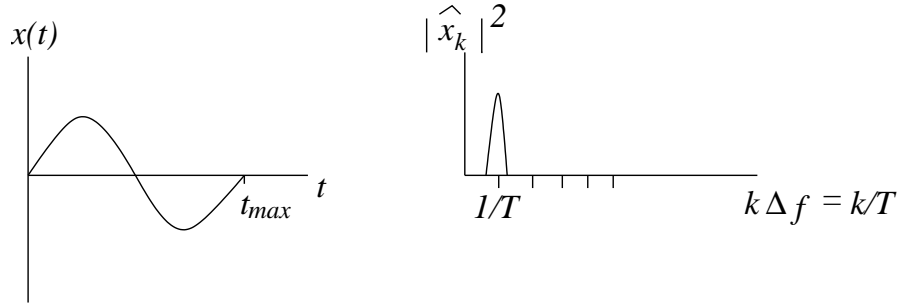
We proceed to calculate the power spectrum analytically, beginning with the DFT:

$$
\begin{aligned}
\hat{x}_k &= \frac{1}{\sqrt{n}} \sum_j x_j \exp\left(\frac{-i2\pi jk}{n}\right) \\
&= \frac{1}{\sqrt{n}} \sum_j \sin\left(\frac{2\pi j\Delta t}{t_{\max}}\right) \exp\left(\frac{-i2\pi jk}{n}\right) \\
&= \frac{1}{2i\sqrt{n}} \sum_j \left[\exp\left(\frac{i2\pi j\Delta t}{t_{\max}}\right) - \exp\left(\frac{-i2\pi j\Delta t}{t_{\max}}\right)\right] \exp\left(\frac{-i2\pi jk}{n}\right) \\
&= \frac{1}{2i\sqrt{n}} \sum_j \left[\exp\left\{i2\pi j\left(\frac{\Delta t}{t_{\max}} - \frac{k}{n}\right)\right\} - \exp\left\{-i2\pi j\left(\frac{\Delta t}{t_{\max}} + \frac{k}{n}\right)\right\}\right] \\
&= \pm\frac{\sqrt{n}}{2i} \qquad \text{when } k = \frac{\pm n\Delta t}{t_{\max}}
\end{aligned}
$$

Thus

$$
|\hat{x}_j|^2 = \frac{n}{4} \qquad \text{for } k = \pm 1.
$$

7.5.2 Non-sinusoidal signal

Consider now a non-sinusoidal yet periodic signal, e.g., a relaxation oscillation as obtained from the van der Pol system.

The non-sinusoidal character of the relaxation oscillation implies that it contains higher-order **harmonics**, i.e., integer multiples of the **fundamental frequency** $1/T$. Thus, pictorially, we expect
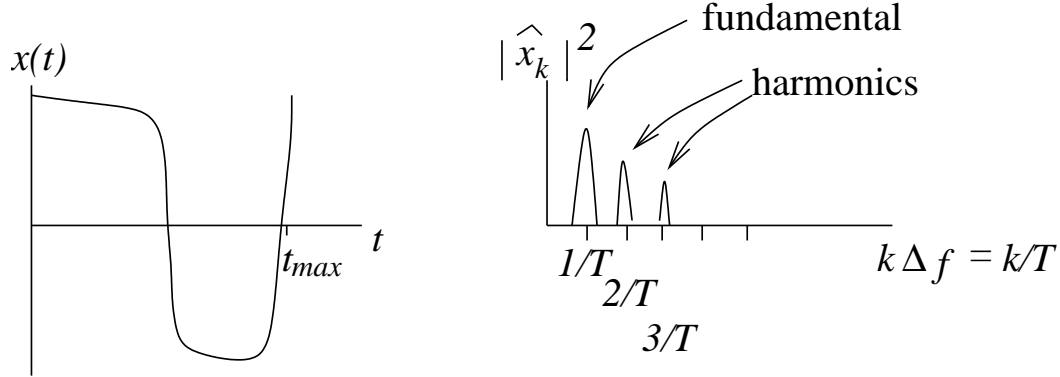
Now suppose $t_{\max} = pT$, where p is an integer. The non-zero components of the power spectrum must still be at frequencies

$$1/T, 2/T, \ldots.$$

But since

$$\Delta f = \frac{1}{t_{\max}} = \frac{1}{pT}$$

the frequency resolution is p times greater. Contributions to the power spectrum would remain at integer multiples of the frequency $1/T$, but spaced p samples apart on the frequency axis.

7.5.3 $t_{\max}/T \neq$ **integer**

If $t_{\max}/T$ is not an integer, the (effectively periodic) signal looks like
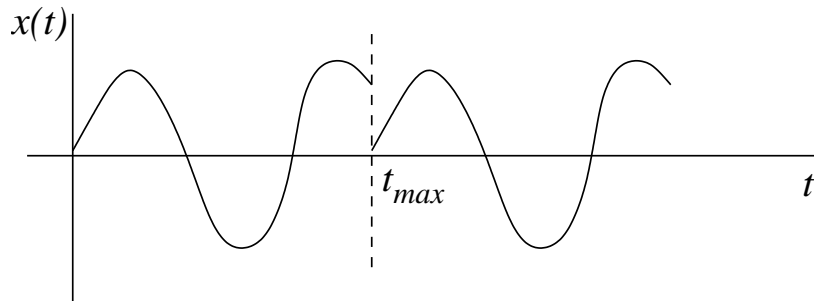
We proceed to calculate the power spectrum of such a signal. Assume the sinusoidal function

$$x(t) = \exp\left(i\frac{2\pi t}{T}\right)$$

which yields

$$x_j = \exp\left(i\frac{2\pi j \Delta t}{T}\right)$$

The DFT is

$$\hat{x}_k = \frac{1}{\sqrt{n}} \sum_{j=0}^{n-1} \exp\left(i\frac{2\pi j \Delta t}{T}\right) \exp\left(-i\frac{2\pi j k}{n}\right)$$

Set

$$\phi_k = \frac{\Delta t}{T} - \frac{k}{n}.$$

Then

$$\hat{x}_k = \frac{1}{\sqrt{n}} \sum_{j=0}^{n-1} \exp\left(i 2\pi \phi_k j\right)$$

Recall the identity

$$\sum_{j=0}^{n-1} x^j = \frac{x^n - 1}{x - 1}$$

Then

$$\hat{x}_k = \frac{1}{\sqrt{n}} \frac{\exp(i 2\pi \phi_k n) - 1}{\exp(i 2\pi \phi_k) - 1}$$

The power spectrum is

$$|\hat{x}_k|^2 = \hat{x}_k \hat{x}_k^* = \frac{1}{n}\left(\frac{1 - \cos(2\pi \phi_k n)}{1 - \cos(2\pi \phi_k)}\right)$$

$$= \frac{1}{n}\left(\frac{\sin^2(\pi \phi_k n)}{\sin^2(\pi \phi_k)}\right)$$

Note that

$$n\phi_k = \frac{n\Delta t}{T} - k = \frac{t_{\max}}{T} - k$$

is the difference between a DFT index k and the "real" non-integral frequency index $t_{\max}/T$.

Assume that n is large and k is close to that "real" frequency index such that

$$n\phi_k = \frac{n\Delta t}{T} - k \ll n.$$

Consequently $\phi_k \ll 1$, so we may also assume

$$\pi\phi_k \ll 1.$$

Then

$$
\begin{aligned}
|\hat{x}_k|^2 &\simeq \frac{1}{n}\frac{\sin^2(\pi\phi_k n)}{(\pi\phi_k)^2} \\
&= n\frac{\sin^2(\pi\phi_k n)}{(\pi\phi_k n)^2} \\
&\propto \frac{\sin^2 z}{z^2}
\end{aligned}
$$

where

$$z = n\pi\phi_k = \pi\left(\frac{n\Delta t}{T} - k\right) = \pi\left(\frac{t_{\max}}{T} - k\right)$$

Thus $|\hat{x}_k|^2$ is no longer a simple spike. Instead, as a function of $z = n\pi\phi_k$ it appears as
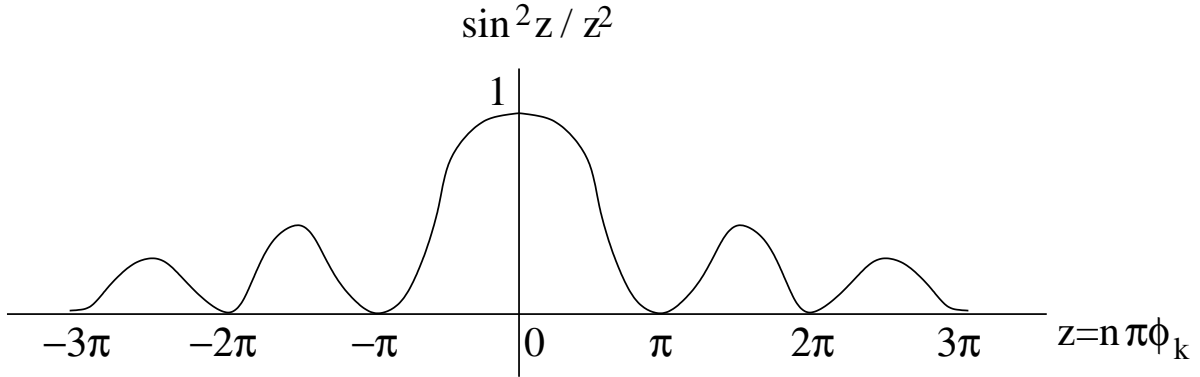
The plot gives the kth component of the power spectrum of $e^{i2\pi t/T}$ as a function of $\pi(t_{\max}/T - k)$.

To interpret the plot, let k_0 be the integer closest to $t_{\max}/T$. There are then two extreme cases:

1. t_{max} is an integral multiple of T:

$$\frac{t_{\text{max}}}{T} - k_0 = 0.$$

The spectrum is perfectly sharp:
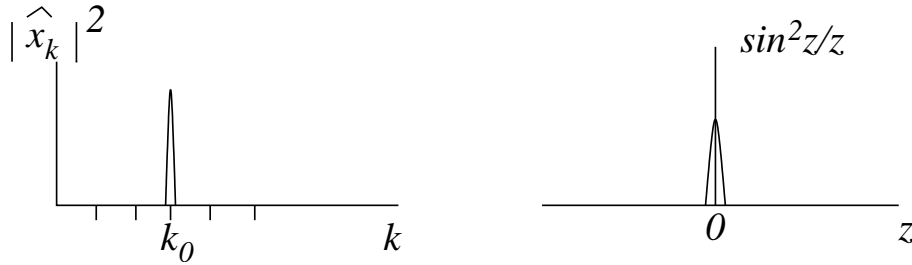
2. t_{max}/T falls midway between two frequencies. Then

$$\frac{t_{\text{max}}}{T} - k_0 = \frac{1}{2}.$$

The spectrum is smeared:
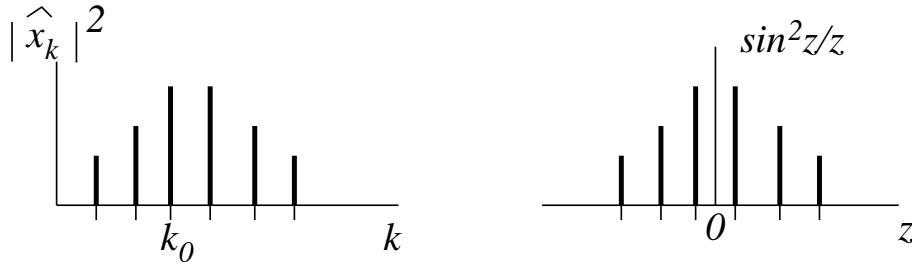
The smear decays like

$$\frac{1}{(k - t_{\text{max}}/T)^2} \sim \frac{1}{k^2}$$

7.5.4   Conclusion

The power spectrum of a periodic signal of period T is composed of:

1. a peak at the frequency $1/T$

2. a smear (sidelobes) near $1/T$

3. possibly harmonics (integer multiples) of $1/T$

4. smears near the harmonics.

7.6 Quasiperiodic signals

Let y be a function of r independent variables:

$$y = y(t_1, t_2, \ldots, t_r).$$

y is **periodic**, of period 2π in *each* argument, if

$$y(t_1, t_2, \ldots, t_j + 2\pi, \ldots, t_r) = y(t_1, t_2, \ldots, t_j, \ldots, t_r), \quad j = 1, \ldots, r$$

y is called **quasiperiodic** if each t_j varies with time at a different rate (i.e., different "clocks"). We have then

$$t_j = \omega_j t, \qquad j = 1, \ldots, r.$$

The quasiperiodic function y has r fundamental frequencies:

$$f_j = \frac{\omega_j}{2\pi}$$

and r periods

$$T_j = \frac{1}{f_j} = \frac{2\pi}{\omega_j}.$$

Example: The astronomical position of a point on Earth's surface changes due to

- rotation of Earth about axis ($T_1 = 24$ hours).

- revolution of Earth around sun ($T_2 \simeq 365$ days).

- we ignore precession and other orbital changes.

Mathematically, we can conceive of such a function on a 2-D torus T^2, existing in a 3-D space.
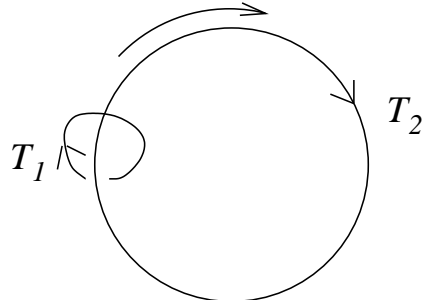
Here we think of a disk spinning with period T_1 while it revolves along the circular path with period T_2.

Such behavior can be conceived as a trajectory on the *surface* of a doughnut or inner tube, or a torus T_2 in $\mathbb{R}^3$.
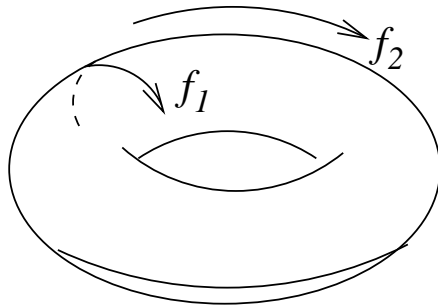
What is the power spectrum of a quasiperiodic signal $x(t)$? There are two possibilities:

1. The quasiperiodic signal is a *linear* combination of independent periodic functions. For example:

$$x(t) = \sum_{i=1}^{r} x_i(\omega_i t).$$

   Because the Fourier transform is a linear transformation, the power spectrum of $x(t)$ is a set of peaks at frequencies

   $$f_1 = \omega_1/2\pi, \ f_2 = \omega_2/2\pi, \ldots$$

   and their harmonics

   $$m_1 f_1, \ m_2 f_2, \ldots \qquad (m_1, m_2, \ldots \text{ positive integers}).$$

2. The quasiperiodic signal $x(t)$ depends nonlinearly on periodic functions. For example,

   $$x(t) = \sin(2\pi f_1 t)\sin(2\pi f_2 t) = \frac{1}{2}\cos(|f_1 - f_2|2\pi t) - \frac{1}{2}\cos(|f_1 + f_2|2\pi t).$$

   The fundamental frequencies are

   $$|f_1 - f_2| \qquad \text{and} \qquad |f_1 + f_2|.$$

The harmonics are

$$m_1|f_1 - f_2| \qquad \text{and} \qquad m_2|f_1 + f_2|, \qquad m_1, m_2 \text{ positive integers.} \quad (21)$$

The nonlinear case requires more attention. In general, if $x(t)$ depends non-linearly on r periodic functions, then the harmonics are

$$|m_1 f_1 + m_2 f_2 + \ldots + m_r f_r|, \qquad m_i \text{ arbitrary integers.}$$

(This is the most general case, for which equation (21) is a specific example. The expression above derives from $m_1 f_1 \pm m_2 f_2 \pm \ldots$, with m_i positive)

We proceed to specialize to $r = 2$ frequencies, and forget about finite Δf.

Each nonzero component of the spectrum of $x(\omega_1 t, \omega_2 t)$ is a peak at

$$f = |m_1 f_1 + m_2 f_2|, \qquad m_1, m_2 \text{ integers .}$$

There are two cases:

1. f_1/f_2 rational $\Rightarrow$ *sparse spectrum.*

2. f_1/f_2 irrational $\Rightarrow$ *dense spectrum.*

To understand this, rewrite f as

$$f = f_2 \left| m_1 \frac{f_1}{f_2} + m_2 \right|.$$

In the rational case,

$$\frac{f_1}{f_2} = \frac{\text{integer}}{\text{integer}}.$$

Then

$$\left| m_1 \frac{f_1}{f_2} + m_2 \right| = \left| \frac{\text{integer}}{f_2} + \text{integer} \right| = \text{ integer multiple of } \frac{1}{f_2}.$$

Thus the peaks of the spectrum must separated (i.e., sparse).

Alternatively, if f_1/f_2 is irrational, then m_1 and m_2 may always be chosen so that

$$\left| m_1 \frac{f_1}{f_2} + m_2 \right| \text{ is not similarly restricted.}$$

These distinctions have further implications.

In the rational case,

$$\frac{f_1}{f_2} = \frac{n_1}{n_2}, \qquad n_1, n_2 \text{ integers.}$$

Since

$$\frac{n_1}{f_1} = \frac{n_2}{f_2}$$

the quasiperiodic function is *periodic* with period

$$T = n_1 T_1 = n_2 T_2.$$

All spectral peaks must then be harmonics of the fundamental frequency

$$f_0 = \frac{1}{T} = \frac{f_1}{n_1} = \frac{f_2}{n_2}.$$

Thus the rational quasiperiodic case is in fact periodic, and some writers restrict quasiperiodicity to the irrational case.

Note further that, in the irrational case, the signal never exactly repeats itself.

One may consider, as an example, the case of a child walking on a sidewalk, attempting with uniform steps to never step on a crack (and breaking his mother's back...).

Then if $x(t)$ were the distance from the closest crack at each step, it would only be possible to avoid stepping on a crack if the ratio

$$\frac{\text{step size}}{\text{crack width}}$$

were rational.

7.7 Aperiodic signals

Aperiodic signals are neither periodic nor quasiperiodic.

Aperiodic signals appear random, though they may have a deterministic foundation.

An example is white noise, which is a signal that is "new" and unpredictable at each instant, e.g.,
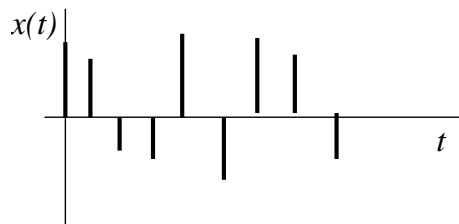
Statistically, each sample of a white-noise signal is independent of the others, and therefore uncorrelated to them.

The power spectrum of white noise is, on average, flat:
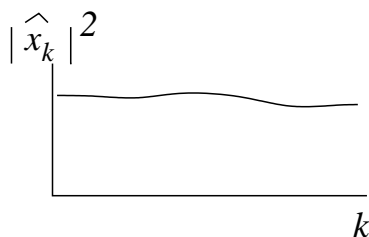
The flat spectrum of white noise is a consequence of its lack of harmonic structure (i.e., one cannot recognize any particular tone, or dominant frequency).

We proceed to derive the spectrum of a white noise signal $x(t)$.

Rather than considering only one white-noise signal, we consider an **ensemble** of such signals, i.e.,
$$x^{(1)}(t), x^{(2)}(t), \ldots$$
where the superscipt denotes the particular realization within the ensemble. Each realization is independent of the others.

Now discretize each signal so that

$$x_j = x(j\Delta t), \qquad j = 0, \ldots, n-1$$

We take the signal to have finite length n but consider the ensemble to contain an infinite number of realizations.

We use angle brackets to denote **ensemble averages** (i.e., averages taken over the ensemble).

The ensemble-averaged mean of the jth sample is then

$$\langle x_j \rangle = \lim_{p \to \infty} \frac{1}{p} \sum_{i=1}^{p} x_j^{(i)}$$

Similarly, the mean-square value of the jth sample is

$$\langle x_j^2 \rangle = \lim_{p \to \infty} \frac{1}{p} \sum_{i=1}^{p} (x_j^{(i)})^2$$

Now assume *stationarity*: $\langle x_j \rangle$ and $\langle x_j^2 \rangle$ are independent of j. We take these mean values to be $\langle x \rangle$ and $\langle x^2 \rangle$, respectively, assume $\langle x \rangle = 0$.

Recall the autocorrelation ψ_m:

$$\psi_m = \frac{1}{n} \sum_{j=0}^{n-1} x_j x_{j+m}.$$

By definition, each sample of white noise is uncorrelated with its past and future. Therefore

$$\langle \psi_m \rangle = \left\langle \frac{1}{n} \sum_j x_j x_{j+m} \right\rangle$$

$$= \langle x^2 \rangle \delta_m$$

where

$$\delta_m = \begin{cases} 1 & m = 0 \\ 0 & \text{else} \end{cases}$$

We obtain the power spectrum from the autocorrelation function by the Wiener-Khintchine theorem:

$$\langle |\hat{x}_k|^2 \rangle = \sum_{m=0}^{n-1} \langle \psi_m \rangle \exp\left(i\frac{2\pi mk}{n} \right)$$

$$= \sum_{m=0}^{n-1} \langle x^2 \rangle \delta_m \exp\left(i\frac{2\pi mk}{n} \right)$$

$$= \langle x^2 \rangle$$

$$= \text{constant.}$$

Thus for white noise, the spectrum is indeed flat, as previously indicated:
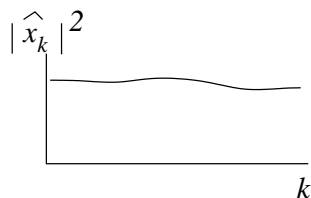
A more common case is "colored" noise: a continuous spectrum, but not constant:
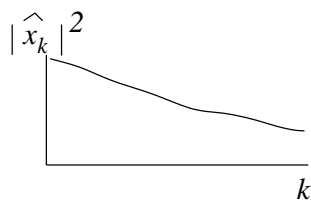
In such (red) colored spectra, there is a relative lack of high frequencies. The signal is still apparently random, but only beyond some interval Δt.

The autocorrelation of colored noise is broader, e.g.,

66
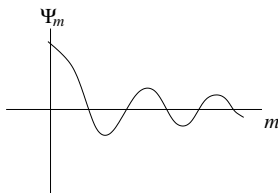
Finally, we note a problem: power spectra can recognize a signal that is approximately aperiodic, but they cannot distinguish between **deterministic** systems and statistical, **random** systems.

Thus we turn to Poincaré sections.

8 Poincaré sections

The dynamical systems we study are of the form

$$\frac{\mathrm{d}}{\mathrm{d}t}\vec{x}(t) = F(\vec{x}, t)$$

Systems of such equations describe a *flow* in phase space.

The solution is often studied by considering the trajectories of such flows.

But the phase trajectory is itself often difficult to determine, if for no other reason than that the dimensionality of the phase space is too large.

Thus we seek a geometric depiction of the trajectories in a lower-dimensional space—in essence, a view of phase space without *all* the detail.

8.1 Construction of Poincaré sections

Suppose we have a 3-D flow Γ. Instead of directly studying the flow in 3-D, consider, e.g., its intersection with a plane $(x_3 = h)$:
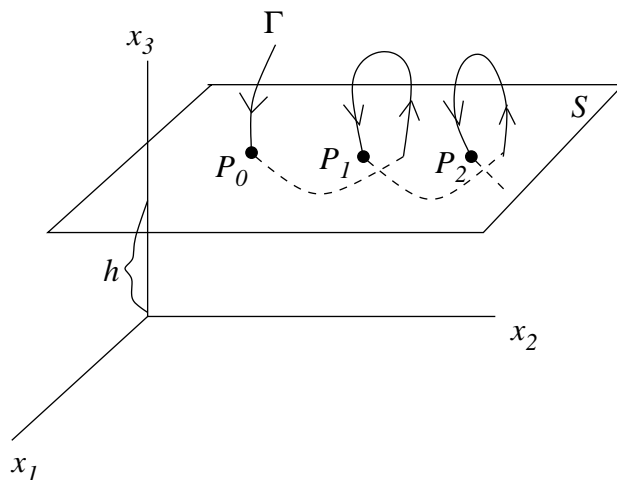
- Points of intersection correspond (*in this case*) to $\dot{x}_3 < 0$ on Γ.

- Height h of plane S is chosen so that Γ continually crosses S.

- The points P_0, P_1, P_2 form the 2-D **Poincaré section**.

The Poincaré section is a continuous mapping T of the plane S into itself:

$$P_{k+1} = T(P_k) = T\left[T(P_{k-1})\right] = T^2(P_{k-1}) = \ldots$$

Since the flow is deterministic, P_0 determines P_1, P_1 determines P_2, etc.

The Poincaré section reduces a *continuous* flow to a **discrete-time mapping**. However the time interval from point to point is not necessarily constant.

We expect some geometric properties of the flow and the Poincaré section to be the same:

- Dissipation $\Rightarrow$ areas in the Poincaré section *should* contract.

- If the flow has an attractor, we should see it in the Poincaré section.

Essentially the Poincaré section provides a means to visualize an otherwise messy, possibly aperiodic, attractor.

8.2 Types of Poincaré sections

As we did with power spectra, we classify three types of flows: periodic, quasiperiodic, and aperiodic.

8.2.1 Periodic

The flow is a closed orbit (e.g., a limit cycle):
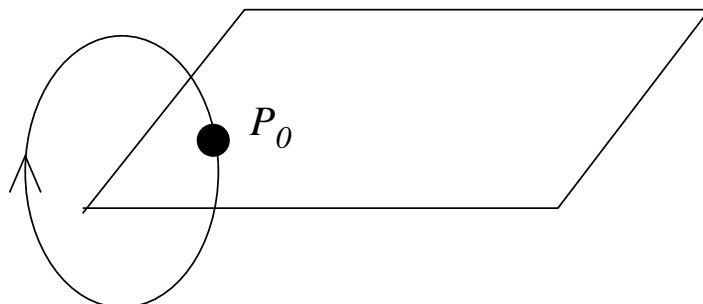
P_0 is a fixed point of the Poincaré map:

$$P_0 = T(P_0) = T^2(P_0) = \ldots.$$

We proceed to analyze the stability of the fixed point.

To first order, a Poincaré map T can be described by a matrix M defined in the neighborhood of P_0:

$$M_{ij} = \left.\frac{\partial T_i}{\partial x_j}\right|_{P_0}.$$

In this context, M is called a *Floquet matrix*. It describes how a point $P_0 + \delta$ moves after one intersection of the Poincaré map.

A Taylor expansion about the fixed point yields:

$$T_i(P_0 + \delta) \simeq T_i(P_0) + \left.\frac{\partial T_i}{\partial x_1}\right|_{P_0} \cdot \delta_1 + \left.\frac{\partial T_i}{\partial x_2}\right|_{P_0} \cdot \delta_2, \qquad i = 1, 2$$

Since $T(P_0) = P_0$,

$$T(P_0 + \delta) \simeq P_0 + M\delta$$

Therefore

$$T\bigg(T(P_0 + \delta)\bigg) \simeq T(P_0 + M\delta)$$

$$\simeq T(P_0) + M^2\delta$$

$$\simeq P_0 + M^2\delta$$

After m interations of the map,

$$T^m(P_0 + \delta) - P_0 \simeq M^m\delta.$$

Stability therefore depends on the properties of M.

Assume that δ is an eigenvector of M. (There will always be a projection onto an eigenvector.) Then

$$M^m\delta = \lambda^m\delta,$$

where λ is the corresponding eigenvalue.

Therefore

$$|\lambda| < 1 \Rightarrow \text{ linearly stable}$$
$$|\lambda| > 1 \Rightarrow \text{ linearly unstable}$$

Conclusion: a periodic map is unstable if one of the eigenvalues of the Floquet matrix crosses the unit circle in the complex plane.

8.2.2 Quasiperiodic flows

Consider a 3-D flow with two fundamental frequencies f_1 and f_2. The flow is a torus T^2:
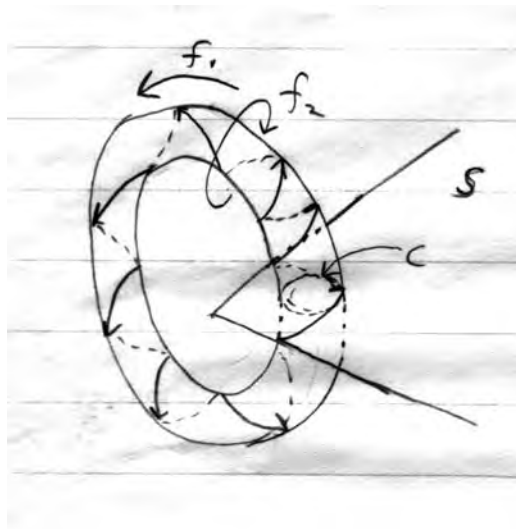
The points of intersection of the flow with the plane S appear on a closed curve C.

As with power spectra, the form of the resulting Poincaré section depends on the ratio f_1/f_2:

- **Irrational** f_1/f_2. The frequencies are called *incommensurate*. The closed curve C appears continuous, e.g.
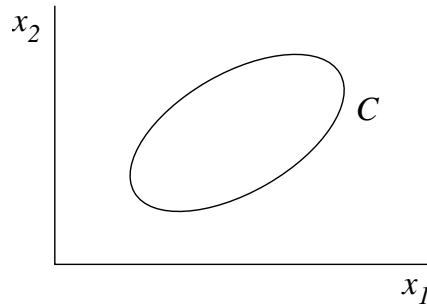
- The trajectory on the torus T^2 never repeats itself exactly.
- The curve is not traversed continuously, but rather

$$T(C) = \text{ finite shift along } C.$$

- **Rational f_1/f_2.**

  - f_1 and f_2 are *frequency locked.*
  - There are finite number of intersections (points) along the curve C.
  - Trajectory repeats itself after n_1 revolutions and n_2 rotations.
  - The Poincaré section is periodic with

$$\text{period } = n_1/f_1 = n_2/f_2$$

  - The Poincaré section contains just n_1 points. Thus

$$P_i = T^{n_1}(P_i)$$

  - Example, $n_1 = 5$:
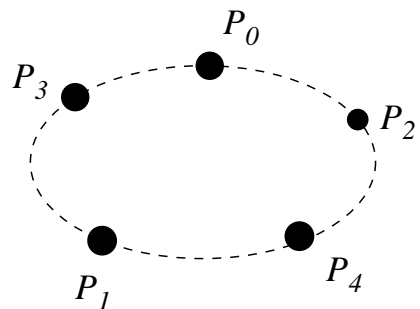
8.2.3 Aperiodic flows

Aperiodic flows may no longer lie on some reasonably simple curve.

In an extreme case, one has just a point cloud:
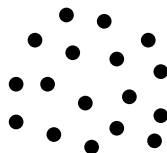
This would be expected for statistical white noise.

Deterministic aperiodic systems often display more order, however. In some cases they create mild departures from a simple curve, e.g.
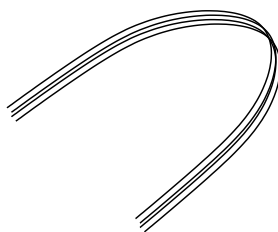
Such cases arise from strong dissipation (and the resulting contraction of areas in phase space).

It then becomes useful to define a coordinate x that falls roughly along this curve, and to study the iterates of x. This is called a *first return map.*

8.3   First-return maps

First return maps are 1-D reductions of the kind of 2-D Poincaré maps that we have been considering.

Such maps are of the form
$$x_{k+1} = f(x_k).$$
We will study these extensively at the end of the course.

We shall give particular attention to the following quadratic mapping of the unit interval onto itself:

$$x_{k+1} = 4\mu x_k(1 - x_k), \qquad 0 \le \mu \le 1.$$

The mapping is easily described graphically. The quadratic rises from $x = 0$, falls to $x = 1$, and has its maximum at $x = 1/2$, where it rises to height μ.

Consider, for example, the case $\mu = 0.7$:
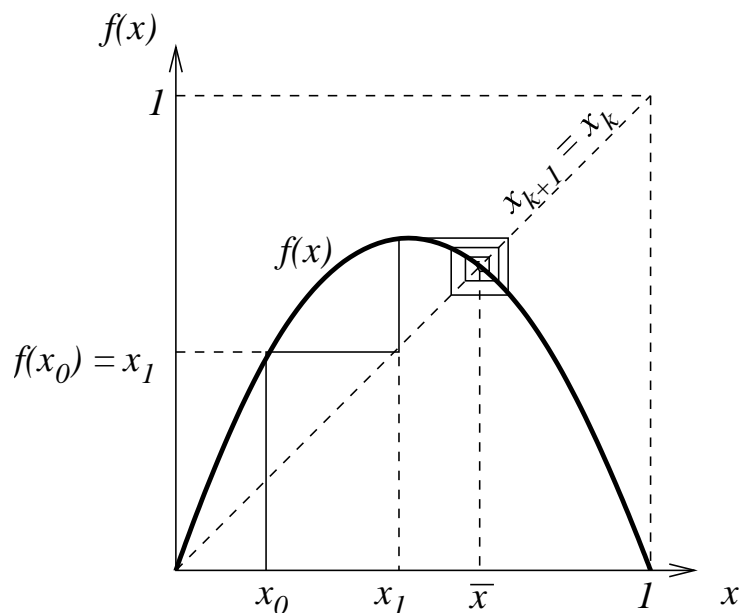
Eventually the interations converge to $x = \bar{x}$, which is where the diagonal (the identity map $x_{k+1} = x_k$) intersects $f(x)$.

Thus $\bar{x}$ is a fixed point of f, i.e.,

$$\bar{x} = f(\bar{x})$$

Another fixed point is $x = 0$, since $f(0) = 0$.

However we can see graphically that $x = 0$ is unstable; iterates initiated at $x_0 = \varepsilon$ still converges to $\bar{x}$.

Thus $x = 0$ is an *unstable* fixed point, while $x = \bar{x}$ is *stable*.

What determines stability? Consider graphically the case $\mu = 0.9$:
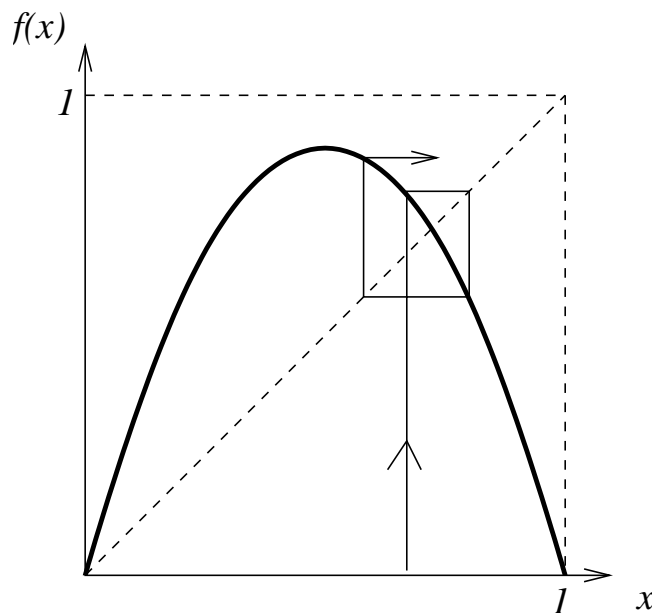
We infer that the slope $f'(\bar{x})$ determines whether $\bar{x}$ is stable. We proceed to show this formally.

Suppose x^* is *any* fixed point such that

$$x^* = f(x^*).$$

Define

$$x_k = x^* + \varepsilon_k, \qquad \varepsilon_k \text{ small.}$$

In general, our mappings are described by

$$x_{k+1} = f(x_k).$$

Then

$$x^* + \varepsilon_{k+1} = f(x^* + \varepsilon_k)$$

$$= f(x^*) + f'(x^*)\varepsilon_k + O(\varepsilon_k^2)$$

Therefore

$$\varepsilon_{k+1} \simeq f'(x^*)\varepsilon_k.$$

Thus

$$|f'(x^*)| < 1 \implies \text{stability.}$$

8.4   1-D flows

It is instructive to compare the stability of 1-D maps to the stability of the continuous 1-D flow
$$\dot{x} = f(x).$$
Consider, for example, a particular $f(x)$ that looks like
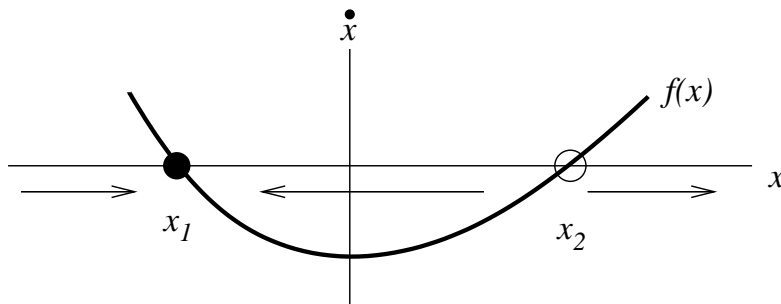
Clearly x_1 and x_2 are fixed points. Which are stable?

The arrows show the direction of flow on the x-axis, i.e., the sign of $\dot{x} = f(x)$.

Thus x_1 is stable while x_2 is not.

Stability of a fixed point x^* is therefore determined as follows:

$$f'(x^*) < 0 \quad \Rightarrow \quad \text{stable}$$

$$f'(x^*) > 0 \quad \Rightarrow \quad \text{unstable}$$

Whereas the stability of a continuous 1-D flow f depends on the sign of f', the stability of a 1-D map depends on the magnitude $|f'|$.

In higher dimensions this same distinction holds for the eigenvalues λ of the Jacobian (which, in the case of mappings, we have called the Floquet matrix). That is, the sign of $\text{Re}(\lambda)$ determines the stability of flows, whereas the magnitude $|\lambda|$ is the relevant quantity for maps.

8.5 Relation of flows to maps

We now consider explicitly how flows may be related to maps.

8.5.1 Example 1: the van der Pol equation

Consider again the van der Pol equation

$$\frac{\mathrm{d}^2\theta}{\mathrm{d}t^2} + \varepsilon(\theta^2 - 1)\frac{\mathrm{d}\theta}{\mathrm{d}t} + \theta = 0$$

Recall that for $\varepsilon > 0$ the rest position is unstable and that the system has a limit cycle.

We draw a ray emanating from the origin, and consider two representative trajectories initiating and terminating on it:
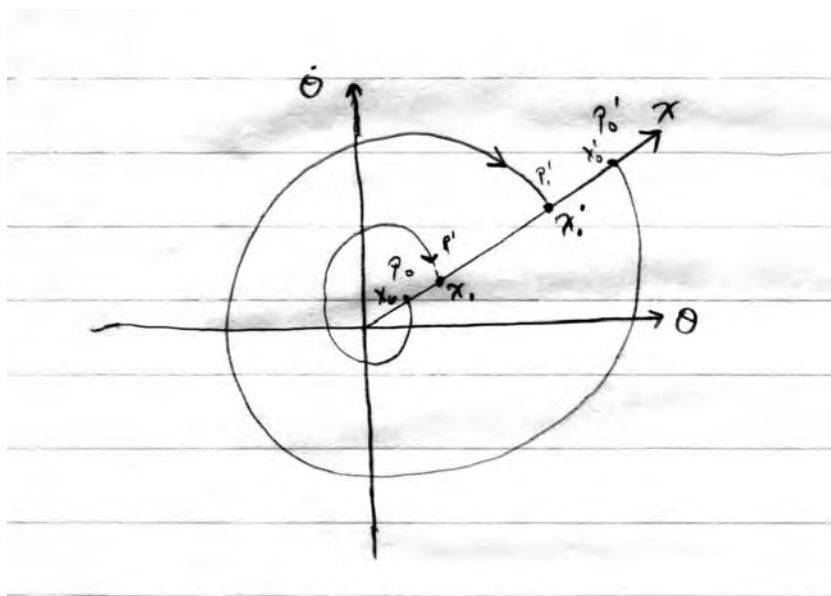
Let x_k be the position of the kth intersection of the trajectory with the ray. There is then some mapping f such that

$$x_{k+1} = f(x_k).$$

The precise form of $f(x)$ is unknown, but physical and mathematical reasoning allows us to state some of its properties:

- f maps x_k to a unique x_{k+1}.

- f is continuous.

- $f'(x) > 1$ near the origin (divergent spirals).

- $f'(x) < 1$ far from the origin (convergent spirals).

- $f'(x) > 0$ for all $x > 0$ (since $f(x + \delta) > f(x)$).

The simplest form of f is therefore a curve rising steeply from the origin, followed by a gentle upward slope:
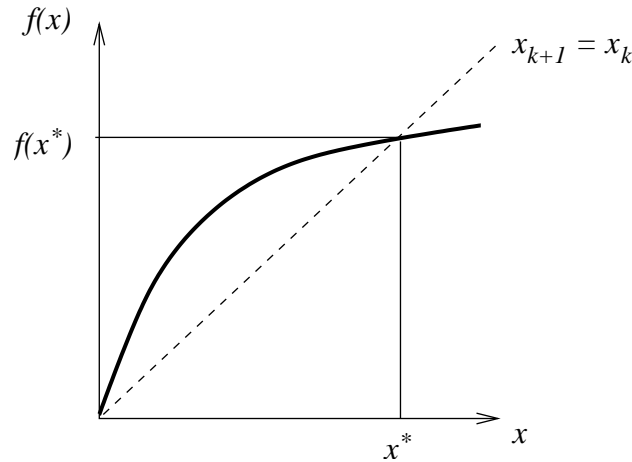
By continuity, there must be a stable fixed point x^* characterized by

$$x^* = f(x^*) \qquad \text{and} \qquad f'(x^*) < 1.$$

Thus x^* gives the effective radius of the stable limit cycle.

8.5.2   Example 2: Rössler attractor

Consider the following 3-D flow (the Rössler attractor):

$$\begin{aligned}
\dot{x} &= -y - z \\
\dot{y} &= x + ay \\
\dot{z} &= b + z(x - c)
\end{aligned}$$

a, b, and c are fixed parameters.

Numerical solutions yield the time series $x(t)$:

Figure IV.11, BPV

The time series $z(t)$:

Figure IV.11, BPV

A Poincaré section in the x-y plane:

Figure IV.12a, BPV

And a 3-D perspective of the flow:

Figure 12.1, unknown source

The time series display great irregularity, but the Poincaré section and the full flow display some order.

Consider now another Poincaré section, in the plane

$$y + z = 0.$$

From the Rössler equations, we identify this plane with extrema in the time series $x(t)$, i.e., each intersection of the plane corresponds to

$$\dot{x} = 0.$$

Consider a sequence x_k of such extrema, but only when the extremum is a maximum (local peak) of $x(t)$.

Then plot x_{k+1} vs. x_k:

Figure IV.10, BPV

Conclusions:

- The 1-D map, even more so than the Poincaré section, reveals that the flow contains much order.

- The time series, however, displays no apparent regularity.

This is the essence of deterministic chaos.

We proceed to show how such Poincaré sections and 1-D maps can be constructed from experimental data.

8.5.3 Example 3: Reconstruction of phase space from experimental data

Suppose we measure some signal $x(t)$ (e.g., the weather, the stock market, etc.)

In most cases it is unlikely that we can specify the equations of motion of the dynamical system that is generating $x(t)$.

How, then, may we visualize the system's phase space and its attractor?

The (heuristic but highly successful) idea, originally due to Santa Cruz undergraduates Packer, Crutchfield, Farmer, and Shaw (1980), is to measure any 3 *independent* quantities from $x(t)$.

For example:

- $x(t)$, $x(t+\tau)$, $x(t+2\tau)$; τ large enough for "independence," i.e., beyond an autocorrelation time. This is the most popular; it is known as the **method of delays**.

- $x(t)$, $\dot{x}(t)$, $\ddot{x}(t)$ (where the derivatives are finite differences $x_k - x_{k-1}$, etc.).

Such a representation of the attractor is not identical to the "real" phase space, but it should retain similar geometric properties.

We use the Rössler attractor as an example.

- Comparison of the projection of the trajectories in the x-y plane to the projection of the trajectories in the x-$\dot{x}$ plane:

$$\boxed{\text{Figure IV.12, BPV}}$$

• Example of different values for τ using the method of delays:

$$\boxed{\text{Figure 78, Schuster}}$$

With the method of delays, τ is typically the period of the forcing, or the period of a characteristic limit cycle.

Here we have discussed only qualitative, geometric properties. We shall see that the various representations also yield similar quantitative properties (e.g., measures of Lyaponov exponents).

9 Fluid dynamics and Rayleigh-Bénard convection

In these lectures we derive (mostly) the equations of viscous fluid dynamics. We then show how they may be generalized to the problem of Rayleigh-Bénard convection—the problem of a fluid heated from below. Later we show how the RB problem itself may be reduced to the famous Lorenz equations.

The highlights of these lectures are as follows:

- Navier-Stokes equations of fluid dynamics (mass and momentum conservation).

- Reynolds number

- Phenomenology of RB convection

- Rayleigh number

- Equations of RB convection

Thus far we have dealt almost exclusively with the temporal behavior of a few variables.

In these lectures we digress, and discuss the evolution of a *continuum.*

9.1 The concept of a continuum

Real fluids are made of atoms or molecules.

The *mean free path* ℓ_{mfp} is the characteristic length scale between molecular collisions.

Let L_{hydro} be the characteristic length scale of macroscopic motions.

Fluids may be regarded as *continuous fields* if

$$L_{\mathrm{hydro}} \gg \ell_{\mathrm{mpf}}.$$

When this condition holds, the evolution of the macroscopic field may be described by *continuum mechanics*, i.e., partial differential equations.

To make this idea clearer, consider a thought experiment in which we measure the density of a fluid over a length scale ℓ using some particularly sensitive device. We then move the device in the x-direction over a distance of roughly 10ℓ.

Suppose $\ell \sim L_1 \sim \ell_{mpf}$. Then we expect the density to vary greatly in space as in Figure (a) below:

(a)   (b)   (c)
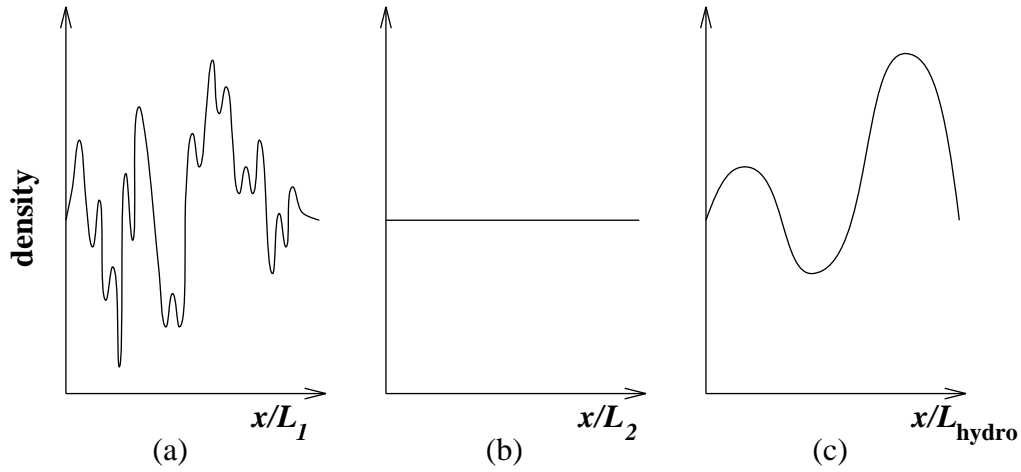
We expect that the fluctuations in (a) should decrease as ℓ increases. (Statistics tells us that these fluctuations should decrease like $1/N^{1/2}$, where $N \propto \ell^3$ is the average number of molecules in a box of size ℓ.)

On the other hand, if $\ell \sim L_{\mathrm{hydro}}$ (see (c)), variations in density should reflect density changes due to macroscopic motions (e.g., a rising hot plume), not merely statistical fluctuations.

Our assumption of a continuum implies that there is an intermediate scale, $\ell \sim L_2$, over which fluctuations are small. Thus the continuum hypothesis implies a *separation of scales* between the molecular scale, $L_1 \sim \ell_{\mathrm{mfp}}$, and the hydrodynamic scale, L_{hydro}.

Thus, rather than dealing with the motion $\sim 10^{23}$ molecules and therefore $\sim 6 \times 10^{23}$ ordinary differential equations of motion (3 equations each for position and momentum), we model the fluid as a continuum.

The motion of the continuum is expressed by *partial differential equations* for evolution of conserved quantities. We begin with the conservation of mass.

9.2 Mass conservation

Let
$$\left.\begin{array}{l} \rho = \text{density} \\ \vec{u} = \text{velocity} \end{array}\right\} \text{ of a macroscopic fluid particle}$$

Consider a volume V of fluid, fixed in space:
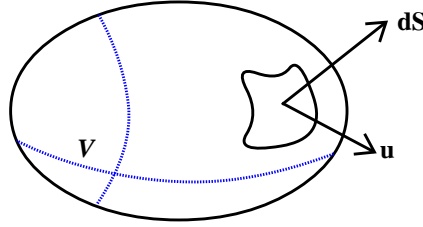
$d\vec{s}$ is an element of the surface, $|d\vec{s}|$ is its area, and it points in the outward normal direction.

$\vec{u}$ is the velocity.

The outward mass flux through the element $d\vec{s}$ is
$$\rho\vec{u} \cdot d\vec{s}.$$

Therefore,
$$\text{rate of mass loss from } V = \int_s \rho\vec{u} \cdot d\vec{s}.$$

The total mass in V is
$$\int_V \rho dv$$

Thus the rate of mass loss may be rewritten as
$$-\frac{d}{dt}\int_V \rho dv = -\int_V \frac{\partial \rho}{\partial t} dv = +\int_s \rho\vec{u} \cdot d\vec{s}$$

Shrinking the volume, we eliminate the integrals and obtain
$$\frac{\partial \rho}{\partial t} = -\lim_{V \to 0}\left[\int \rho\vec{u} \cdot d\vec{s}/V\right].$$

Recall that the RHS above is the definition of the divergence operator. We thus obtain

$$\frac{\partial \rho}{\partial t} = -\vec{\nabla} \cdot (\rho \vec{u})$$

We see that to conserve mass, a net divergence creates a corresponding change in density.

For *incompressible* fluids,

$$\rho \sim \text{constant.}$$

$\Big($This result is not an assumption, but instead derives from the assumption that the Mach number, the square of the ratio of the fluid velocity to the speed of sound, is much less than unity.$\Big)$

Then

$$\vec{\nabla} \cdot \vec{u} = 0.$$

which is the *equation of continuity* for incompressible fluids.

9.3   Momentum conservation

We seek an expression of Newton's second law:

$$\frac{\mathrm{d}}{\mathrm{d}t}(\text{momentum of fluid particle}) = \text{force acting on fluid particle} \qquad (22)$$

9.3.1   Substantial derivative

We first focus on the LHS of (22).

There is a conceptual problem: $\frac{\mathrm{d}}{\mathrm{d}t}$(particle momentum) cannot be given at a fixed location, because

- the momentum field itself changes with respect to time; and

- fluid particle can change its momentum by *flowing* to a place where the velocity is different.

To better understand this problem physically, consider how a scalar property—the temperature T—of a fluid particle changes in time.

A small change δT is produced by a small changes δt in time and δx, δy, δz in the position of the fluid particle:

$$\delta T = \frac{\partial T}{\partial t}\delta t + \frac{\partial T}{\partial x}\delta x + \frac{\partial T}{\partial y}\delta y + \frac{\partial T}{\partial z}\delta z$$

Divide by δt to obtain the rate of change:

$$\frac{\delta T}{\delta t} = \frac{\partial T}{\partial t} + \frac{\partial T}{\partial x}\frac{\delta x}{\delta t} + \frac{\partial T}{\partial y}\frac{\delta y}{\delta t} + \frac{\partial T}{\partial z}\frac{\delta z}{\delta t}$$

In the limit $\delta t \to 0$,

$$\frac{\delta x}{\delta t} \to u_x, \qquad \frac{\delta y}{\delta t} \to u_y, \qquad \frac{\delta z}{\delta t} \to u_z$$

The rate of change of T of a fluid particle is then

$$\begin{aligned} \frac{\mathrm{D}T}{\mathrm{D}t} &= \frac{\partial T}{\partial t} + u_x\frac{\partial T}{\partial x} + u_y\frac{\partial T}{\partial y} + u_z\frac{\partial T}{\partial z} \\[2mm] &= \frac{\partial T}{\partial t} + \vec{u}\cdot\vec{\nabla}T \end{aligned}$$

where

$$\frac{\mathrm{D}}{\mathrm{D}t} = \frac{\partial}{\partial t} + \vec{u}\cdot\vec{\nabla}$$

is the *substantial derivative* or *convective derivative* operator.

Thus we see that the temperature of a fluid particle can change because

- the temperature field changes "in place" (via $\partial/\partial t$); and

- the particle can flow to a position where the temperature is different (via $\vec{u}\cdot\vec{\nabla}$).

Note that the same analysis applies to *vector* fields such as the velocity $\vec{u}$:

$$\frac{\mathrm{D}\vec{u}}{\mathrm{D}t} = \frac{\partial\vec{u}}{\partial t} + (\vec{u}\cdot\vec{\nabla})\vec{u}$$

Therefore the velocity $\vec{u}$ enters $\mathrm{D}\vec{u}/\mathrm{D}t$ in 2 ways:

- $\vec{u}$ changes (in place) as the fluid moves $(\partial/\partial t)$

- $\vec{u}$ governs *how fast* that change occurs $(\vec{u} \cdot \vec{\nabla})$.

This dual role of velocity is the essential nonlinearity of fluid dynamics and thus the cause of turbulent instabilities.

We can now express the rate-of-change of momentum per unit volume (i.e., LHS of (22)):
$$\rho\frac{\mathrm{D}\vec{u}}{\mathrm{D}t} = \rho\frac{\partial\vec{u}}{\partial t} + \rho(\vec{u} \cdot \vec{\nabla})\vec{u}$$
ρ is outside the differential because a fluid particle does not lose mass. Density changes thus mean volume changes, which are irrelevant to the momentum change of that particle. Above we have written the (rate of change of momentum) per unit volume, which need not be equal to the rate of change of (momentum per unit volume).

9.3.2 Forces on fluid particle

To obtain the full dynamical equation, we need the RHS of

$$\rho\frac{\mathrm{D}\vec{u}}{\mathrm{D}t} = \text{ Force acting on fluid particle / unit volume.}$$

These forces are

- body force (i.e., gravity)

- pressure

- viscous friction (internal stresses)

Body force. We represent the externally imposed body force by $\vec{F}$.

Pressure. Fluid flows from high to low pressure. Thus

$$\frac{\text{pressure force}}{\text{unit volume}} = -\frac{\partial p}{\partial x} \quad \text{in 1-D}$$

$$= -\vec{\nabla}p \quad \text{in 3-D}$$

Viscous friction. Viscous stresses are the source of dissipation in fluids. They resist relative movements between fluid particles.

For example, the shear flow
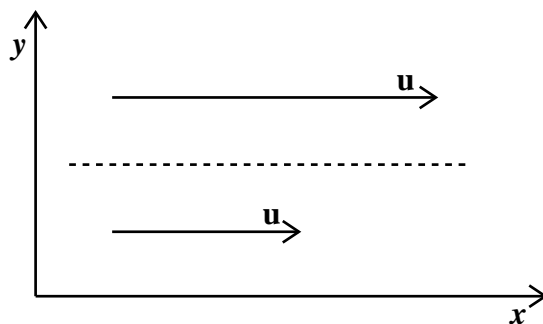
is resisted more by high viscosity fluids than low viscosity fluids.

This resistance derives from molecular motions. (A nice analog is Reif's picture of two mail trains, one initially fast and the other initially slow, that trade mailbags.)

In the simple shear flow above, there is a flux of x-momentum in the y-direction.

In *Newtonian fluids*, this flux, which we call P_{xy}, is proportional to the gradient:

$$P_{xy} = -\eta \frac{\partial u_x}{\partial y}$$

where η is called the dynamic viscosity. η has units of mass/(length $\times$ time).

The shear stress can occur at any orientation. Analogous to the 1-D Newtonian condition above, we define the *viscous momentum flux*

$$P_{ij} = -\eta \frac{\partial u_i}{\partial x_j}.$$

The conservation of momentum requires that the divergence of the momentum flux P_{ij} be balanced by a change in the momentum of a fluid particle. Loosely stated,

$$\frac{\partial(\rho u_i)}{\partial t}\bigg|_{\text{viscous}} = -\vec{\nabla} \cdot P_{ij} = -\sum_j \frac{\partial}{\partial x_j} P_{ij} = \eta \sum_j \frac{\partial^2}{\partial x_j^2} u_i$$

We thus find that

$$\frac{\text{viscous force}}{\text{unit volume}} = \eta \nabla^2 \vec{u}.$$

$\Big($A careful derivation requires consideration of the tensorial relationship between viscous stress and the rate of deformation.$\Big)$

Newton's second law then gives the *Navier-Stokes equation* for incompressible fluids:

$$\underbrace{\rho \frac{\partial \vec{u}}{\partial t} + \rho(\vec{u} \cdot \vec{\nabla})\vec{u}}_{\text{(mass per unit vol)}\times\text{acceleration}} = \underbrace{-\vec{\nabla}p + \eta \nabla^2 \vec{u}}_{\text{stresses on fluid element per unit vol}} + \underbrace{\vec{F}}_{\text{body force per unit vol}}$$

Incompressibility arose from our negelect of compressive forces on fluid elements.

9.4   Nondimensionalization of Navier-Stokes equations

Define the characteristic length scale L and velocity scale U. We obtain the non-dimensional quantities

$$x' = \frac{x}{L}, \quad y' = \frac{y}{L}, \quad z' = \frac{z}{L}$$

$$\vec{u}' = \frac{\vec{u}}{U}, \quad t' = t\frac{U}{L}, \quad p' = \frac{p}{\rho U^2}$$

The dynamical equations (without body force) become

$$\vec{\nabla}' \cdot \vec{u}' = 0$$

$$\frac{\partial \vec{u}'}{\partial t'} + (\vec{u}' \cdot \vec{\nabla}')\vec{u}' = -\vec{\nabla}'p' + \frac{1}{\text{Re}}\nabla'^2 \vec{u}'$$

where
$$\mathrm{Re} = \text{ Reynolds number } = \frac{\rho U L}{\eta}$$
is the *dimensionless* control parameter.

The Reynolds number quantifies the relative importance of the nonlinear term to the viscous term. To see why, note the following dimensional quantities:

$$|\rho \vec{u} \cdot \vec{\nabla} \vec{u}| \ \sim \ \frac{\rho U^2}{L} \qquad \text{nonlinearity}$$

$$|\eta \nabla^2 \vec{u}| \ \sim \ \frac{\eta U}{L^2} \qquad \text{dissipation}$$

Their ratio is
$$\frac{|\rho \vec{u} \cdot \vec{\nabla} \vec{u}|}{|\eta \nabla^2 \vec{u}|} \sim \frac{\rho U L}{\eta} = \text{Reynolds number}$$

High Re is associated with turbulence (i.e., nonlinearities). Low Re is associated with *laminar* or *creeping* flows dominated by viscous friction.

Note that as long as Re remains the same, the dimensional parameters like U and L can change but the the flow (i.e., the equation it solves) does not. This is *dynamical similarity.*

An example is running vs. swimming:

$$\left(\frac{\eta}{\rho} \right)\bigg|_{\text{air}} = 0.15 \text{ cm}^2/\text{sec} \qquad \text{and} \qquad \left(\frac{\eta}{\rho} \right)\bigg|_{\text{water}} = 0.01 \text{ cm}^2/\text{sec}$$

On the other hand, comparing 100 meter world records,

$$U_{\text{run}} \ \sim \ \frac{10^4 \text{ cm}}{10 \text{ sec}} = 10^3 \text{ cm/sec}$$

$$U_{\text{swim}} \ \sim \ \frac{10^4 \text{ cm}}{55 \text{ sec}} \sim 2 \times 10^2 \text{ cm/sec}$$

Taking $L \sim 100$ cm,

$$\mathrm{Re}(\text{swim}) \sim 2 \times 10^4 \qquad \text{and} \qquad \mathrm{Re}(\text{run}) \sim 6 \times 10^3$$

Thus for both swimming and running, Re $\sim 10^4$, well into the turbulent regime. Surprisingly, despite the slower speed of swimming, Re(swim) is somewhat greater.

Another example: bacteria swimming in water is roughly like us swimming in molasses, since the the small size and slow speed of bacteria would correspond to a larger and faster body in a more viscous fluid.

9.5 Rayleigh-Bénard convection

In a thermally expansive fluid, hot fluid rises.

R-B convection concerns the study of the instabilities caused by rising hot fluid and falling cold fluid.

Typically,, fluid is confined between two horizontal, heat-conducting plates:
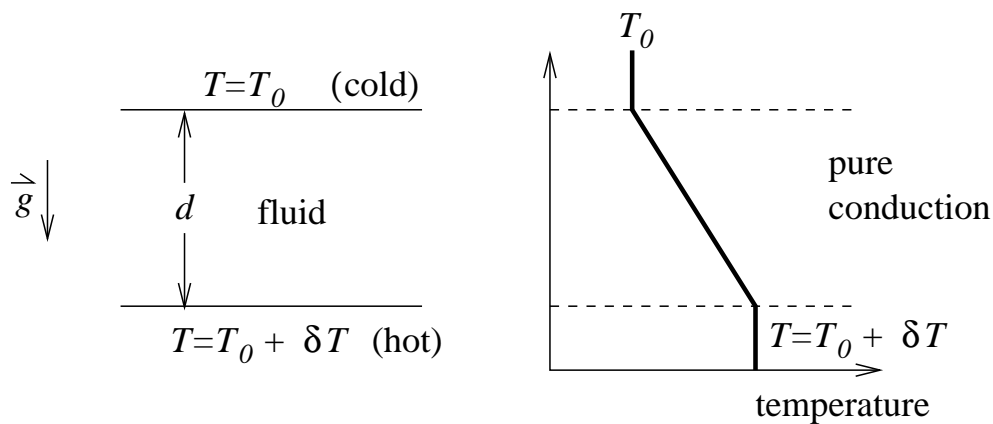
In the absence of convection—the transport of hot fluid *up* and cold fluid *down*—the temperature gradient is constant.

Two cases of interest:

- δT small: no convective motion, due to stabilizing effects of viscous friction.

- δT large: convective motion occurs.

How large is a "large δT"? We seek a non-dimensional formulation.

The following fluid properties are important:

- viscosity
- density
- thermal expansivity
- thermal diffusivity (heat conductivity)

Convection is also determined by

- d, the box size
- δT (of course)

Consider a small displacement of a cold blob downwards and a hot blob upwards:
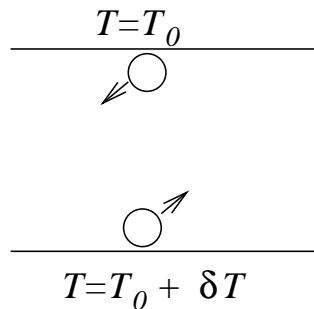
Left undisturbed, buoyancy forces would allow the hot blob to continue rising and cold blob to continue falling.

There are however damping (dissipation) mechanisms:

- diffusion of heat
- viscous friction

Let D_T = thermal diffusivity, which has units

$$[D_T] = \frac{\text{length}^2}{\text{time}}$$

The temperature difference between the two blobs can therefore be maintained at a characteristic time scale

$$\tau_{\text{th}} \sim \frac{d^2}{D_T}$$

We also seek a characteristic time scale for buoyant displacement over the length scale d.

Let

$$\begin{aligned} \rho_0 &= \text{mean density} \\ \Delta\rho &= -\alpha\rho_0\Delta T, \qquad \alpha = \text{expansion coefficient} \end{aligned}$$

Setting $\Delta T = \delta T$,

$$\begin{aligned} \text{buoyancy force density} &= |\vec{g}\Delta\rho| \\ &= g\alpha\rho_0\,\delta T. \end{aligned}$$

Note units:

$$[g\alpha\rho_0\delta T] = \frac{\text{mass}}{(\text{length})^2(\text{time})^2}$$

The buoyancy force is resisted by viscous friction between the two blobs separated by $\sim d$.

The viscous friction between the two blobs diminishes like $1/d$ (since viscous stresses $\propto$ velocity gradients). The rescaled viscosity has units

$$\left[\frac{\eta}{d}\right] = \frac{\text{mass}}{(\text{length})^2(\text{time})}$$

Dividing the rescaled viscosity by the buoyancy force, we obtain the characteristic time τ_m for convective motion:

$$\tau_m \sim \frac{\eta/d}{\text{buoyancy force}} = \frac{\eta}{g\alpha\rho_0\,d\,\delta T}.$$

Convection (sustained motion) occurs if

time for motion $<$ diffusion time for temperature difference

$$\tau_\mathrm{m} \quad < \quad \tau_\mathrm{th}$$

Thus convection requires

$$\frac{\tau_\mathrm{th}}{\tau_\mathrm{m}} > \mathrm{constant}$$

or

$$\frac{\rho_0 g \alpha d^3}{\eta D_T} \delta T \equiv \mathrm{Ra} > \mathrm{constant}$$

Ra is the *Rayleigh number*. A detailed stability calculation reveals that the critical constant is 1708.

Our derivation of the Rayleigh number shows that the convective instability is favored by

- large δT, α, d, ρ_0.

- small η, D_T.

In other words, convection occurs when the buoyancy force $\rho_0 g \alpha d^3 \, \delta T$ exceeds the dissipative effects of viscous drag and heat diffusion.

Note that box height enters Ra as d^3. This means that small increases in box size can have a dramatic effect on Ra.

9.6 Rayleigh-Bénard equations

9.6.1 Dimensional form

We employ the *Boussinesq approximation*: density perturbations affect only the gravitational force.

The momentum equation is therefore the Navier-Stokes equation augmented by the buoyancy force:

$$\frac{\partial \vec{u}}{\partial t} + \vec{u} \cdot \vec{\nabla} \vec{u} = -\frac{1}{\rho_0} \vec{\nabla} p + \nu \nabla^2 \vec{u} - \vec{g} \alpha (T - T_0)$$

Here we have written the *kinematic viscosity*

$$\nu = \eta/\rho_0$$

The mass conservation equation is again

$$\vec{\nabla} \cdot \vec{u} = 0.$$

We now additionally require an equation for the convection and diffusion of heat:

$$\frac{\partial T}{\partial t} + (\vec{u} \cdot \nabla)T = D_T \nabla^2 T.$$

9.6.2 Dimensionless equations

The equations are nondimensionalized using

$$
\begin{aligned}
\text{length scale} &= d \\
\text{time scale} &= d^2/D_T \\
\text{temperature scale} &= \delta T/\text{Ra}.
\end{aligned}
$$

An additional dimensionless parameter arises:

$$\text{Pr} = \text{Prandtl number} = \nu/D_T,$$

which is like the ratio of momentum diffusion to thermal diffusion.

We shall employ the dimensionless temperature fluctuation

$\theta = $ deviation of dimensionless T from the simple conductive gradient

The mass conservation equation is

$$\vec{\nabla} \cdot \vec{u} = 0$$

Momentum conservation yields ($\hat{z}$ is a unit upward normal)

$$\frac{1}{\text{Pr}} \left[\frac{\partial \vec{u}}{\partial t} + \vec{u} \cdot \vec{\nabla} \vec{u} \right] = -\vec{\nabla} p + \theta \hat{z} + \nabla^2 \vec{u}$$

The heat equation becomes

$$\frac{\partial \theta}{\partial t} + \vec{u} \cdot \vec{\nabla} \theta = \mathrm{Ra}(\vec{u} \cdot \hat{z}) + \nabla^2 \theta$$

Note that there are two nonlinear terms:

- $\vec{u} \cdot \vec{\nabla} \vec{u}$

- $\vec{u} \cdot \vec{\nabla} \theta$

Their relative importance depends on Pr:

- small $\mathrm{Pr} \Rightarrow \vec{u} \cdot \vec{\nabla} \vec{u}$ dominates. Instabilities are "hydrodynamic."

- large $\mathrm{Pr} \Rightarrow \vec{u} \cdot \vec{\nabla} \theta$ dominates. Instabilities are thermally induced.

9.6.3 Bifurcation diagram

For $\mathrm{Ra} < \mathrm{Ra}_c$, there is no convection.

For $\mathrm{Ra} > \mathrm{Ra}_c$, but not too large, a regular structure of convection "rolls" forms, with hot fluid rising and cold fluid falling:
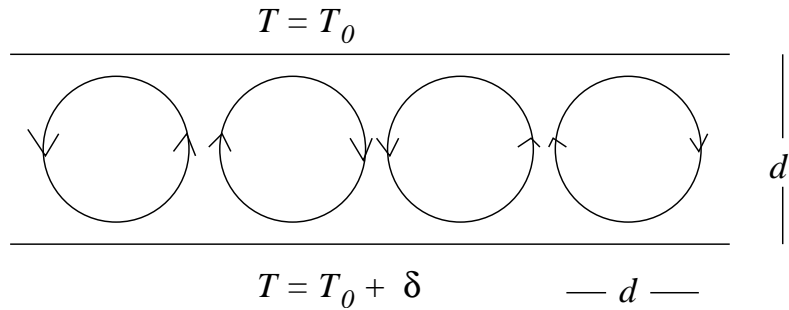
Now imagine placing a probe that measures the vertical component v of velocity, somewhere in the box midway between the top and bottom. A plot of $v(\mathrm{Ra})$ looks like
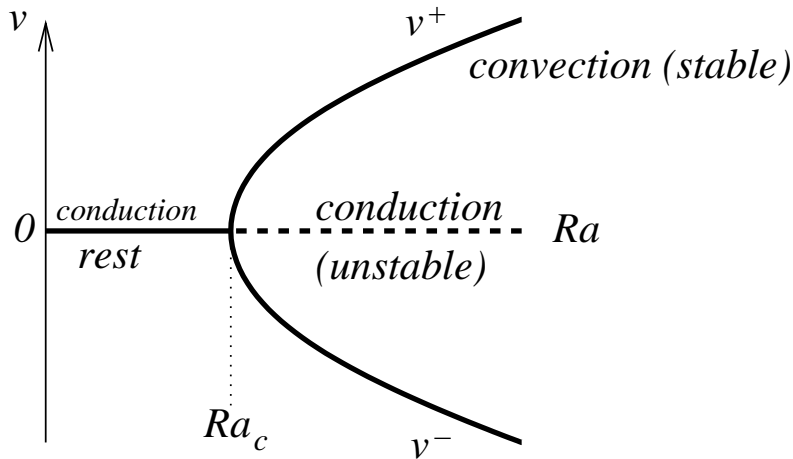
Such a plot is called a *bifurcation* diagram. Here the stable states are bold and the unstable states are dashed.

Note that we cannot know in advance whether the velocity will be up or down. This is called *symmetry breaking.*

9.6.4   Pattern formation

Rayleigh-Bénard convection makes fascinating patterns. Some examples:

- Figures 22.3–8, Tritton.

- Plate 1, Schuster, showing quasiperiodic regime. (The 40 sec period is not precise: note details in upper right are not quite periodic.)

- Plumes: Figure 22.12, Tritton

- Plumes in the wind: Zocchi, Moses, and Libchaber (1990)

- Collective plumes: Zhang et al (1997).

9.6.5   Convection in the Earth

The Earth's radius is about 6378 km. It is layered, with the main divisions being the inner core, outer core, mantle, and crust.

The Earth's crust—the outermost layer—is about 30 km thick.

The mantle ranges from about 30–2900 km.

The mantle is widely thought to be in a state of thermal convection. The source of heat is thought to be the radioactive decay of isotopes of uranium, thorium, and potassium. Another heat source is related to the heat deriving from the gravitational energy dissipated by the formation of the Earth roughly 4.5 Ga.

At long time scales mantle rock is thought to flow like a fluid. However its effective viscosity is the subject of much debate.

One might naively think that the huge viscosity would make the Rayleigh number quite small. Recall, however, that Ra scales like d^3, where d is the "box size". For the mantle, d is nearly 3000 km!!!

Consequently Ra is probably quite high. Current estimates suggest that

$$3 \times 10^6 \lesssim \mathrm{Ra_{mantle}} \lesssim 10^9$$

which corresponds to roughly

$$10^3 \times \mathrm{Ra}_c \lesssim \mathrm{Ra_{mantle}} \lesssim 10^6 \mathrm{Ra}_c$$

The uncertainty derives principally from the viscosity, and its presumed variation by a factor of about 300 with depth.

Some pictures illustrate these ideas:

- Science cover, 26 May 1989

- van der Hilst seismic tomography, showing cold slab descending toward the core-mantle boundary.

- Gurnis (1988) simulation/cartoon showing breakup of continents.

- Zhang and Libchaber (2000) showing floater-plates.

Thermal convection is the "engine" that drives plate tectonics and volcanism.

It turns out that volcanism is, over the long-term, responsible for the CO_2 in the atmosphere, and thus the source of carbon that is fixed by plants. (Weathering reactions remove C from the atmosphere.)

Thus in some sense thermal convection may be said to also sustain life.

That is, without convection, there probably would be no CO_2 in the atmosphere, and therefore we wouldn't be around to discuss it...

10 Introduction to Strange Attractors

Thus far, we have studied only classical attractors such as fixed points and limit cycles. In this lecture we begin our study of *strange attractors*. We emphasize their generic features.

10.1 Dissipation and attraction

Our studies of oscillators have revealed explicitly how forced systems can reach a stationary (yet dynamic) state characterized by an energy balance:

$$\text{average energy supplied} = \text{average energy dissipated}$$

An example is a limit cycle:
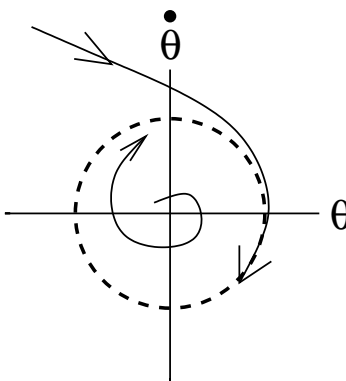
Initital conditions inside or outside the limit cycle always evolve to the limit cycle.

Limit cycles are a specific way in which

$$\text{dissipation} \Rightarrow \text{attraction}.$$

More generally, we have an n-dimensional flow

$$\frac{\mathrm{d}}{\mathrm{d}t}\vec{x}(t) = \vec{F}[\vec{x}(t)], \qquad \vec{x} \in \mathbb{R}^n \tag{23}$$

Assume that the flow $\vec{x}(t)$ is dissipative, with attractor A.

Properties of the attractor A:

- A is invariant with flow (i.e., it does not change with time).

- A is contained within B, the *basin of attraction*. B is that part of phase space from which all initial conditions lead to A as $t \to \infty$:
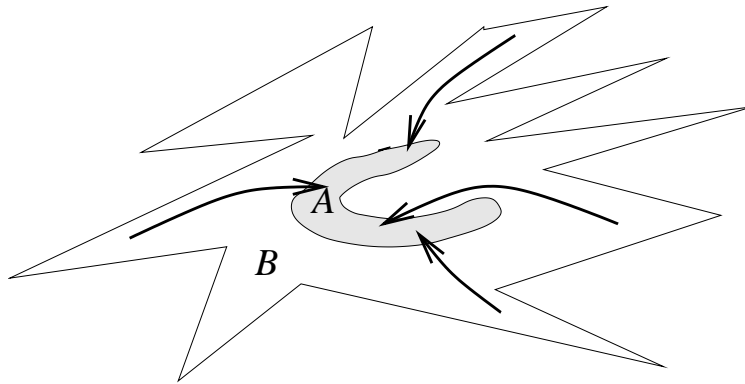
- A has dimension $d < n$.
  Consider, for example, the case of a limit cycle:
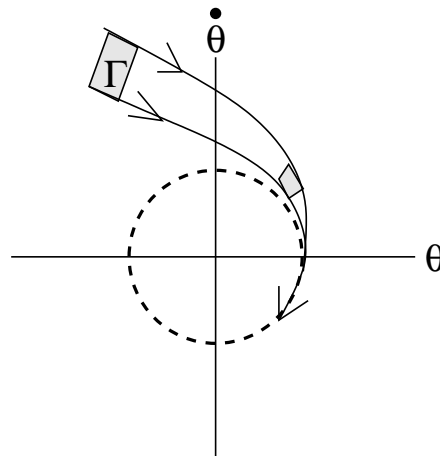
  The surface Γ is reduced by the flow to a line segment on the limit cycle (the attractor). Here

  $$
  \begin{aligned}
  d &= \text{attractor dimension} = 1 \\
  n &= \text{phase-space dimension} = 2.
  \end{aligned}
  $$

  This phenomenon is called **reduction of dimensionality**.

  Consequence: loss of information on initial conditions.

We have already quantified volume contraction. Given an initial volume V evolving according to the flow (23), the Lie derivative tells us that V changes as

$$\frac{1}{V}\frac{\mathrm{d}V}{\mathrm{d}t} = \nabla \cdot \dot{\vec{x}} = \sum_i^n \frac{\partial \dot{x}_i}{\partial x_i}$$

As we showed earlier, dissipation yields volume *contraction*; i.e.,

$$\frac{\mathrm{d}V}{\mathrm{d}t} < 0.$$

Consequently, the attractor cannot have n-dimensional volumes, so $d < n$.

What, then, is the dimension of the attractor?

We proceed by example, by considering the case $d = 2$.

10.2   Attractors with $d = 2$

What happens when d (the dimension of the attractor) is 2?

Assume a quasiperiodic attractor on a torus T^2:
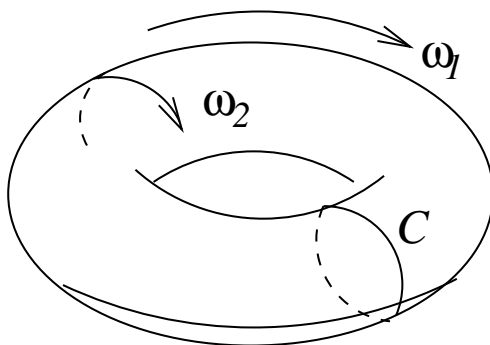
Cut the torus on a small circle C and open it:
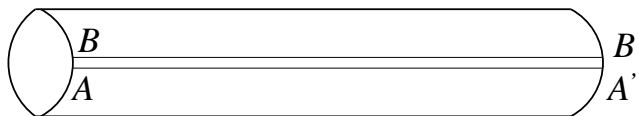
Finally, cut the long way, from A to A', and open it again:
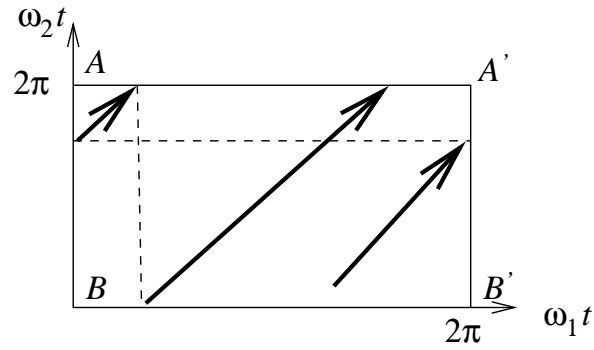
Note the parallel trajectories.

As usual, the quasiperiodic flows are characterized by two cases: ω_1/ω_2 rational or irrational.

- Rational. Consider, e.g., $\omega_1/\omega_2 = 1/3$:
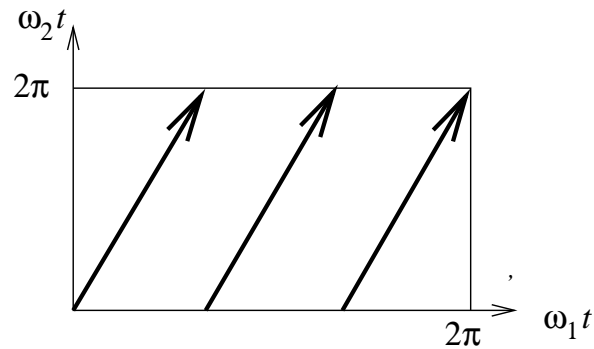
  The trajectory repeats itself exactly every three times around the 2-axis, or each timen around the 1-axis.

- Irrational.
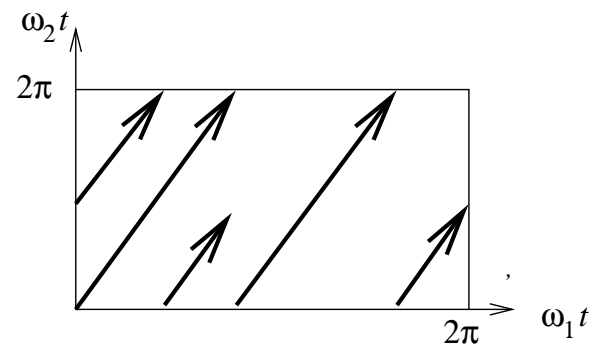
  The trajectories densely fill the plane.

Determinism forbids non-parallel trajectories, because they would cross:
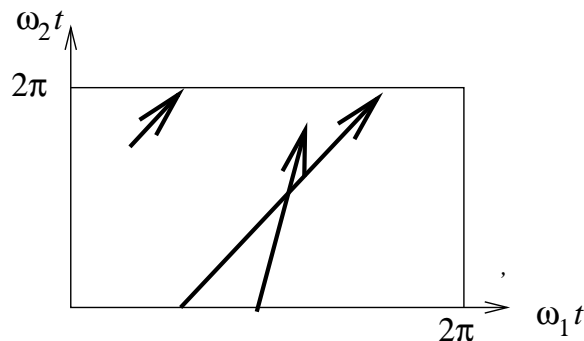
Thus a torus T^2 can only be a periodic or quasiperiodic attractor.

The attractor cannot be aperiodic if $d = 2$.

10.3 Aperiodic attractors

We have already shown that the power spectrum of an aperiodic signal $x(t)$ is continuous:
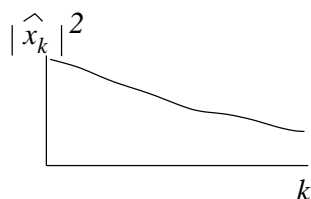
And the autocorrelation $\Psi_m = \langle x_j x_{j+m} \rangle$ has finite width:
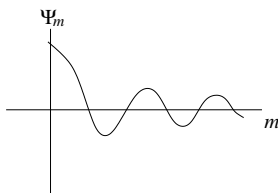
The finite width of Ψ_m implies that knowledge of no finite interval of $x(t)$ allows prediction of all future $x(t)$.

This "unpredictability" is associated with what we call "chaos." We seek, however, a more precise definition of chaos.

On an aperiodic attractor, small differences in initial conditions *on the at-tractor* lead at later times to large differences, *still on the attractor.*

In phase space, trajectories on an aperiodic attractor can diverge, e.g.,
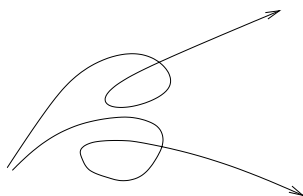
We shall see that the divergence of trajectories is exponential in time.

This phenomenon is called **sensitivity to initial conditions** (SIC). It defini-tively identifies *chaos*, i.e., a chaotic attractor.

Note that, despite the precision of this definition, we are left with an apparent conundrum: simultaneously we have

- attraction, such that trajectories *converge.*

- sensitivity to initial conditions, such that trajectories *diverge.*

The conundrum is solved by noting that trajectories converge *to* the attractor, but diverge *on* the attractor.

Note further that divergence on the attractor implies that the attractor di-mension

$$d > 2,$$

since phase tractories cannot diverge in two dimensions.

Thus we conclude that an aperiodic (chaotic) attractor must have phase space dimension

$$n \geq 3.$$

Assume $n = 3$. How may trajectories converge, but still remain bounded on an attractor?

The trajectories are successively **stretched** (by SIC) and **folded** (thus remaining bounded).

To illustrate these ideas, see

Figures 4.1.9–10, Abraham and Shaw

- Trajectories diverge in plane by spiralling out (stretching).

- Trajectories leave plane.

- Trajectories return to plane (folding), back to center of spiral.

At the same time, we must have volume contraction. One dimension can expand while another contracts, e.g.

Figures 4.3.1, Abraham and Shaw

10.4 Example: Rössler attractor

We proceed to consider stretching and folding in more detail, using the Rössler attractor:

$$\begin{aligned}
\dot{x} &= -y - z \\
\dot{y} &= x + ay \\
\dot{z} &= b + z(x - c)
\end{aligned}$$

where we assume

$$a > 0.$$

Assume z and $\dot{z}$ are small. Then in the x, y plane the system is apprxoximated by

$$\begin{aligned}
\dot{x} &= -y \\
\dot{y} &= x + ay.
\end{aligned}$$

Then

$$\ddot{x} = -\dot{y} = -x + a\dot{x}$$

106

yielding the *negatively damped* oscillator

$$\ddot{x} - a\dot{x} + x = 0.$$

Consequently the trajectories spiral out of the origin.

How is the spreading confined? From the equation for $\dot{z}$, we see that, for small b,

$$x < c \;\; \Rightarrow \;\; \dot{z} < 0$$
$$x > c \;\; \Rightarrow \;\; \dot{z} > 0$$

Thus we expect trajectories to behave as follows:

- Divergence from the origin creates $x > c$.

- $x > c \Rightarrow z$ increases $\Rightarrow x$ decreases.

- Eventually x decreases such that $x < c$.

- Then $x < c \Rightarrow z$ decreases $\Rightarrow$ back in the x, y plane.

- The process repeats.

Thus we have

- *stretching*, from the outward spiral; and

- *folding*, from the feedback of z into x.

A sequence of figures shows how endless divergence can occur in a bounded region:

Figures 4.3.2–4, Abraham and Shaw

Trajectories never close exactly as a surface, but more like filo dough:

Figures 4.4.1–4, Abraham and Shaw

10.5 Conclusion

We arrive at the following conclusions:

- Aperiodic attractors must have

$$d > 2.$$

- Since dissipation contracts volumes,

$$d < n,$$

   where n is the dimension of the phase space.

- Suppose $n = 3$. Then a chaotic attractor must have

$$2 < d < 3.$$

How can $2 < d < 3$? The attractor has a *fractal* dimension.

Chaotic attractors have three properties:

- Attraction
- SIC
- Non-integer fractal dimension.

The combination of these three properties defines a **strange attractor**. The "strangeness" arises not so much from each individual property but their combined presence.

Next we study the most celebrated strange attractor—the *Lorenz attractor*.

11   Lorenz equations

In this lecture we derive the Lorenz equations, and study their behavior.

The equations were first derived by writing a severe, low-order truncation of the equations of R-B convection.

One motivation was to demonstrate SIC for weather systems, and thus point out the impossibility of accurate long-range predictions.

Our derivation emphasizes a simple physical setting to which the Lorenz equations apply, rather than the mathematics of the low-order truncation.

See Strogatz, Ch. 9, for a slightly different view. This lecture derives from Tritton, Physical Fluid Dynamics, 2nd ed. The derivation is originally due to Malkus and Howard.

11.1   Physical problem and parameterization

We consider convection in a vertical loop or torus, i.e., an empty circular tube:
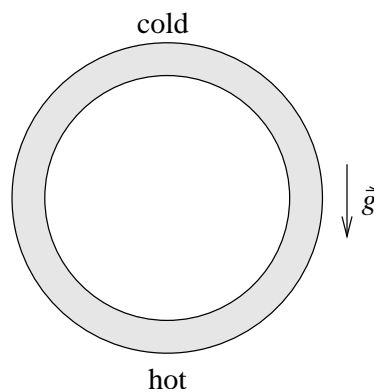
We expect the following possible flows:

- Stable pure conduction (no fluid motion)

- Steady circulation

- Instabilities (unsteady circulation)

The precise setup of the loop:
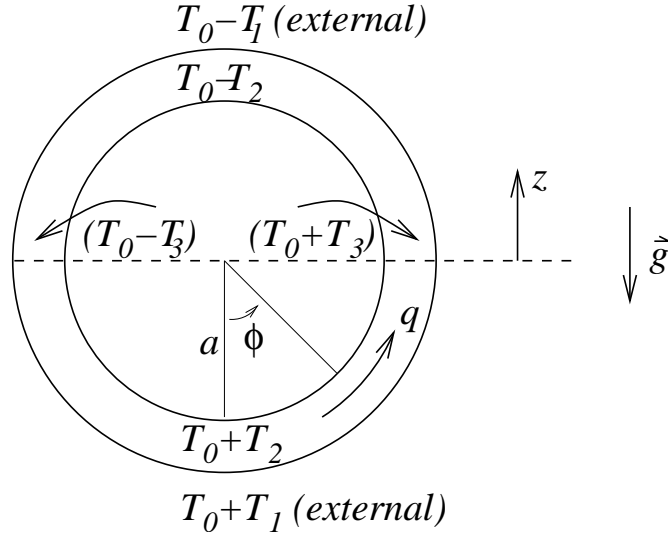
ϕ = position round the loop.

External temperature T_E varies linearly with height:

$$T_E = T_0 - T_1 z/a = T_0 + T_1 \cos\phi \qquad (24)$$

Let a be the radius of the loop. Assume that the tube's inner radius is much smaller than a.

Quantities inside the tube are averaged cross-sectionally:

$$
\begin{aligned}
\text{velocity} \;&=\; q = q(\phi, t) \\
\text{temperature} \;&=\; T = T(\phi, t) \qquad \text{(inside the loop)}
\end{aligned}
$$

As in the Rayleigh-Bénard problem, we employ the Boussinesq approximation (here, roughly like incompressiblity) and therefore assume

$$\frac{\partial \rho}{\partial t} = 0.$$

Thus mass conservation, which would give $\nabla \cdot \vec{u}$ in the full problem, here gives

$$\frac{\partial q}{\partial \phi} = 0. \qquad (25)$$

Thus motions inside the loop are equivalent to a kind of solid-body rotation, such that

$$q = q(t).$$

The temperature $T(\phi)$ could in reality vary with much complexity. Here we assume it depends on only two parameters, T_2 and T_3, such that

$$T - T_0 = T_2 \cos \phi + T_3 \sin \phi. \tag{26}$$

Thus the temperature difference is

- $2T_2$ between the top and bottom, and

- $2T_3$ between sides at mid-height.

T_2 and T_3 vary with time:

$$T_2 = T_2(t), \qquad T_3 = T_3(t)$$

11.2   Equations of motion

11.2.1   Momentum equation

Recall the Navier-Stokes equation for convection:

$$\frac{\partial \vec{u}}{\partial t} + \vec{u} \cdot \vec{\nabla} \vec{u} = -\frac{1}{\rho} \vec{\nabla} p - \vec{g} \alpha \Delta T + \nu \nabla^2 \vec{u}$$

We write the equivalent equation for the loop as

$$\frac{\partial q}{\partial t} = -\frac{1}{\rho a} \frac{\partial p}{\partial \phi} + g\alpha(T - T_0) \sin \phi - \Gamma q. \tag{27}$$

The terms have the following interpretation:

- $\vec{u} \to q$

- $\vec{u} \cdot \nabla \vec{u} \to 0$ since $\partial q / \partial \phi = 0$.

- $\nabla p \to \frac{1}{a}\frac{\partial p}{\partial \phi}$ by transformation to polar coordinates.

- A factor of $\sin\phi$ modifies the buoyancy force $F = g\alpha(T - T_0)$ to obtain the tangential component:
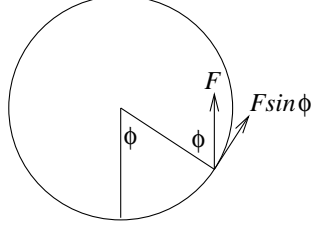
  The sign is chosen so that hot fluid rises.

- Γ is a generalized friction coefficient, corresponding to viscous resistance proportional to velocity.

Now substitute the expression for $T - T_0$ (equation (26)) into the momentum equation (27):

$$\frac{\partial q}{\partial t} = -\frac{1}{\rho a}\frac{\partial p}{\partial \phi} + g\alpha(T_2 \cos\phi + T_3 \sin\phi)\sin\phi - \Gamma q$$

Integrate once round the loop, with respect to ϕ, to eliminate the pressure term:

$$2\pi\frac{\partial q}{\partial t} = g\alpha \int_0^{2\pi}(T_2 \cos\phi \sin\phi + T_3 \sin^2\phi)\mathrm{d}\phi - 2\pi\Gamma q.$$

The pressure term vanished because

$$\int_0^{2\pi}\frac{\partial p}{\partial \phi}\mathrm{d}\phi = 0,$$

i.e., there is no net pressure gradient around the loop.

The integrals are easily evaluated:

$$\int_0^{2\pi}\cos\phi \sin\phi\,\mathrm{d}\phi = \frac{1}{2}\sin^2\phi\Big|_0^{2\pi} = 0$$

and

$$\int_0^{2\pi}\sin^2\phi\,\mathrm{d}\phi = \pi.$$

Then, after dividing by 2π, the momentum equation is

$$\frac{\mathrm{d}q}{\mathrm{d}t} = -\Gamma q + \frac{g\alpha T_3}{2} \tag{28}$$

where we have written $\mathrm{d}q/\mathrm{d}t$ instead of $\partial q/\partial t$ since $\partial q/\partial \phi = 0$.

We see that the motion is driven by the horizontal temperature difference, $2T_3$.

11.2.2 Temperature equation

We now seek an equation for changes in the temperature T. The full temperature equation for convection is

$$\frac{\partial T}{\partial t} + \vec{u} \cdot \vec{\nabla} T = \kappa \nabla^2 T$$

where κ is the heat diffusivity.

We approximate the temperature equation by considering only cross-sectional averages within the loop:

$$\frac{\partial T}{\partial t} + \frac{q}{a}\frac{\partial T}{\partial \phi} = K(T_E - T) \tag{29}$$

Here we have made the following assumptions:

- RHS assumes that heat is transferred through the walls at rate $K(T_{\text{external}} - T_{\text{internal}})$.

- Conduction round the loop is negligible (i.e., no $\nabla^2 T$).

- $\frac{q}{a}\frac{\partial T}{\partial \phi}$ is the product of averages, not (as it should be) the average of a product; i.e., q is taken to be uncorrelated to $\partial T/\partial \phi$.

Recall that we parameterized the internal temperature with two time-dependent variables, $T_2(t)$ and $T_3(t)$. We also have the external temperature T_E varying linearly with height. Specifically:

$$
\begin{aligned}
T_E &= T_0 + T_1 \cos\phi \\
T - T_0 &= T_2 \cos\phi + T_3 \sin\phi
\end{aligned}
$$

Subtracting the second from the first,

$$T_E - T = (T_1 - T_2)\cos\phi - T_3\sin\phi.$$

Substitute this into the temperature equation (29):

$$\frac{\mathrm{d}T_2}{\mathrm{d}t}\cos\phi + \frac{\mathrm{d}T_3}{\mathrm{d}t}\sin\phi - \frac{q}{a}T_2\sin\phi + \frac{q}{a}T_3\cos\phi = K(T_1 - T_2)\cos\phi - KT_3\sin\phi.$$

Here the partial derivatives of T have become total derivatives since T_2 and T_3 vary only with time.

Since the temperature equation must hold for all ϕ, we may separate $\sin\phi$ terms and $\cos\phi$ terms to obtain

$$\sin\phi: \qquad \frac{\mathrm{d}T_3}{\mathrm{d}t} - \frac{qT_2}{a} = -KT_3$$

$$\cos\phi: \qquad \frac{\mathrm{d}T_2}{\mathrm{d}t} + \frac{qT_3}{a} = K(T_1 - T_2)$$

These two equations, together with the momentum equation (28), are the three o.d.e.'s that govern the dynamics.

We proceed to simplify by defining

$$T_4(t) = T_1 - T_2(t),$$

which is the difference between internal and external temperatures at the top and bottom—loosely speaking, the extent to which the system departs from a "conductive equilibrium." Substitution yields

$$\frac{\mathrm{d}T_3}{\mathrm{d}t} = -KT_3 + \frac{qT_1}{a} - \frac{qT_4}{a}$$

$$\frac{\mathrm{d}T_4}{\mathrm{d}t} = -KT_4 + \frac{qT_3}{a}$$

11.3   Dimensionless equations

Define the nondimensional variables

$$X = \frac{q}{aK}, \qquad Y = \frac{g\alpha T_3}{2a\Gamma K}, \qquad Z = \frac{g\alpha T_4}{2a\Gamma K}$$

Here

$$X = \text{dimensionless velocity}$$
$$Y = \text{dimensionless temperature difference between up and down currents}$$
$$Z = \text{dimensionless departure from conductive equilibrium}$$

Finally, define the dimensionless time

$$t' = tK.$$

Drop the prime on t to obtain

$$\frac{dX}{dt} = -PX + PY$$

$$\frac{dY}{dt} = -Y + rX - XZ$$

$$\frac{dZ}{dt} = -Z + XY$$

where the dimensionless parameters r and P are

$$r = \frac{g\alpha T_1}{2a\Gamma K} = \text{``Rayleigh number''}$$

$$P = \frac{\Gamma}{K} = \text{``Prandtl number''}$$

These three equations are essentially the same as Lorenz's celebrated system, but with one difference. Lorenz's system contained a factor b in the last equation:

$$\frac{dZ}{dt} = -\underline{b}Z + XY$$

The parameter b is related to the horizontal wavenumber of the convective motions.

11.4 Stability

We proceed to find the fixed points and evaluate their stability. For now, we remain with the loop equations ($b = 1$).

The fixed points, or steady solutions, occur where

$$\dot{X} = \dot{Y} = \dot{Z} = 0.$$

An obvious fixed point is

$$X^* = Y^* = Z^* = 0,$$

which corresponds, respectively, to a fluid at rest, pure conduction, and a temperature distribution consistent with conductive equilibrium.

Another steady solution is

$$\begin{aligned} X^* &= Y^* = \pm\sqrt{r-1} \\ Z^* &= r-1 \end{aligned}$$

This solution corresponds to flow around the loop at constant speed; the $\pm$ signs arise because the circulation can be in either sense. That $\mathrm{sgn}(X) = \mathrm{sgn}(Y)$ implies that hot fluid rises and cold fluid falls.

Note that the second (convective) solution exists only for $r > 1$. Thus we see that, effectively, $r = \mathrm{Ra}/\mathrm{Ra}_c$, i.e., the convective instability occurs when $\mathrm{Ra} > \mathrm{Ra}_c$.

As usual, we determine the stability of the steady-state solutions by determining the sign of the eigenvalues of the Jacobian.

Let

$$\vec{\phi} = \begin{pmatrix} X \\ Y \\ Z \end{pmatrix}, \qquad \phi^* = \begin{pmatrix} X^* \\ Y^* \\ Z^* \end{pmatrix}$$

Then the Jacobian matrix is

$$\left.\frac{\partial \dot{\phi}_i}{\partial \phi_j}\right|_{\phi^*} = \begin{bmatrix} -P & +P & 0 \\ r - Z^* & -1 & -X^* \\ Y^* & X^* & -1 \end{bmatrix}$$

The eigenvalues σ are found by equating the following determinant to zero:

$$\begin{vmatrix} -(\sigma + P) & P & 0 \\ r - Z^* & -(\sigma + 1) & -X^* \\ Y^* & X^* & -(\sigma + 1) \end{vmatrix} = 0$$

For the steady state without circulation $(X^* = Y^* = Z^* = 0)$, we have

$$\begin{vmatrix} -(\sigma + P) & P & 0 \\ r & -(\sigma + 1) & 0 \\ 0 & 0 & -(\sigma + 1) \end{vmatrix} = 0.$$

This yields

$$-(\sigma + P)(\sigma + 1)^2 + rP(\sigma + 1) = 0$$

or

$$(\sigma + 1)\left[\sigma^2 + \sigma(P + 1) - P(r - 1)\right] = 0.$$

There are three roots:

$$\sigma_1 = -1$$
$$\sigma_{2,3} = \frac{-(P + 1)}{2} \pm \frac{\sqrt{(P + 1)^2 + 4P(r - 1)}}{2}$$

As usual,

$$\text{Re}\{\sigma_1, \sigma_2, \textbf{and } \sigma_3\} < 0 \implies \text{stable}$$
$$\text{Re}\{\sigma_1, \sigma_2, \textbf{or } \sigma_3\} > 0 \implies \text{unstable}$$

Therefore $X^* = Y^* = Z^* = 0$ is

$$\text{stable} \quad \text{for} \quad 0 < r < 1$$
$$\text{unstable} \quad \text{for} \quad r > 1$$

We now calculate the stability of the second fixed point, $X^* = \pm\sqrt{r - 1}$, $Y^* = \pm\sqrt{r - 1}$, $Z^* = r - 1$.

The eigenvalues σ are now the solution of

$$\begin{vmatrix} -(\sigma + P) & P & 0 \\ 1 & -(\sigma + 1) & -S \\ S & S & -(\sigma + 1) \end{vmatrix} = 0, \qquad S = \pm\sqrt{r - 1}.$$

(Explicitly,

$$-(\sigma + p)(\sigma + 1)^2 - Ps^2 - S^2(\sigma + P) + P(\sigma + 1) = 0$$
$$(\sigma + 1)[\sigma^2 + \sigma(P + 1)] + \sigma S^2 + 2PS^2 = 0.)$$

117

The characteristic equation is cubic:

$$\sigma^3 + \sigma^2(P+2) + \sigma(P+r) + 2P(r-1) = 0$$

This equation is of the form

$$\sigma^3 + A\sigma^2 + B\sigma + C = 0 \tag{30}$$

where A, B, and C are all real and positive.

Such an equation has either

- 3 real roots; or

- 1 real root and 2 complex conjugate roots, e.g.,

3 real roots   or   1 real and 2 complex conjugates
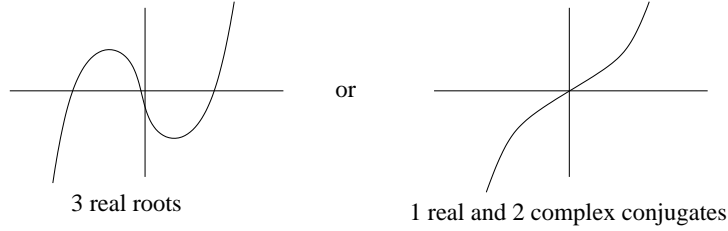
Rearranging equation (30),

$$\sigma \underbrace{(\sigma^2 + B)}_{\text{positive real}} = \underbrace{-A\sigma^2 - C}_{\text{negative real}} < 0.$$

Consequently any real $\sigma < 0$, and we need only consider the complex roots (since only they may yield $\text{Re}\{\sigma\} > 0$).

Let σ_1 be the (negative) real root, and let

$$\sigma_{2,3} = \alpha \pm i\beta.$$

Then

$$(\sigma - \sigma_1)(\sigma - \alpha - i\beta)(\sigma - \alpha + i\beta) = 0$$

and

$$
\begin{aligned}
A &= -(\sigma_1 + 2\alpha) \\
B &= 2\alpha\sigma_1 + \alpha^2 + \beta^2 \\
C &= -\sigma_1(\alpha^2 + \beta^2)
\end{aligned}
$$

A little trick:
$$C - AB = 2\alpha \underbrace{\left[(\sigma_1 + \alpha)^2 + \beta^2\right]}_{\text{positive real}}.$$

Since α is the real part of both complex roots, we have

$$\text{sgn}(\text{Re}\{\sigma_{2,3}\}) = \text{sgn}(\alpha) = \text{sgn}(C - AB).$$

Thus instability occurs for $C - AB > 0$, or

$$2P(r - 1) - (P + 2)(P + r) > 0, .$$

Rearranging,
$$r(2P - P - 2) > 2P + P(P + 2)$$

and we find that instability occurs for

$$r > r_c = \frac{P(P + 4)}{P - 2}.$$

This condition, which exists only for $P > 2$, gives the critical value of r for which steady *circulation* becomes unstable.

Loosely speaking, this is analogous to a transition to turbulence.

Summary: The rest state, $X^* = Y^* = Z^* = 0$, is

$$\begin{aligned}
\text{stable} \quad &\text{for} \quad 0 < r < 1 \\
\text{unstable} \quad &\text{for} \quad r > 1.
\end{aligned}$$

The convective state (steady circulation), $X^* = Y^* = \pm\sqrt{r - 1}$, $Z^* = r - 1$, is

$$\begin{aligned}
\text{stable} \quad &\text{for} \quad 1 < r < r_c \\
\text{unstable} \quad &\text{for} \quad r > r_c.
\end{aligned}$$

What happens for $r > r_c$?

Before addressing that interesting question, we first look at contraction of volumes in phase space.

11.5 Dissipation

We now study the "full" equations, with the parameter b, such that

$$\dot{Z} = -bZ + XY, \qquad b > 0.$$

The rate of volume contraction is given by the Lie derivative

$$\frac{1}{V}\frac{dV}{dt} = \sum_i \frac{\partial \dot{\phi_i}}{\partial \phi_i}, \qquad i = 1, 2, 3, \qquad \phi_1 = X, \phi_2 = Y, \phi_3 = Z.$$

For the Lorenz equations,

$$\frac{\partial \dot{X}}{\partial X} + \frac{\partial \dot{Y}}{\partial Y} + \frac{\partial \dot{Z}}{\partial Z} = -P - 1 - b.$$

Thus

$$\frac{dV}{dt} = -(P + 1 + b)V$$

which may be solved to yield

$$V(t) = V(0)e^{-(P+1+b)t}.$$

The system is clearly dissipative, since $P > 0$ and $b > 0$.

The most common choice of parameters is that chosen by Lorenz

$$P = 10$$
$$b = 8/3 \qquad \text{(corresponding to the first wavenumber to go unstable).}$$

For these parameters,

$$V(t) = V(0)e^{-\frac{41}{3}t}.$$

Thus after 1 time unit, volumes are reduced by a factor of $e^{-\frac{41}{3}} \sim 10^{-6}$. The system is therefore *highly* dissipative.

11.6 Numerical solutions

For the full Lorenz system, instability of the convective state occurs for

$$r > r_c = \frac{P(P + 3 + b)}{P - 1 - b}$$

For P=10, b=8/3, one has

$$r_c = 24.74.$$

In the following examples, $r = 28$.

Time series of the phase-space variables are shown in

Tritton, Fig 24.2, p. 397

- $X(t)$ represents variation of velocity round the loop.

  - Oscillations around each fixed point X_+^* and X_-^* represent variation in speed but the same direction.
  - Change in sign represents change in direction.

- $Y(t)$ represents the temperature difference between up and downggoing currents. Intuitively, we expect some correlation between $X(t)$ and $Y(t)$.

- $Z(t)$ represents the departure from conductive equilibrium. Intuitively, we may expect that pronounced maxima of Z (i.e., overheating) would foreshadow a change in sign of X and Y, i.e., a destabilization of the sense of rotation.

Projection in the Z-Y plane, showing oscillations about the unstable convective fixed points, and flips after maxima of Z:

BPV, Fig. VI.12

A 3-D perspective, the famous "butterfly:"

BPV, Fig. VI.14

Note the system is symmetric, being invariant under the transformation $X \to -X$, $Y \to -Y$, $Z \to Z$.

A slice (i.e., a Poincaré section) through the plane $Z = r - 1$, which contains the convective fixed points:

BPV, Fig. VI.15

- The trajectories lie on roughly straight lines, indicating the attractor dimension $d \simeq 2$.

- These are really closely packed sheets, with (as we shall see) a fractal dimension of 2.06.

- $d \simeq 2$ results from the strong dissipation.

Since $d \simeq 2$, we can construct, as did Lorenz, the first return map

$$z_{k+1} = f(z_k),$$

where z_k is the kth maximum of $Z(t)$. The result is

BPV, Fig. VI.16

(These points intersect the plane $XY - bZ = 0$, which corresponds to $\dot{Z} = 0$.)

The first-return map shows that the dynamics can be approximated by a 1-D map. It also reveals the stability properties of the fixed point $Z = r - 1$:

BPV, Fig. VI.17

Finally, sensitivity to initial conditions is documented by

BPV, Fig. VI.18

11.7 Conclusion

The Lorenz model shows us that the apparent unpredictability of turbulent fluid dynamics is deterministic. Why?

Lorenz's system is much simpler than the Navier-Stokes equations, but it is essentially contained within them.

Because the simpler system exhibits deterministic chaos, surely the Navier-Stokes equations contain sufficient complexity to do so also.

Thus any doubt concerning the deterministic foundation of turbulence, such as assuming that turbulence represents a failure of deterministic equations, is now removed.

A striking conclusion is that only a few (here, three) degrees of freedom are required to exhibit this complexity. Previous explanations of transitions to turbulence (e.g., Landau) had invoked a successive introduction of a large number of degrees of freedom.

12 Hénon attractor

The chaotic phenomena of the Lorenz equations may be exhibited by even simpler systems.

We now consider a discrete-time, 2-D mapping of the plane into itself. The points in $\mathbb{R}^2$ are considered to be the the Poincaré section of a flow in higher dimensions, say, $\mathbb{R}^3$.

The restriction that $d > 2$ for a strange attractor does not apply, because maps generate discrete points; thus the flow is not restricted by continuity (i.e., lines of points need not be parallel).

12.1 The Hénon map

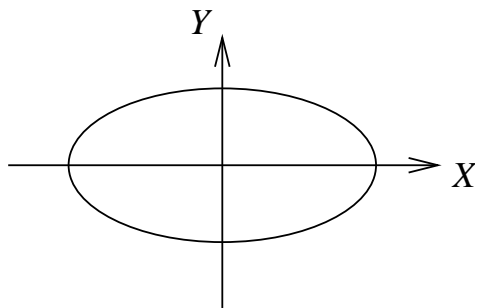The discrete time, 2-D mapping of Hénon is

$$X_{k+1} \;=\; Y_k + 1 - \alpha X_k^2$$

$$Y_{k+1} \;=\; \beta X_k$$

- α controls the nonlinearity.

- β controls the dissipation.

Pictorially, we may consider a set of initial conditions given by an ellipse:

Now bend the elllipse, but preserve the area inside it (we shall soon quantify area preservation):

Map T_1 :
$$\begin{aligned} X' &= X \\ Y' &= 1 - \alpha X^2 + Y \end{aligned}$$
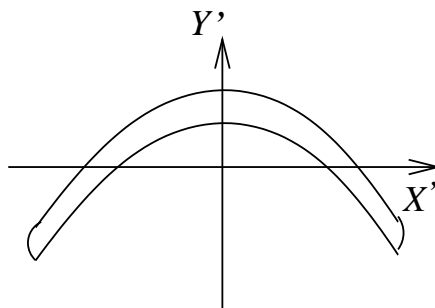
Next, contract in the x-direction $(|\beta| < 1)$

Map T_2 :
$$\begin{aligned} X'' &= \beta X' \\ Y'' &= Y' \end{aligned}$$
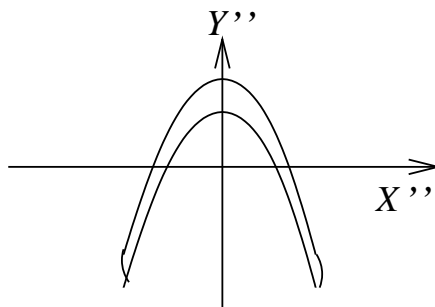
Finally, reorient along the x axis (i.e. flip across the diagonal).

Map T_3 :
$$\begin{aligned} X''' &= Y'' \\ Y''' &= X'' \end{aligned}$$
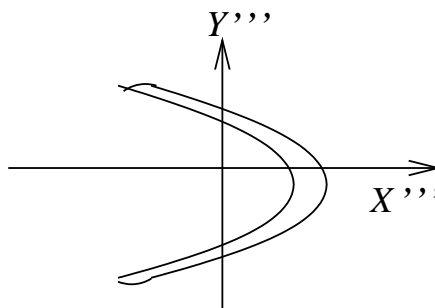
The composite of these maps is

$$T = T_3 \circ T_2 \circ T_1.$$

We readily find that T is the Hénon map:

$$\begin{aligned} X''' &= 1 - \alpha X^2 + Y \\ Y''' &= \beta X \end{aligned}$$

125

12.2 Dissipation

The rate of dissipation may be quantified directly from the mapping via the Jacobian.

We write the map as

$$
\begin{aligned}
X_{k+1} &= f(X_k, Y_k) \\
Y_{k+1} &= g(X_k, Y_k)
\end{aligned}
$$

Infinitesimal changes in mapped quantities as a function of infinitesimal changes in inputs follow

$$
\mathrm{d}f = \frac{\partial f}{\partial X_k} \mathrm{d}X_k + \frac{\partial f}{\partial Y_k} \mathrm{d}Y_k
$$

We may approximate, to first order, the increment ΔX_{k+1} due to small increments $(\Delta X_k, \Delta Y_k)$ as

$$
\Delta X_{k+1} \simeq \frac{\partial f}{\partial X_k} \Delta X_k + \frac{\partial f}{\partial Y_k} \Delta Y_k
$$

When $(\Delta X_k, \Delta Y_k)$ are perturbations about a point (x_0, y_0), we have, to first order,

$$
\begin{bmatrix} \Delta X_{k+1} \\ \Delta Y_{k+1} \end{bmatrix} = \begin{bmatrix} f'_{X_k}(x_0, y_0) & f'_{Y_k}(x_0, y_0) \\ g'_{X_k}(x_0, y_0) & g'_{Y_k}(x_0, y_0) \end{bmatrix} \begin{bmatrix} \Delta X_k \\ \Delta Y_k \end{bmatrix}.
$$

Rewrite simply as

$$
\begin{bmatrix} \Delta x' \\ \Delta y' \end{bmatrix} = \begin{bmatrix} a & b \\ c & d \end{bmatrix} \begin{bmatrix} \Delta x \\ \Delta y \end{bmatrix}.
$$

Geometrically, this system describes the transformation of a rectangular area determined by the vertex $(\Delta x, \Delta y)$ to a parallelogram as follows:
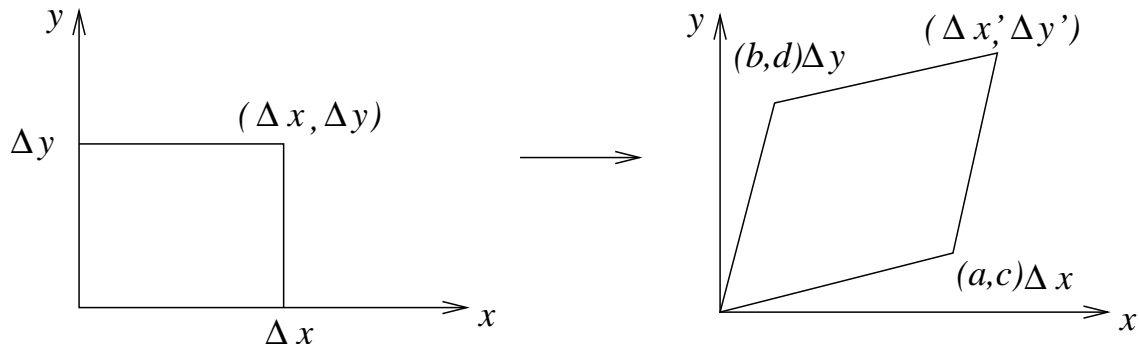
Here we have taken account of transformations like

$$(\Delta x, 0) \rightarrow (a\Delta x, c\Delta x)$$
$$(0, \Delta y) \rightarrow (b\Delta y, d\Delta y)$$

If the original rectangle has unit area (i.e., $\Delta x \Delta y = 1$), then the area of the parallelogram is given by the magnitude of the cross product of (a, c) and (b, d), or, in general, the Jacobian determinant

$$J = \begin{vmatrix} a & b \\ c & d \end{vmatrix} = \begin{vmatrix} \dfrac{\partial X_{k+1}}{\partial X_k} & \dfrac{\partial X_{k+1}}{\partial Y_k} \\ \dfrac{\partial Y_{k+1}}{\partial X_k} & \dfrac{\partial Y_{k+1}}{\partial Y_k} \end{vmatrix}_{(x_0, y_0)}$$

Therefore

$$|J| > 1 \implies \text{dilation}$$
$$|J| < 1 \implies \text{contraction}$$

For the Hénon map,

$$J = \begin{vmatrix} -2\alpha X_k & 1 \\ \beta & 0 \end{vmatrix} = -\beta$$

Thus areas are multipled at each iteration by $|\beta|$.

After k iterations of the map, an initial area a_0 becomes

$$a_k = a_0 |\beta|^k.$$

12.3   Numerical simulations

Hénon chose $\alpha = 1.4$, $\beta = 0.3$. The dissipation is thus considerably less than the factor of 10^{-6} in the Lorenz model.

An illustration of the attractor is given by

BPV, Figure VI.19

Numerical simulations show the basin of attraction to be quite complex.

Sensitivity to initial conditions is confirmed by

BPV, Figure VI.20

The weak dissipation allows one to see the fractal structure induced by the repetitive folding

BPV, Figure VI.21

Note the apparent scale-invariance: at each magnification of scale, we see that the upper line is composed of 3 separate lines.

The fractal dimension $D = 1.26$. (We shall soon discuss how this is computed.)

The action of the Hénon map *near* the attractor is evident in the deformation of a small circle of initial conditions:

BPV, Figure VI.22

At the scale of the attractor we can see the combined effects of *stretching* and *folding*:

BPV, Figure VI.23

13 Experimental attractors

In this brief lecture we show examples of strange attractors found in experiments.

13.1 Rayleigh-Bénard convection

BPV, Figure VI.25

Two dynamical variables, (ΔT) and $(\Delta T)'$, represent time-dependent thermal gradients measured measured by the refraction of light, inside the convecting system.

A 3-D phase space is defined by the coordinates

$$(\Delta T), (\dot{\Delta T}), \text{ and } (\Delta T)'.$$

The Poincaré section in the plane $(\Delta T), (\dot{\Delta T})$ is obtained by strobing the system at the dominant frequency of the fluctuations of one of the dynamical variables.

Like the Hénon attractor, the points are arranged in a "complex but well-defined structure" (BPV, p. 137).

13.2 Belousov-Zhabotinsky reaction

See Strogatz, Section 8.3.

The B-Z reaction is a particularly well studied chemical reaction that is of interest for

- dynamics, because it is oscillatory; and
- pattern formation and nonlinear waves.

An example of the pattern formation is

Strogatz, Plate 1, Section 8.3

For us the dynamical aspects are of greater interest. This chemical reaction, like many others, can be envisioned as a flux of reactants into a reactor, and a flux of products out of the reactor:
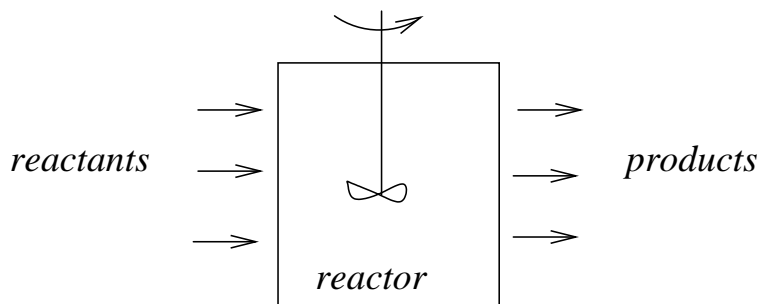
Nonlinearities arise from chemical reactions like

$$A + B \rightarrow C$$

which yield terms like

$$\frac{\mathrm{d}C}{\mathrm{d}t} = AB$$

The control parameter is typically the reactant flux.

The dynamical variable $X(t)$ measures the concentration of a particular chemical species within the reactor.

Phase portraits are obtained in the 3-D phase space formed by

$$X(t), X(t + \tau), X(t + 2\tau).$$

The periodic regime (limit cycle) is evident in the 2-D projection given by

BPV, Figure VI.26

The chaotic regime is evident in the 2-D projection given by

BPV, Figure VI.27

A Poincaré section reveals evidence of strong dissipation, as seen in a plot of intersections with a plane perpendicular to $X(t), X(t + \tau)$:

BPV, Figure VI.28

The straightness of the line is insignificant, but its thinness indicates strong dissipation.

Due to dissipation, a nice 1-D first-return map can be formed by plotting X_{k+1} vs. X_k, where X_k is the kth observation of $X(t)$:

BPV, Figure VI.29a

That all the points essentially lie on a simple curve implies *deterministic order* in the system.

Attraction is demonstrated by inducing a small perturbation and then observing the re-establishment of the first return map:

BPV, Figure VI.29b

Sensitivity to initial conditions is observedby plotting the distribution of points that results after passage close to the same point:

BPV, Figure VI.30

Stretching and folding may also be observed. Plotting the data with a different choice of τ:

BPV, Figure VI.31

Nine different slices through the system reveal stretching (from 9 to 1) and folding (between 2 and 8):

BPV, Figure VI.32

14 Fractals

We now proceed to quantify the "strangeness" of strange attractors. There are two processes of interest, each associated with a measurable quantity:

- sensitivity to initial conditions, quantified by Lyaponov exponents.

- repetitive folding of attractors, quantified by the fractal dimension.

Now we consider fractals, and defer Lyaponov exponents to the next lecture.

We shall see that the fractal dimension can be associated with the effective number of degrees of freedom that are "excited" by the dynamics, e.g.,

- the number of independent variables;

- the number of oscillatory modes; or

- the number of peaks in the power spectrum

14.1 Definition

Consider an attractor A formed by a set of points in a p-dimensional space:
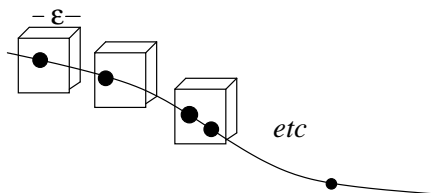
We contain each point within a (hyper)-cube of linear dimension ε.

Let $N(\varepsilon)$ = smallest number of cubes of size ε needed to cover A.

Then if

$$N(\varepsilon) = C\varepsilon^{-D}, \qquad \text{as } \varepsilon \to 0, \qquad C = \text{const.}$$

then D is called the *fractal* (or *Hausdorf*) dimension.

Solve for D (in the limit $\varepsilon \to 0$):

$$D = \frac{\ln N(\varepsilon) - \ln C}{\ln(1/\varepsilon)}.$$

Since $\ln C / \ln(1/\varepsilon) \to 0$ as $\varepsilon \to 0$, we obtain the formal definition

$$D = \lim_{\varepsilon \to 0} \frac{\ln N(\varepsilon)}{\ln(1/\varepsilon)}.$$

14.2   Examples

Suppose A is a line segment of length L:

$$\underbrace{\rule{5cm}{0.4pt}}_{L}$$
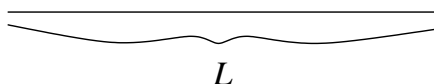
Then the "boxes" that cover A are just line segments of length ε, and it is obvious that

$$N(\varepsilon) = L\varepsilon^{-1} \implies D = 1.$$

Next suppose A is a surface or area S. Then

$$N(\varepsilon) = S\varepsilon^{-2} \implies D = 2.$$

But we have yet to learn anything from D.

Consider instead the Cantor set. Start with a unit line segment:

$$\overline{}$$
0   *1*
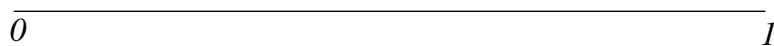
The successively remove the middle third:

0   *1/3*   *2/3*   *1*

   1/9   *2/9*

etc   *etc*

Note that the structure is *scale-invariant*: from far away, you see the middle 1/3 missing; closer up, you see a different middle 1/3 missing.

The effect is visually similar to that seen in the Lorenz, Hénon, and Rössler attractors.

The fractal dimension of the Cantor set is easily calculated from the definition of D:

$$\text{Obviously,} \qquad N\left(\varepsilon = \frac{1}{3}\right) = 2$$

$$\text{Then} \qquad N\left(\varepsilon = \frac{1}{9}\right) = 4$$

$$N\left(\frac{1}{27}\right) = 8\ldots$$

Thus

$$N\left(\frac{1}{3^m}\right) = 2^m.$$

Taking $\varepsilon = 1/3$ and using the definition of D,

$$D = \lim_{m \to \infty} \frac{\ln 2^m}{\ln 3^m} = \frac{\ln 2}{\ln 3} \simeq 0.63$$

14.3 Correlation dimension ν

We proceed now to an alternative procedure for the calculation of the fractal dimension, which offers additional (physical) insight.

Rather than calculating the fractal dimension via its definition, we calculate the *correlation dimension ν*.

We shall show that $\nu \leq D$. But first we define it.

14.3.1 Definition

Consider a set of points distributed on a plane.

Let $N(r) =$ number of points located inside a circle of radius r.

Assume the points are uniformly distributed on a curve like
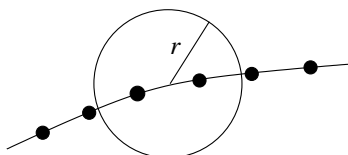
For r sufficiently small compared to the curvature of the curve, we have

$$N(r) \propto r$$

or

$$N(r) \propto r^\nu, \qquad \nu = 1.$$

Now assume the points are uniformly distributed along a surface in two dimensions:

Now

$$N(r) \propto r^2 \implies \nu = 2.$$

Next, reconsider the Cantor set:

We expect that $N(r)$ will grow more slowly than r.

Indeed, calculations show that $\nu \simeq 0.63 = D$, just as before.

14.3.2 Computation

Our implicit definition of ν is clearly generalized by considering

- an attractor in a p-dimensional space, and

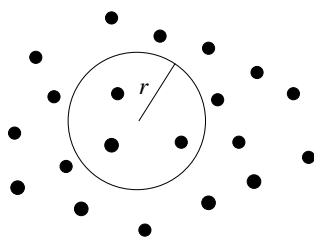- $N(r)$ = number of points in a p-dimensional hypersphere of radius r.

For a time series $x(t)$, we reconstruct a p-dimensional phase space with the coordinates

$$x(t), x(t + \tau), x(t + 2\tau), \ldots x(t + (p - 1)\tau) = \vec{x}(t).$$

Suppose there are m points on the attractor. We quantify the spatial correlation of these points by defining

$$C(r) = \lim_{m \to \infty} \frac{1}{m^2} \left(\text{number of pairs } i, j \text{ for which } |\vec{x}_i - \vec{x}_j| < r\right).$$

More formally,

$$C(r) = \lim_{m \to \infty} \frac{1}{m^2} \sum_i^m \sum_j^m H(r - |\vec{x}_i - \vec{x}_j|)$$

where

$$H(x) = \begin{cases} 1 & x > 0 \\ 0 & \text{else.} \end{cases}$$

The summation is performed by centering hyperspheres on *each* of the m points.

In practice, one *embeds* the signal $x(t)$ in a phase space of dimension p, for

$$p = 2, 3, 4, 5, \ldots$$

p is called the **embedding dimension**.

For each p, we calculate $C(r)$. Then, assuming

$$C(r) = r^\nu$$

we plot $\log C$ vs. $\log r$ and estimating the slope ν:
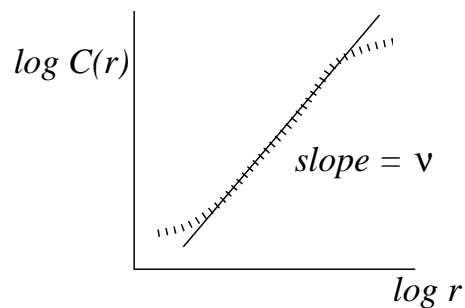
Consider the example of white noise. Then $x(t)$ is a series of uncorrelated random numbers, and we expect

$$C(r) \propto r^p, \qquad p = \text{embedding dimension.}$$

Graphically, one expect a series of plots like
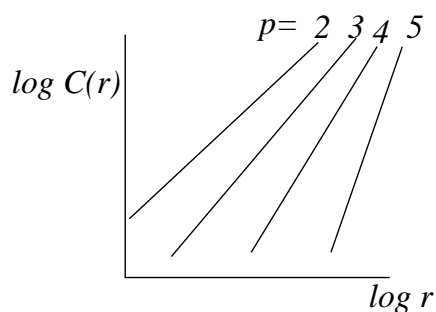
Here

$$\nu(p) = p,$$

a consequence of the fact that white noise has as many degrees of freedom (i.e., independent "modes") as there are data points.

Consider instead $X(t) = $ periodic function, i.e., a limit cycle, with only one fundamental frequency.

Then the attractor looks like

Provided that r is sufficiently smaller than the curvature of the limit cycle, we expect

$$C(r) \propto r^1, \qquad \text{for } p = 2, 3, 4, \ldots$$

Graphically, we obtain
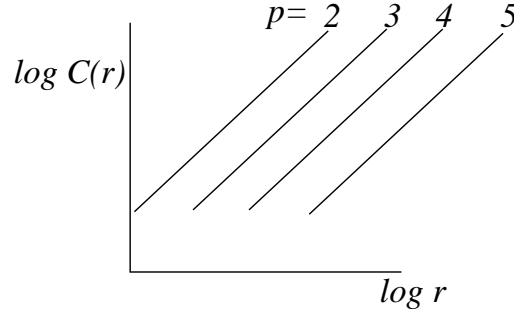
and therefore

$$\nu(p) = 1, \qquad \text{independent of } p.$$

We conclude that ν measures something related to the "number of degrees of freedom" needed to parameterize an attractor.

Specifically, suppose a dynamical regime has n oscillatory modes. The attractor is then a torus T^n, and we expect

$$C(r) \propto r^n.$$

Thus

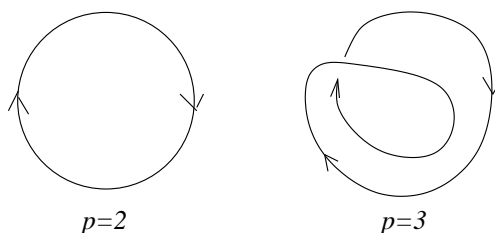$$p \leq n \implies C(r) \propto r^p$$

and

$$p > n \implies C(r) \propto r^n, \qquad \text{independent of } p.$$

Conclusion: If, for embedding dimensions $p \geq p_0$, ν is independent of p, then ν is the number of degrees of freedom *excited* by the system.

This conclusion provides for an appealing conjecture: since white noise gives

$$\nu(p) = p,$$

ν independent of p (and reasonably small) implies that the signal is deterministic, and characterizable by $\sim\nu$ variables.

138

(There are some practical limitations:

- r must be small compared to the attractor size.

- r and m must be large enough for reasonable statistics.)

14.4 Relationship of ν to D

$\big($Grassberger and Procaccia, Physica **9D**, 183 (1983)$\big)$

The correlation dimension is not strictly the same as the fractal dimension, however it can be. We now derive their mathematical relation.

Suppose we cover an attractor A with $N(r)$ hypercubes of size r.

If the points are *uniformly* distributed on A, the probability that a point falls into the ith hypercube is
$$p_i = 1/N(r).$$
By definition, for an attractor containing m points,

$$C(r) = \lim_{m \to \infty} \frac{1}{m^2} \sum_i^m \sum_j^m H(r - |\vec{x}_i - \vec{x}_j|), \qquad H(x) = \begin{cases} 1 & x > 0 \\ 0 & \text{else} \end{cases}$$

$C(r)$ measures the number of pairs of points within a distance r of each other. In a box of size r, there are on average mp_i points, all within the range r. Therefore, within a factor of $O(1)$ (i.e., ignoring box boundaries and factors of two arising from counting pairs twice),

$$C(r) \simeq \frac{1}{m^2} \sum_{i=1}^{N(r)} (mp_i)^2$$

$$= \sum_{i=1}^{N(r)} p_i^2$$

Then, using angle brackets to represent mean quantities, we have, from Schwartz's inequality,

$$C(r) = N(r) \langle p_i^2 \rangle \geq N(r) \langle p_i \rangle^2 = \frac{1}{N(r)}.$$

If the attractor has fractal dimension D, then

$$N(r) \propto r^{-D}, \qquad r \to 0.$$

The definition of the correlation dimension ν, on the other hand, gives

$$C(r) \propto r^{\nu}.$$

Substituting these relations into both sides of the inequality, we find

$$r^{\nu} \geq r^{D}$$

Thus as $r \to 0$, we see that
$$\nu \leq D$$

The equality is obtained when $\langle p_i^2 \rangle = \langle p_i \rangle^2$.

Thus $\nu < D$ results from non-uniformity of points on the attractor.

15   Lyapunov exponents

Whereas fractals quantify the geometry of strange attractors, Lyaponov exponents quantify the sensitivity to initial conditions that is, in effect, their most salient feature.

In this lecture we point broadly sketch some of the mathematical issues concerning Lyaponov exponents. We also briefly describe how they are computed. We then conclude with a description of a simple model that shows how both fractals and Lyaponov exponents manifest themselves in a simple model.

15.1   Diverging trajectories

Lyapunov exponents measure the rate of divergence of trajectories on an attractor.

Consider a flow $\vec{\phi}(t)$ in phase space, given by

$$\frac{\mathrm{d}\phi}{\mathrm{d}t} = \vec{F}(\vec{\phi})$$

If instead of initiating the flow at $\vec{\phi}(0)$, it is initiated at $\vec{\phi}(0) + \varepsilon(0)$, sensitivity to initial conditions would produce a divergent trajectory:
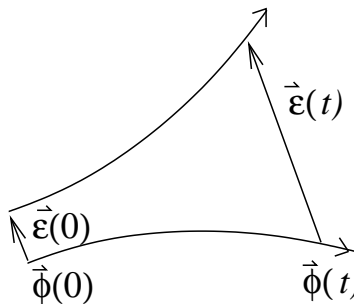
Here $|\vec{\varepsilon}|$ grows with time. To the first order,

$$\frac{\mathrm{d}(\vec{\phi} + \vec{\varepsilon})}{\mathrm{d}t} \simeq \vec{F}(\vec{\phi}) + M(t)\,\vec{\varepsilon}$$

where

$$M_{ij}(t) = \left.\frac{\partial F_i}{\partial \phi_j}\right|_{\vec{\phi}(t)}.$$

We thus find that

$$\frac{\mathrm{d}\vec{\varepsilon}}{\mathrm{d}t} = M(t)\,\vec{\varepsilon}. \qquad (31)$$

Consider the example of the Lorenz model. The Jacobian M is given by

$$M(t) = \begin{bmatrix} -P & P & 0 \\ -Z(t) + r & -1 & -X(t) \\ Y(t) & X(t) & -b \end{bmatrix}.$$

We cannot solve for $\vec{\varepsilon}$ because of the unknown time dependence of $M(t)$. However one may numerically solve for $\vec{\phi}(t)$, and thus $\vec{\varepsilon}(t)$, to obtain (formally)

$$\vec{\varepsilon}(t) = L(t)\,\vec{\varepsilon}(0).$$

15.2 Example 1: M independent of time

Consider a simple 3-D example in which M is time-independent.

Assume additionally that the phase space coordinates correspond to M's eigenvectors.

Then M is diagonal and

$$L(t) = \begin{bmatrix} e^{\lambda_1 t} & 0 & 0 \\ 0 & e^{\lambda_2 t} & 0 \\ 0 & 0 & e^{\lambda_3 t} \end{bmatrix}$$

where the λ_i are the eigenvalues of M. $\big($Recall that if $\dot{\vec{\varepsilon}} = M\vec{\varepsilon}$, then $\vec{\varepsilon}(t) = e^{Mt}\vec{\varepsilon}(0)$, where, in the coordinate system of the eigenvectors, $e^{Mt} = L(t)$.$\big)$

As t increases, the eigenvalue with the largest real part dominates the flow $\vec{\varepsilon}(t)$.

To express this formally, let L^* be the conjugate (Hermitian) transpose of L, i.e.

$$L^*_{ij} = L_{ji}.$$

Also let
$$\mathrm{Tr}(L) = \text{diagonal sum} \ = \sum_{i=j} L_{ij}.$$

Then
$$\mathrm{Tr}[L^*(t)L(t)] = e^{(\lambda_1 + \lambda_1^*)t} + e^{(\lambda_2 + \lambda_2^*)t} + e^{(\lambda_3 + \lambda_3^*)t}$$

Define
$$\overline{\lambda} = \lim_{t \to \infty} \frac{1}{2t} \ln \left(\mathrm{Tr}[L^*(t)L(t)] \right)$$

$\overline{\lambda}$ is the *largest Lyapunov exponent*. Its sign is crucial:
$$\overline{\lambda} < 0 \implies \varepsilon(t) \text{ decays exponentially}$$
$$\overline{\lambda} > 0 \implies \varepsilon(t) \text{ grows exponentially.}$$

15.3 Example 2: Time-dependent eigenvalues

Now suppose that $M(t)$ varies with time in such a way that only its eigenvalues, but not its eigenvectors, vary.

Let
$$\vec{\phi} = \begin{bmatrix} X(t) \\ Y(t) \\ Z(t) \end{bmatrix}$$
and consider small displacements $\delta X(t), \delta Y(t), \delta Z(t)$ in the reference frame of the eigenvectors.

Then, analogous to equation (31), and again assuming that phase space coordinates correspond to M's eigenvectors,
$$\begin{bmatrix} \delta \dot{X}(t) \\ \delta \dot{Y}(t) \\ \delta \dot{Z}(t) \end{bmatrix} = \begin{bmatrix} A[\phi(t)] & 0 & 0 \\ 0 & B[\phi(t)] & 0 \\ 0 & 0 & C[\phi(t)] \end{bmatrix} \begin{bmatrix} \delta X(t) \\ \delta Y(t) \\ \delta Z(t) \end{bmatrix}.$$
Here A, B, C are the time-dependent eigenvalues (assumed to be real).

The solution for $\delta X(t)$ is
$$\delta X(t) = \delta X(0) \, \exp \left[\int_0^t \mathrm{d}t' A[\phi(t')] \right]$$

Rearranging and dividing by t,

$$\frac{1}{t} \ln \left| \frac{\delta X(t)}{\delta X(0)} \right| = \frac{1}{t} \int_0^t dt' A[\phi(t')]$$

The RHS represents the time-average of the eigenvalue A. We assume that for sufficiently long times this average is equivalent to an average of A for all possible flows ϕ evaluated at the same time.

In other words, we assume that the flow is *ergodic*.

We denote this average by angle brackets:

$$\langle A \rangle = \phi\text{-average of } A[\phi(t)]$$

$$= \text{time-average of } A[\phi(t)]$$

$$= \lim_{t \to \infty} \frac{1}{t} \int_0^t dt' A[\phi(t')]$$

$$= \lim_{t \to \infty} \frac{1}{t} \ln \left| \frac{\delta X(t)}{\delta X(0)} \right|$$

$\langle A \rangle$ is one of the three Lyapunov exponents for $\phi(t)$.

More sophisticated analyses show that the theory sketched above applies to the general case in which both eigenvectors and eigenvalues vary with time.

15.4 Numerical evaluation
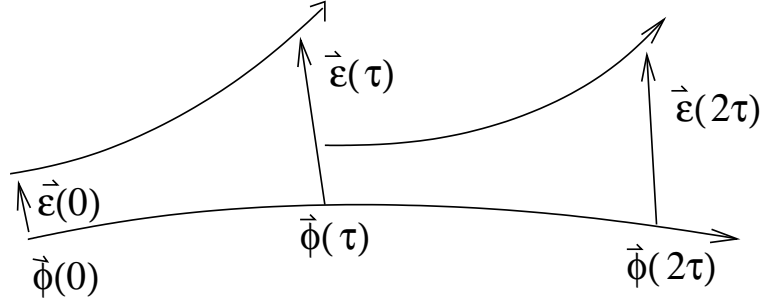
Lyaponov exponents are almost always evaluated numerically.

The most obvious method is the one used in the problem sets: For some $\vec{\varepsilon}(0)$, numerically evaluate $\vec{\varepsilon}(t)$, and then find $\overline{\lambda}$ such that

$$|\vec{\varepsilon}(t)| \simeq |\vec{\varepsilon}(0)| e^{\overline{\lambda} t}.$$

This corresponds to the definition of $\langle A \rangle$ above.

A better method avoids saturation at the size of the attractor by successively averaging small changes over the same trajectory:

Here $\vec{\varepsilon}$ is renormalized at each step such that

$$\vec{\varepsilon}(\tau) \;=\; \vec{\varepsilon}(0)e^{\gamma_1\tau}$$

$$\vec{\varepsilon}(2\tau) \;=\; \frac{\vec{\varepsilon}(\tau)}{|\vec{\varepsilon}(\tau)|}e^{\gamma_2\tau}$$

The largest Lyaponov exponent is given by the long-time average:

$$\overline{\lambda} = \lim_{n\to\infty}\frac{1}{n}\sum_{i=1}^{n}\gamma_i = \lim_{n\to\infty}\frac{1}{n\tau}\sum_{i}\ln|\vec{\varepsilon}(i\tau)|$$

Experimental data poses greater challenges, because generally we have only a single time series $X(t)$.

One way is to compare two intervals on $X(t)$, say

$$[t_1, t_2] \qquad \text{and} \qquad [t_1', t_2'],$$

where $X(t)$ is nearly the same on both intervals.

Then the comparison of $X(t)$ beyond t_2 and t_2' may yield the largest Lyaponov exponent.

Another way is to reconstruct phase space by, say, the method of delays. Then all trajectories that pass near a certain point may be compared to see the rate at which they diverge.

15.5 Lyaponov exponents and attractors in 3-D

Consider an attractor in a 3-D phase space. There are 3 Lyaponov exponents.

Their signs depend on the type of attractor:

Type	Signs of Lyapunov exponents
Fixed point	$(-,-,-)$
Limit cycle	$(-,-,0)$
Torus T^2	$(-,0,0)$
Strange attractor	$(-,0,+)$

If the attractor is a fixed point, all three exponents are negative.

If it is a limit cycle with one frequency, only two are negative, and the third is zero. The zero-exponent corresponds to the direction of flow—which can neither be expanding nor contracting.

Of the other cases in the table below, the most interesting is that of a strange attractor:

- The largest exponent is, by definition, positive.

- There must also be a zero-exponent corresponding to the flow direction.

- The smallest exponent must be negative—and of greater magnitude than the largest, since volumes must be contracting.

15.6 Smale's horseshoe attractor
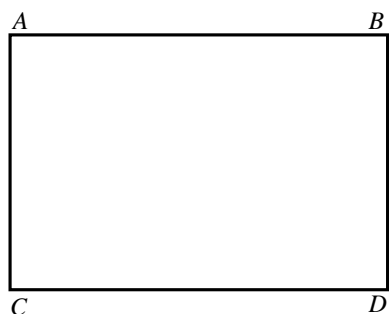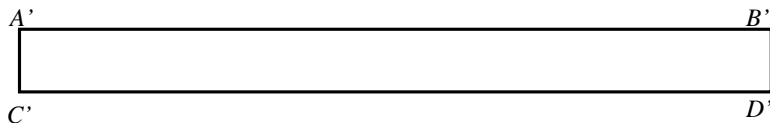
We have seen that

- Lyaponov exponents measure "stretching."
- Fractal dimensions measure "folding."

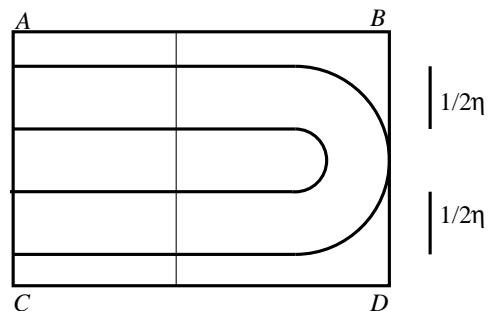Smale's *horseshoe attractor* exemplifies both, and allows easy quantification.
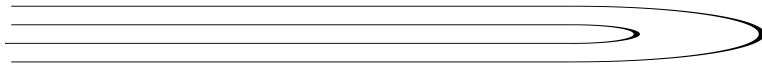
Start with a rectangle:

Stretch by a factor of 2; squash by a factor of $1/(2\eta)$, $\eta > 1$:

Now fold like a horseshoe and put back in $ABCD$:

Now iterate the process. Stretch and squash:

Fold and place back in $ABCD$:
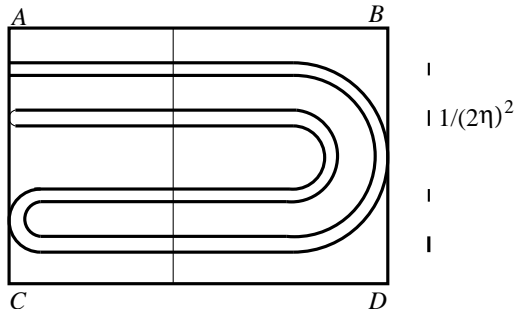
Each dimension is successively scaled by its own multiplier, called a *Lyaponov number*:

$$\begin{aligned}
\Lambda_1 &= 2 & (x-\text{stretch}) \\
\Lambda_2 &= \frac{1}{2\eta} & (y-\text{squash})
\end{aligned}$$

Area contraction is given by

$$\Lambda_1\Lambda_2 = 1/\eta.$$

The *Lyapunov exponents* are

$$\begin{aligned}
\lambda_1 &= \ln\Lambda_1 \\
\lambda_2 &= \ln\Lambda_2
\end{aligned}$$

Note also that vertical cuts through the attractor appear as the early iterations of a Cantor set.

To obtain the fractal dimension, we use the definition

$$D = \lim_{\varepsilon\to 0}\frac{\ln N(\varepsilon)}{\ln(1/\varepsilon)}.$$

Taking the initial box height to be unity, the ε, N pairs for the number N of segments of length ε required to cover the attractor is

148

ε	N
1	1
$1/(2\eta)$	2
$1/(2\eta)^2$	4
...	...
$1/(2\eta)^m$	2^m

Therefore the dimension D of the Cantor set is

$$D = \frac{\ln 2}{\ln 2\eta}.$$

The dimension D' of the attractor in the plane $ABCD$ is

$$D' = 1 + \frac{\ln 2}{\ln 2\eta},$$

where we have neglected the "bend" in the horseshoe (i.e., we've assumed the box's width is much greater than its height.

Note that,

$$\text{as } \eta \to 1, \quad D' \to 2,$$

because iterates nearly fill the plane. Conversely,

$$\text{as } \eta \to \infty, \quad D' \to 1,$$

meaning that the attractor is nearly squashed to a simple line.

16 Period doubling route to chaos

We now study the "routes" or "scenarios" towards chaos.

We ask: How does the transition from periodic to strange attractor occur?

The question is analogous to the study of phase transitions: How does a solid become a melt; or a liquid become a gas?

We shall see that, just as in the study of phase transitions, there are *universal* ways in which systems become chaotic.
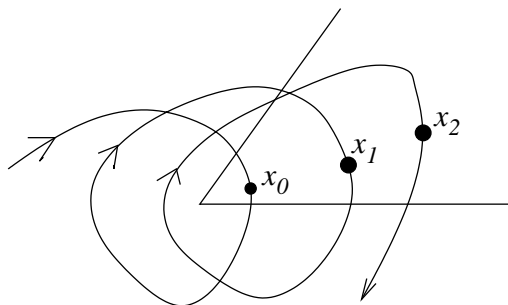
There are three universal routes:

- Period doubling

- Intermittency

- Quasiperiodicity

We shall focus the majority of our attention on period doubling.

16.1 Instability of a limit cycle

To analyze how a periodic regime may lose its stability, consider the Poincaré section:

The periodic regime is linearly unstable if

$$|\vec{x}_1 - \vec{x}_0| < |\vec{x}_2 - \vec{x}_1| < \dots$$

or
$$|\delta\vec{x}_1| < |\delta\vec{x}_2| < \dots$$

Recall that, to first order, a Poincaré map T in the neighborhood of $\vec{x}_0$ is described by the Floquet matrix

$$M_{ij} = \frac{\partial T_i}{\partial X_j}.$$

In a periodic regime,

$$\vec{x}(t + \tau) = \vec{x}(t).$$

But the mapping T sends

$$\vec{x}_0 + \delta\vec{x} \rightarrow \vec{x}_0 + M\delta\vec{x}.$$

Thus stability depends on the 2 (possibly complex) eigenvalues λ_i of M.

If $|\lambda_i| > 1$, the fixed point is unstable.

There are three ways in which $|\lambda_i| > 1$:
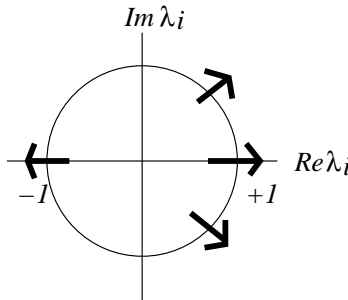
1. $\lambda = 1 + \varepsilon$, ε real, $\varepsilon > 0$. $\delta\vec{x}$ is amplified is in the same direction:
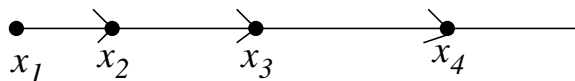
   This transition is associated with Type 1 intermittency.

2. $\lambda = -(1 + \varepsilon)$. $\delta\vec{x}$ is amplified in *alternating* directions:
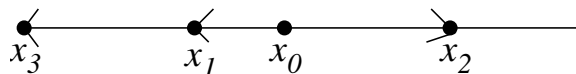
   This transition is associated with period doubling.

3. $\lambda = \alpha \pm i\beta = (1 + \varepsilon)e^{\pm i\gamma}$. $|\delta\vec{x}|$ is amplified, $\delta\vec{x}$ is rotated:
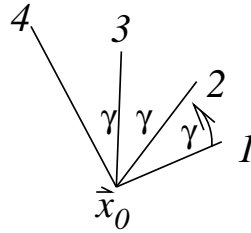
This transition is associated with quasiperiodicity.

In each of these cases, nonlinear effects eventually cause the instability to saturate.

Let's look more closely at the second case, $\lambda \simeq -1$.

Just before the transition, $\lambda = -(1 - \varepsilon)$, $\varepsilon > 0$.

Assume the Poincaré section goes through $x = -0$. Then an initial perturbation x_0 is damped with alternating sign:
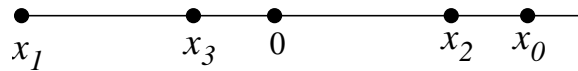
Now vary the control parameter such that $\lambda = -1$. The iterations no longer converge:
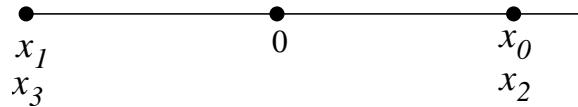
We see that a new cycle has appeared with period twice that of the original cycle through $x = 0$.

This is a *period doubling* bifurcation.

16.2   Logistic map

We now focus on the simplest possible system that exhibits period doubling.

In essence, we set aside n-dimensional $(n \geq 3)$ trajectories and focus only on the Poincaré section and the eigenvector whose eigenvalue crosses (-1).

Thus we look at discrete intervals $T, 2T, 3T, \ldots$ and study the iterates of a transformation on an axis.

We therefore study first return maps

$$x_{k+1} = f(x_k)$$

and shall argue that these maps are highly relevant to n-dimensional flows.

For clarity, we adopt a biological interpretation.

Imagine an island with an insect population that breeds in summer and leaves egges that hatch the following summer.

Let x_j = ratio of actual population in jth summer to some reference population.

Assume that next summer's population is determined by this summer's population according to

$$x_{j+1} = r x_j - s x_j^2.$$

The term $r x_{j+1}$ represents natural growth; if $r > 1$ the population grows (exponentially) by a factor r each year.

The term $s x_j^2$ represents a reduction of natural growth due to crowding and competition for resources.

Now rescale $x_j \rightarrow (r/s) x_j$. Then

$$x_{j+1} = r x_j - r x_j^2.$$

Set $r = 4\mu$:

$$x_{j+1} = 4\mu x_j (1 - x_j).$$

This is called the *logistic map*.

16.3 Fixed points and stability

We seek the long-term dependence of x_j on the control parameter μ. Remarkably, we shall see that μ plays a role not unlike that of the Rayleigh number in thermal convection.

So that $0 < x_j < 1$, we consider the range

$$0 < \mu < 1.$$

Recall that we have already discussed the graphical interpretation of such maps. Below is a sketch for $\mu = 0.7$:

The fixed points solve

$$x^* = f(x^*) = 4\mu x^*(1 - x^*),$$

which yields

$$x^* = 0 \quad \text{and} \quad x^* = 1 - \frac{1}{4\mu},$$

where the second fixed point exists only for $\mu > 1/4$.

Recall that stability requires

$$|f'(x^*)| < 1 \quad \implies \quad |4\mu(1 - 2x^*)| < 1.$$

The stability condition for $x^* = 0$ is therefore

$$\mu < 1/4.$$

The non-trivial fixed point, $x^* = 1 - 1/(4\mu)$, is stable for

$$1/4 < \mu < 3/4.$$

The long-time behavior of the insect population x for $0 < \mu < 3/4$ then looks like
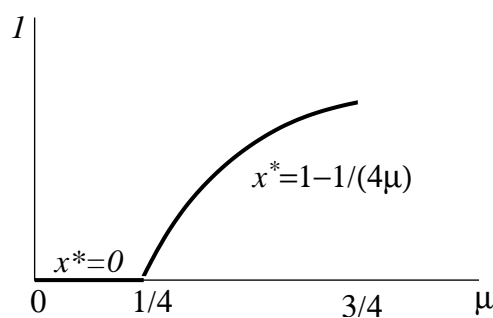
16.4 Period doubling bifurcations

What happens for $\mu > 3/4$?

At $\mu = 3/4$, $x^* = 1 - 1/(4\mu)$ is marginally stable. Just beyond this point, the period of the asymptotic iterates doubles:
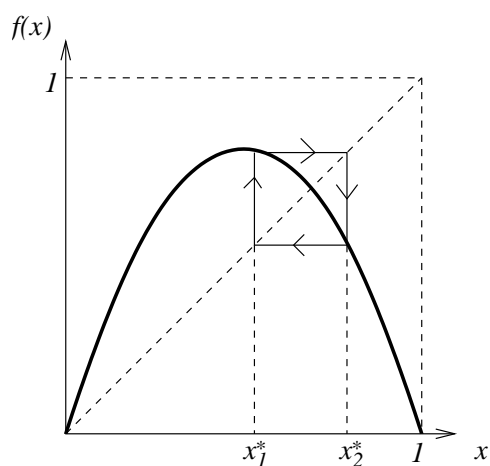
Let's examine this transition more closely. First, look at both $f(x)$ and $f^2(x) = f(f(x))$ just *before the transition*, at $\mu = 0.7$.

- Since $f(x)$ is symmetric about $x = 1/2$, so is $f^2(x)$.

- If x^* is a fixed point of $f(x)$, x^* is also a fixed point of $f^2(x)$.

We shall see that period doubling depends on the relationship of the slope of $f^2(x^*)$ to the slope of $f(x^*)$.

Feigenbaum, Fig. 2.
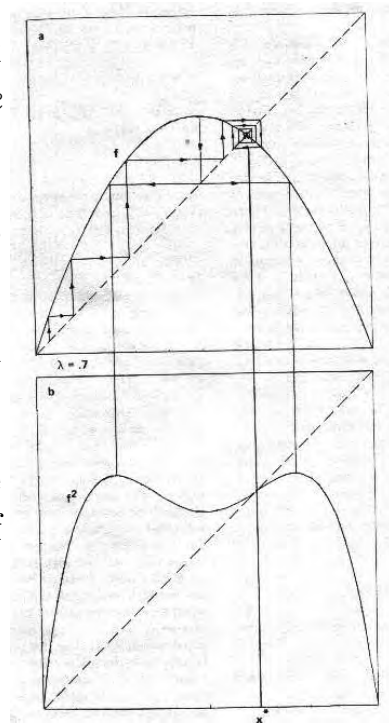
The two slopes are related by the chain rule. By definition,

$$x_1 = f(x_0), x_2 = f(x_1) \implies x_2 = f^2(x_0).$$

Using the chain rule,

$$
\begin{aligned}
f^{2\prime}(x_0) &= \frac{\mathrm{d}}{\mathrm{d}x} f\big(f(x)\big)\big|_{x_0} \\[2mm]
&= f'(x_0)\, f'\big(f(x_0)\big) \\[2mm]
&= f'(x_0)\, f'(x_1)
\end{aligned}
$$

Thus, in general,

$$f^{n\prime}(x_0) = f'(x_0)\, f'(x_1) \ldots f'(x_{n-1}). \tag{32}$$

Now, suppose $x_0 = x^*$, a fixed point of f. Then

$$x_1 = x_0 = x^*$$

and

$$f^{2\prime}(x^*) = f'(x^*)\, f'(x^*) = |f'(x^*)|^2.$$

156

For the example of $\mu < 3/4$,

$$|f'(x^*)| < 1 \implies |f^{2'}(x^*)| < 1.$$

Moreover, if we start at $x_0 = 1/2$, the extremum of f, then equation (32) shows that

$$f'(1/2) = 0 \implies f^{2'}(1/2) = 0$$
$$\implies x = 1/2 \text{ is an extremum of } f^2.$$

Equation (32) also shows us that f^2 has an extremum at the x_0 that iterates, under f, to $x = 1/2$. These *inverses* of $x = 1/2$ are indicated on the figure for $\mu = 0.7$.

What happens *at the transition*, where $\mu = 3/4$?

At $\mu = 3/4$,

$$f'(x^*) = -1 \implies f^2(x^*) = 1.$$

Therefore $f^2(x^*)$ is tangent to the identity map.

Feigenbaum, Fig. 3, $\mu = 0.75$.
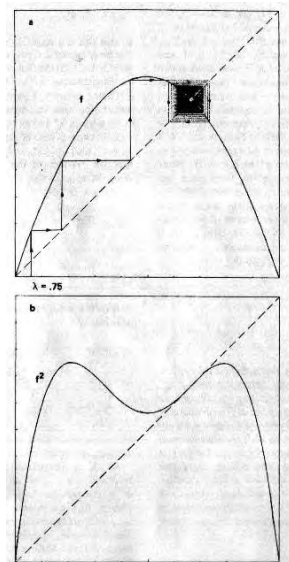
Just *after the transition*, where $\mu > 3/4$, the peaks of f^2 increase, the minimum decreases, and

$$|f'(x^*)| > 1 \implies |f^{2'}(x^*)| > 1.$$

f^2 develops 2 new fixed points, x_1^* and x_2^*, such that

$$x_1^* = f(x_2^*), \quad x_2^* = f(x_1^*).$$

We thus find a cycle of period 2. The cycle is stable because

$$|f^{2'}(x_1^*)| < 1 \quad \text{and} \quad |f^{2'}(x_2^*)| < 1.$$

Feigenbaum, Fig. 4, $\mu = 0.785$.
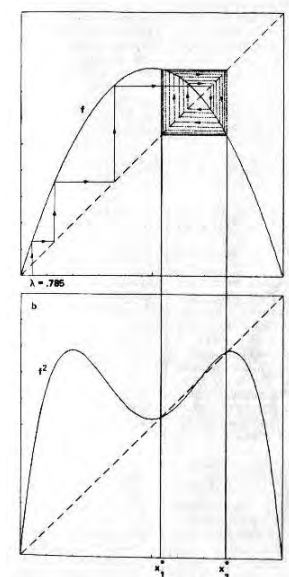
Importantly, the slopes at the fixed points of f^2 are *equal*:

$$f^{2'}(x_1^*) = f^{2'}(x_2^*).$$

This results trivially from equation (32), since the period-2 oscillation gives

$$f^{2'}(x_1^*) = f'(x_1^*) f'(x_2^*) = f'(x_2^*) f'(x_1^*) = f^{2'}(x_2^*).$$

In general, if x_1^*, x_2^*, ..., x_n^* is a cycle of period n, such that

$$\begin{aligned} x_{r+1}^* &= f(x_r^*), && r = 1, 2, \ldots, n-1 \\ \text{and} \quad x_1^* &= f(x_n^*) \end{aligned}$$

then each x_r^* is a fixed point of f^n:

$$x_r^* = f^n(x_r^*), \qquad r = 1, 2, \ldots, n$$

and the slopes $f^{n'}(x_r^*)$ are all equal:

$$f^{n'}(x_r^*) = f'(x_1^*) f'(x_2^*) \ldots f'(x_n^*), \qquad r = 1, 2, \ldots, n.$$

This slope equality is a crucial observation:

- Just as the sole fixed point x^* of $f(x)$ gives rise to 2 stable fixed points x_1^* and x_2^* of $f^2(x)$ as μ increases past $\mu = 3/4$, both x_1^* and x_2^* give rise to 2 stable fixed points of $f^4(x) = f^2(f^2(x))$ as μ increases still further.

- The *period doubling* bifurcation derives from the equality of the fixed points—because each fixed point goes unstable for the same μ.

We thus perceive a sequence of bifurcations at increasing values of μ.

At $\mu = \mu_1 = 3/4$, there is a transition to a cycle of period 2^1.

Eventually, $\mu = \bar{\mu}_1$, where the 2^1-cycle is *superstable*, i.e.,

$$f^{2'}(x_1^*) = f^{2'}(x_2^*) = 0.$$

At $\mu = \mu_2$, the 2-cycle bifurcates to a $2^2 = 4$ cycle, and is superstable at $\mu = \bar{\mu}_2$.

We thus perceive the sequence

$$\mu_1 < \bar{\mu}_1 < \mu_2 < \bar{\mu}_2 < \mu_3 < \ldots$$

where

- μ_n = value of μ at transition to a cycle of period 2^n.

- $\bar{\mu}_n$ = value of μ where 2^n cycle is *superstable*.
  Note that one of the superstable fixed points is always at $x = 1/2$.
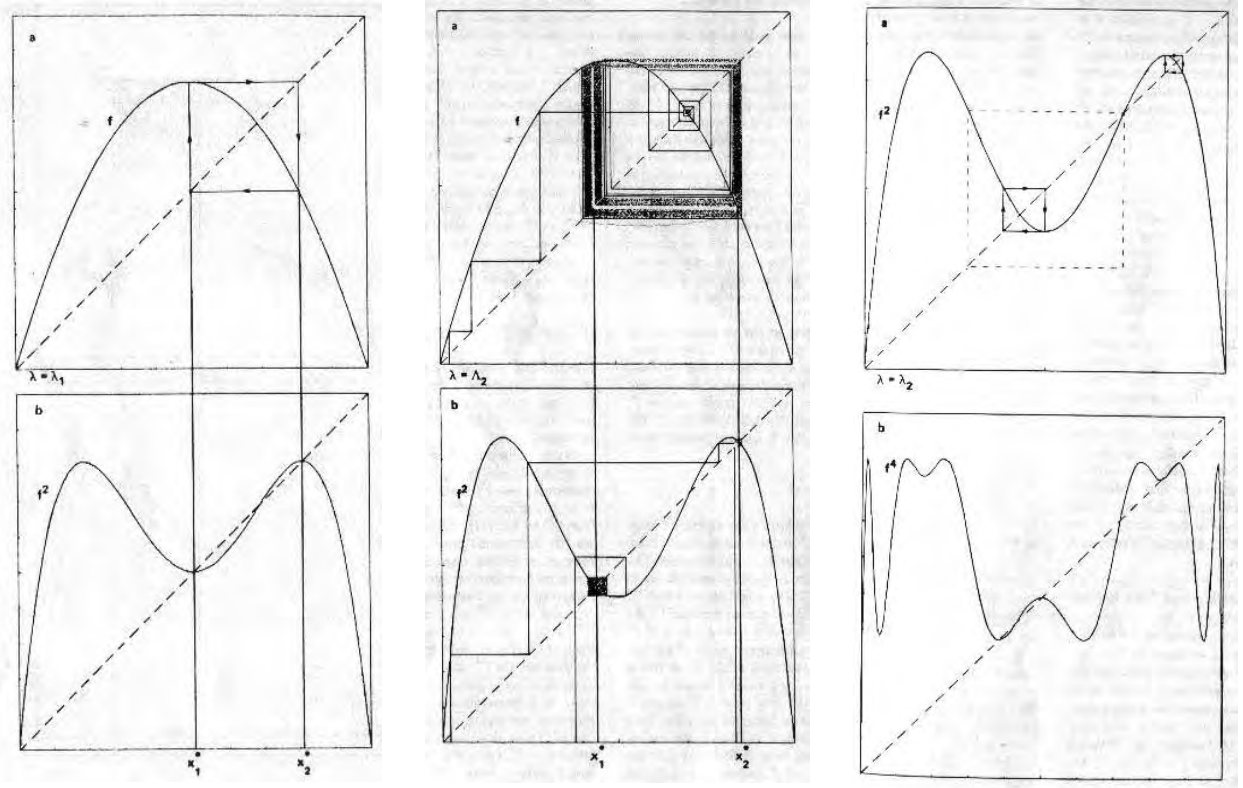
$\mu = \bar{\mu}_1$, superstable 2-cycle (Feigenbaum, Fig. 5).

$\mu = \mu_2$, transition to period 4 (Feigenbaum, Fig. 6).

$\mu = \bar{\mu}_2$, superstable 4-cycle (Feigenbaum, Fig. 7).

Note that in the case $\mu = \bar{\mu}_2$, we consider the fundamental function to be f_2, and its doubling to be $f^4 = f^2(f^2)$.

In general, we are concerned with the functional compositions

$$f^{2^{n+1}} = f^{2^n}\left(f^{2^n}\right)$$

159

Cycles of period 2^{n+1} are always born from the instability of the fixed points of cycles of period 2^n.

Period doubling occurs *ad infinitum.*

16.5   Scaling and universality

The period-doubling bifurcations obey a precise **scaling law**.

Define

$$\mu_\infty = \text{value of } \mu \text{ when the iterates become aperiodic}$$
$$= 0.892486\ldots\text{(obtained numerically, for the logistic map).}$$

There is geometric convergence:

$$\boxed{\mu_\infty - \mu_n \propto \delta^{-n}} \quad \text{for large } n.$$

That is, each increment in μ from one doubling to the next is reduced in size by a factor of $1/\delta$, such that

$$\delta_n = \frac{\mu_{n+1} - \mu_n}{\mu_{n+2} - \mu_{n+1}} \to \delta \quad \text{for large } n.$$

The truly amazing result, however, is not the scaling law itself, but that

$$\boxed{\delta = 4.669\ldots}$$

is **universal**, valid for *any* unimodal map with quadratic maximum.

"Unimodal" simply means that the map goes up and then down.

The quadratic nature of the maximum means that in a Taylor expansion of $f(x)$ about $x_{\max}$, i.e.,

$$f(x_{\max} + \varepsilon) = f(x_{\max}) + \varepsilon f'(x_{\max}) + \frac{\varepsilon^2}{2} f''(x_{\max}) + \ldots$$

the leading order nonlinearity is quadratic, i.e.,

$$f''(x_{\max}) \neq 0.$$

(There is also a relatively technical requirement that the Schwartzian derivative of f must be negative over the entire interval (Schuster))

This is an example of **universality**: if *qualitative* properties are present to enable periodic doubling, then *quantitative* properties are *predetermined.*

Thus we expect that *any* system—fluids, populations, oscillators, etc.— whose dynamics can be approximated by a unimodal map would undergo period doubling bifurcations in the same *quantitative* manner.

How may we understand the foundations of this universal behavior?

Recall that

- the 2^n-cycle generated by f^{2^n} is *superstable* at $\mu = \bar{\mu}_n$;
- superstable fixed points always include $x = 1/2$; and
- all fixed points have the same slope.

Therefore an understanding f^{2^n} near its extremum at $x = 1/2$ will suffice to understand the period-doubling cascade.

To see how this works, consider $f_{\bar{\mu}_1}(x)$ and $f^2_{\bar{\mu}_2}(x)$ (top of Figures 5 and 7).

The parabolic curve within the dashed (red) square, for $f^2_{\bar{\mu}_2}(x)$ looks just like $f_{\bar{\mu}_1}(x)$, after

- reflection through $x = 1/2$, $y = 1/2$; and
- magnification such that the squares are equal size.

The superposition of the first 5 such functions $(f, f^2, f^4, f^8, f^{16})$ rapidly converges to a single function.

Feigenbaum, Figure 8.
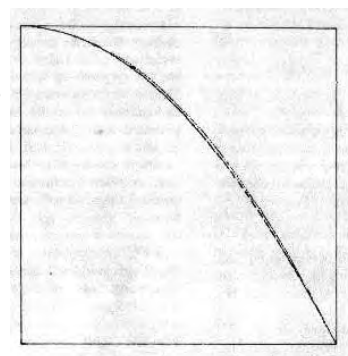
Thus as n increases, a progressively smaller and smaller region near f's maximum becomes relevant—so only the order of the maximum matters.

The composition of doubled functions therefore has a "stable fixed point" in the space of functions, in the infinite period-doubling limit.

The scale reduction is based only on the functional composition

$$f^{2^{n+1}} = f^{2^n}\left(f^{2^n}\right)$$

which is the *same scale factor* for each n (n large).

This scale factor converges to a constant. What is it?

The bifurcation diagram looks like
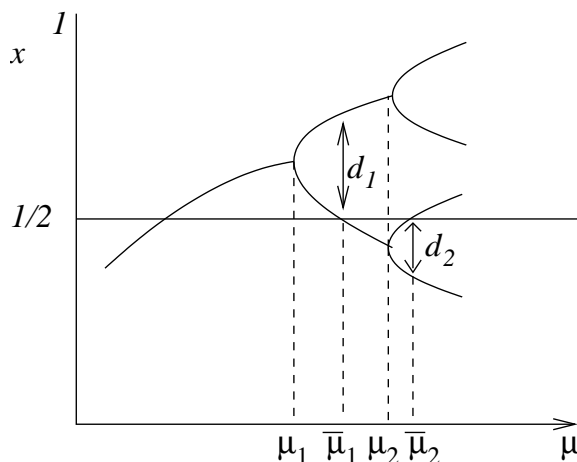
Define d_n = distance from $x = 1/2$ to nearest value of x that appears in the superstable 2^n cycle (for $\mu = \bar{\mu}_n$).

From one doubling to the next, this separation is reduced by the same scale factor:

$$\frac{d_n}{d_{n+1}} \simeq -\alpha.$$

The negative sign arises because the adjacent fixed point is alternately greater than and less than $x = 1/2$.

We shall see that α is also universal:

$$\alpha = 2.502\ldots$$

16.6 Universal limit of iterated rescaled f's

How may we describe the rescaling by the factor α?

For $\mu = \bar{\mu}_n$, d_n is the 2^{n-1} iterate of $x = 1/2$, i.e.,

$$d_n = f_{\bar{\mu}_n}^{2^{n-1}}(1/2) - 1/2.$$

For simplicity, shift the x axis so that $x = 1/2 \to x = 0$. Then

$$d_n = f_{\bar{\mu}_n}^{2^{n-1}}(0).$$

The observation that, for $n \gg 1$,

$$\frac{d_n}{d_{n+1}} \simeq -\alpha \implies \lim_{n \to \infty} (-\alpha)^n d_{n+1} \equiv r_n \quad \text{converges.}$$

Stated differently,

$$\lim_{n \to \infty} (-\alpha)^n f_{\bar{\mu}_{n+1}}^{2^n}(0) \quad \text{must exist.}$$

Our superposition of successive plots of f^{2^n} suggests that this result may be generalized to the whole interval.

Thus a rescaling of the x-axis describes convergence to the limiting function

$$g_1(x) = \lim_{n \to \infty} (-\alpha)^n f_{\bar{\mu}_{n+1}}^{2^n} \left[\frac{x}{(-\alpha)^n} \right].$$

Here the nth interated function has its argument rescaled by $1/(-\alpha)^n$ and its value magnified by $(-\alpha)^n$.

The rescaling of the x-axis shows explicitly that only the behavior of $f_{\bar{\mu}_{n+1}}^{2^n}$ near $x = 0$ is important.

Thus g_1 should be *universal* for all f's with quadratic maximum.

- Figure 5 (top), at $\bar{\mu}_1$, is g_1 for $n = 0$.

- Figure 7 (top), at $\bar{\mu}_2$, when rescaled by α, is g_1 for $n = 1$.

- g_1 for n large looks like $\left(\text{Feigenbaum, Figure 9}\right)$
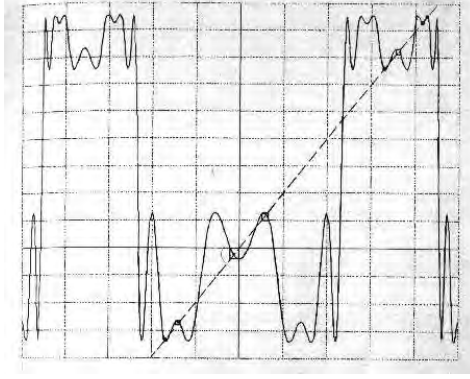
The function g_1 is the universal limit of interated and rescaled f's. Moreover, the location of the elements of the doubled cycles (the circulation squares) is itself universal.

16.7 Doubling operator

We generalize g_1 by introducing a family of functions

$$g_i = \lim_{n \to \infty} (-\alpha)^n f_{\bar{\mu}_{n+i}}^{2^n} \left[\frac{x}{(-\alpha)^n} \right], \qquad i = 0, 1, \dots \tag{33}$$

Note that

$$g_{i-1} = \lim_{n \to \infty} (-\alpha)^n f_{\bar{\mu}_{n+i-1}}^{2^n} \left[\frac{x}{(-\alpha)^n} \right]$$

$$= \lim_{n \to \infty} (-\alpha)(-\alpha)^{n-1} f_{\bar{\mu}_{n-1+i}}^{2^{n-1+1}} \left[\frac{1}{(-\alpha)} \frac{x}{(-\alpha)^{n-1}} \right]$$

Set $m = n - 1$. Then

$$f^{2^{n-1+1}} = f^{2^{m+1}} = f^{2^m} \left(f^{2^m} \right)$$

164

and

$$
\begin{aligned}
g_{i-1} &= \lim_{m \to \infty} (-\alpha)(-\alpha)^m f_{\bar\mu_{m+i}}^{2^m} \left\{ \frac{1}{(-\alpha)^m} \underbrace{(-\alpha)^m f_{\bar\mu_{m+i}}^{2^m} \left[\frac{1}{(-\alpha)} \frac{x}{(-\alpha)^m} \right]}_{g_i\left(\frac{x}{-\alpha}\right)} \right\} \\
&= -\alpha g_i \left[g_i \left(\frac{x}{-\alpha} \right) \right]
\end{aligned}
$$

We thus define the *doubling operator* T such that

$$
g_{i-1}(x) = T \, g_i(x) = -\alpha g_i \left[g_i \left(\frac{x}{-\alpha} \right) \right]
$$

Taking the limit $i \to \infty$, we also define

$$
g(x) \equiv \lim_{i \to \infty} g_i(x)
$$

$$
= \lim_{n \to \infty} (-\alpha)^n f_{\bar\mu_\infty}^{2^n} \left[\frac{x}{(-\alpha)^n} \right]
$$

We therefore conclude that g is a fixed point of T:

$$
g(x) = T \, g(x) = -\alpha g \left[g \left(\frac{x}{-\alpha} \right) \right]. \tag{34}
$$

$g(x)$ is the limit, as $n \to \infty$, of rescaled f^{2^n}, evaluated for μ_∞.

Whereas g is a fixed point of T, $T g_i$, where i is finite, interates away from g.

Thus g is an *unstable* fixed point of T.

16.8 Computation of α

To determine α, first write

$$
g(0) = -\alpha g \left[g(0) \right].
$$

We must set a scale, and therefore set

$$
g(0) = 1 \implies g(1) = -1/\alpha.
$$

There is no general theory that can solve equation (34) for g.

We can however obtain a unique solution for α by specifying the nature (order) of g's maximum (at zero) and requiring that $g(x)$ be smooth.

We thus assume a quadratic maximum, and use the short power law expansion

$$g(x) = 1 + bx^2.$$

Then, from equation (34),

$$
\begin{aligned}
g(x) = 1 + bx^2 &= -\alpha g\left(1 + \frac{bx^2}{\alpha^2}\right) \\
&= -\alpha\left[1 + b\left(1 + \frac{bx^2}{\alpha^2}\right)^2\right] \\
&= -\alpha(1 + b) - \frac{2b^2}{\alpha}x^2 + O(x^4)
\end{aligned}
$$

Equating terms,

$$\alpha = \frac{-1}{1 + b}, \qquad \alpha = -2b$$

which yields,

$$b = \frac{-2 \pm \sqrt{12}}{4} \simeq -1.366 \quad (\text{neg root for max at } x = 0)$$

and therefore

$$\alpha \simeq 2.73,$$

which is within 10% of Feigenbaum's $\alpha = 2.5028\ldots$, obtained by using terms up to x^{14}.

16.9   Linearized doubling operator

We shall see that δ determines how quickly we move away from g under application of the doubling operator T.

In essence, we shall calculate the eigenvalue that corresponds to instability of an unstable fixed point.

Thus our first task will be to linearize the doubling operator T. δ will then turn out to be one of its eigenvalues.

We seek to predict the scaling law

$$\bar{\mu}_n - \bar{\mu}_\infty \propto \delta^{-n},$$

now expressed in terms of $\bar{\mu}_i$ rather than μ_i.

We first expand $f_{\bar{\mu}}(x)$ around $f_{\bar{\mu}_\infty}(x)$:

$$f_{\bar{\mu}}(x) \simeq f_{\bar{\mu}_\infty}(x) + (\bar{\mu} - \bar{\mu}_\infty)\,\delta f(x),$$

where the incremental change in function space is given by

$$\delta f(x) = \left.\frac{\partial f_{\bar{\mu}}(x)}{\partial \bar{\mu}}\right|_{\bar{\mu}_\infty}$$

Now apply the doubling operator T to $f_{\bar{\mu}}$ and linearize with respect to δf:

$$
\begin{aligned}
Tf_{\bar{\mu}} &= -\alpha f_{\bar{\mu}}\left[f_{\bar{\mu}}\left(\frac{x}{-\alpha}\right)\right] \\
&\simeq -\alpha\,[f_{\bar{\mu}_\infty} + (\bar{\mu} - \bar{\mu}_\infty)\,\delta f] \circ \left[f_{\bar{\mu}_\infty}\left(\frac{x}{-\alpha}\right) + (\bar{\mu} - \bar{\mu}_\infty)\,\delta f\left(\frac{x}{-\alpha}\right)\right] \\
&= Tf_{\bar{\mu}_\infty} + (\bar{\mu} - \bar{\mu}_\infty)L_{f_{\bar{\mu}_\infty}}\,\delta f + O(\delta f^2)
\end{aligned}
$$

where L_f is the *linearized doubling operator* defined by

$$L_f\,\delta f = -\alpha\left\{f'\left[f\left(\frac{x}{-\alpha}\right)\right]\delta f\left(\frac{x}{-\alpha}\right) + \delta f\left[f\left(\frac{x}{-\alpha}\right)\right]\right\}. \qquad (35)$$

The first term on the RHS derives from an expansion like $g[f(x)+\delta f(x)] \simeq g[f(x)]+g'[f(x)]\delta f(x)$.

A second application of the doubling operator yields

$$T\big(T(f_{\bar{\mu}})\big) = T^2 f_{\bar{\mu}_\infty} + (\bar{\mu} - \bar{\mu}_\infty)L_{Tf_{\bar{\mu}_\infty}}L_{f_{\bar{\mu}_\infty}}\,\delta f + O\big((\delta f)^2\big).$$

Therefore n applications of the doubling operator produce

$$T^n f_{\bar{\mu}} = T^n f_{\bar{\mu}_\infty} + (\bar{\mu} - \bar{\mu}_\infty)\,L_{T^{n-1}f_{\bar{\mu}_\infty}}\cdots L_{f_{\bar{\mu}_\infty}}\,\delta f + O\big((\delta f)^2\big). \qquad (36)$$

167

For $\bar{\mu} = \bar{\mu}_\infty$, we expect convergence to the fixed point $g(x)$:

$$T^n f_{\bar{\mu}_\infty} = (-\alpha)^n f_{\bar{\mu}_\infty}^{2^n} \left[\frac{x}{(-\alpha)^n} \right] \simeq g(x), \qquad n \gg 1.$$

Substituting $g(x)$ into equation (36) and assuming, similarly, that $L_{Tf_{\bar{\mu}_\infty}} \simeq L_g$,

$$T^n f_{\bar{\mu}}(x) \simeq g(x) + (\bar{\mu} - \bar{\mu}_\infty) \, L_g^n \, \delta f(x), \qquad n \gg 1. \tag{37}$$

We simplify by introducing the eigenfunctions ϕ_ν and eigenvalues λ_ν of L_g:

$$L_g \phi_\nu = \lambda_\nu \phi_\nu, \qquad \nu = 1, 2, \ldots$$

Write δf as a weighted sum of ϕ_ν:

$$\delta f = \sum_\nu c_\nu \phi_\nu$$

Thus n applications of the linear operator L_g may be written as

$$L_g^n \, \delta f = \sum_\nu \lambda_\nu^n c_\nu \phi_\nu.$$

Now *assume* that only one of λ_ν is greater than one:

$$\lambda_1 > 1, \quad \lambda_\nu < 1 \text{ for } \nu \neq 1.$$

(This conjecture, part of the original theory, was later proven.)

Thus for large n, λ_1 dominates the sum, yielding the approximation

$$L_g^n \, \delta f \simeq \lambda_1^n c_1 \phi_1, \qquad n \gg 1.$$

We can now simplify equation (36):

$$T^n f_{\bar{\mu}}(x) = g(x) + (\bar{\mu} - \bar{\mu}_\infty) \cdot \delta^n \cdot a \cdot h(x), \qquad n \gg 1$$

where

$$\delta = \lambda_1, \quad a = c_1, \quad \text{and} \quad h(x) = \phi_1.$$

Now note that when $x = 0$ and $\bar{\mu} = \bar{\mu}_n$,

$$T^n f_{\bar{\mu}_n}(0) = g(0) + (\bar{\mu}_n - \bar{\mu}_\infty) \cdot \delta^n \cdot a \cdot h(0).$$

Recall that $x = 0$ is a fixed point of $f_{\bar{\mu}_n}^{2^n}$ (due to the x-shift). Therefore

$$T^n f_{\bar{\mu}_n}(0) = (-\alpha)^n f_{\bar{\mu}_n}^{2^n}(0) = 0.$$

Recall also that we have scaled g such that $g(0) = 1$. We thus obtain the Feigenbaum scaling law:

$$\lim_{n \to \infty} (\bar{\mu}_n - \bar{\mu}_\infty) \delta^n = \frac{-1}{a \cdot h(0)} = \text{constant!}$$

16.10 Computation of δ

Recall that δ is the eigenvalue that corresponds to the eigenfunction $h(x)$.

Then applying the linearized doubling operator (35) to $h(x)$ yields

$$L_g h(x) = -\alpha \left\{ g' \left[g \left(\frac{x}{-\alpha} \right) \right] h \left(\frac{x}{-\alpha} \right) + h \left[g \left(\frac{x}{-\alpha} \right) \right] \right\}$$

$$= \delta \cdot h(x).$$

Now approximate $h(x)$ by $h(0)$, the first term in a Taylor expansion about $x = 0$.

Seting $x = 0$, we obtain

$$-\alpha \left\{ g' \left[g(0) \right] h(0) + h \left[g(0) \right] \right\} = \delta \cdot h(0).$$

Note that the approximation

$$h(x) \simeq h(0) \implies h[g(0)] = h(1) \simeq h(0).$$

Thus $h(0)$ cancels in each term and, recalling that $g(0) = 1$,

$$-\alpha \left[g'(1) + 1 \right] = \delta. \tag{38}$$

To obtain $g'(1)$, differentiate $g(x)$ twice:

$$g(x) = -\alpha g\left[g\left(\frac{-x}{\alpha}\right)\right]$$

$$g'(x) = -\alpha\left\{g'\left[g\left(\frac{-x}{\alpha}\right)\right]\cdot\left(\frac{-1}{\alpha}\right)g'\left(\frac{-x}{\alpha}\right)\right\}$$

$$g''(x) = \frac{-1}{\alpha}\left\{g''\left[g\left(\frac{x}{-\alpha}\right)\right]\left[g'\left(\frac{-x}{\alpha}\right)\right]^2 + g'\left[g\left(\frac{-x}{\alpha}\right)\right]g''\left(\frac{-x}{\alpha}\right)\right\}$$

Substitute $x = 0$. Note that

$$g'(0) = 0 \quad \text{and} \quad g''(0) \neq 0$$

because we have assumed a quadratic maximum at $x = 0$. Then

$$g''(0) = \frac{-1}{\alpha}\left[g'(1)g''(0)\right].$$

Therefore

$$g'(1) = -\alpha.$$

Substituting into equation (38), we obtain

$$\boxed{\delta = \alpha^2 - \alpha}.$$

This result derives from the crude approximation $h(0) = h(1)$. Better approximations yield greater accuracy (Feigenbaum, 1979).)
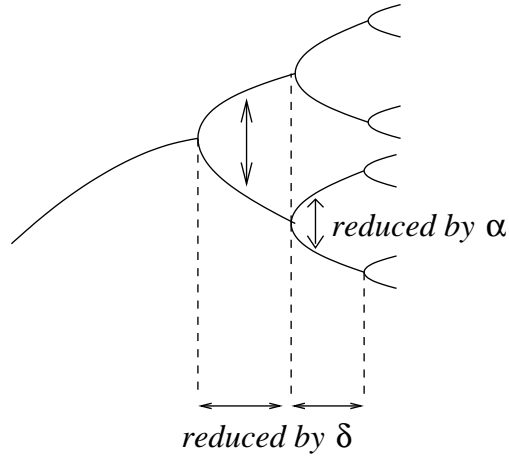
Recall that we previously estimated $\alpha \simeq 2.73$. Substituting that above, we obtain

$$\delta \simeq 4.72,$$

which is within 1% of the exact value $\delta = 4.669\ldots$.

16.11 Comparison to experiments

We have established the universality of α and δ:

reduced by α

reduced by δ

These *quantitative* results hold if a *qualitative* condition—the maximum of f must be locally quadratic—holds.

At first glance this result may appear to pertain only to mathematical maps. However we have seen that more complicated systems can also behave as if they depend on only a few degrees of freedom. Due to dissipation, one may expect that a one-dimensional map is contained, so to speak, within them.

The first experimental verification of this idea was due to Libchaber, in a Rayleigh-Bénard system.

As the Rayleigh number increases beyond its critical value, a single convection roll develops an oscillatory wave:

$Ra=Ra_c$ $Ra>Ra_c$ *probe*
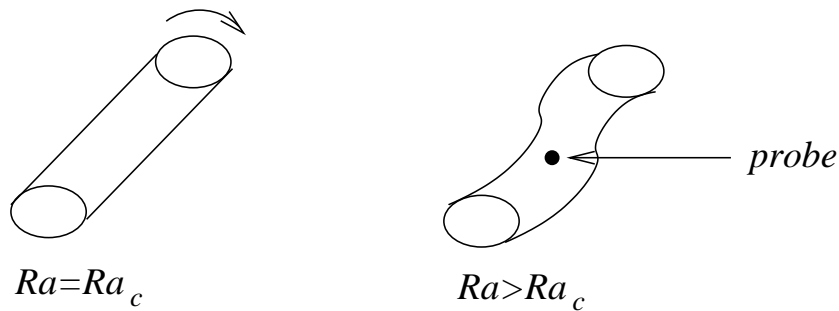
A probe of temperature $X(t)$ is then oscillatory with frequency f_1 and period $1/f_1$.

Successive increases of Ra then yield a sequence of period doubling bifurca-

tions at Rayleigh numbers

$$\mathrm{Ra}_1 < \mathrm{Ra}_2 < \mathrm{Ra}_3 < \ldots$$

The experimental results are shown in

BPV, Figure VIII.13a and VIII.13b .

Identifying Ra with the control parameter μ in Feigenbaum's theory, Libchaber found

$$\delta \simeq 4.4$$

which is amazingly close to Feigenbaum's prediction, $\delta = 4.669\ldots$.

Such is the power of scaling and universality!

17   Intermittency (and quasiperiodicity)

In this lecture we discuss the other two generic routes to chaos, intermittency and quasiperiodicity.

Almost all our remarks will be on intermittency; we close with a brief description of quasiperiodicity.

Definition: Intermittency is the occurrence of a signal that alternates randomly between regular (laminar) phases and relatively short irregular bursts.

In the exercises we have already seen examples, particulary in the Lorenz model (where it was discovered, by Manneville and Pomeau).

Examples:

- The Lorenz model, near $r = 166$.

    Figure 1a,b Manneville and Pomeau (1980)

- Rayleigh-Benard convection.

    BPV, Figure IX.9

17.1   General characteristics of intermittency

Let r = control parameter. The following summarizes the behavior with respect to r:

- For $r < r_i$, system displays stable oscillations (e.g., a limit cycle).

- For $r > r_i$ ($r - r_i$ small), system in in the *intermittent* regime: stable oscillations are interrupted by fluctuations.

- As $r \to r_i$ from above, the fluctuations become increasingly rare, and disappear for $r < r_i$.

- Only the *average intermission time* between fluctuations varies, not their amplitude nor their duration.

We seek theories for

- Linear stability of the limit cycle and "relaminarization." (i.e. return to stability after irregular bursts).

- Scaling law for intermission times.

- Scaling law for Lyaponov exponents.

17.2 One-dimensional map

We consider the instability of a Poincaré map due to the crossing of the unit circle at $(+1)$ by an eigenvalue of the Floquet matrix.

This corresponds to the specific case of *Type I intermittency.*

Let u be the coordinate in the plane of the Poincaré section that points in the direction of the eigenvector whose eigenvalue λ crosses $+1$.

The lowest-order approximation of the 1-D map constructed along this line is

$$u' = \lambda(r)u. \tag{39}$$

Taking $\lambda(r_i) = 1$ at the intermittency threshold, we have

$$u' = \lambda(r_i)u = u. \tag{40}$$

We consider this to be the leading term of a Taylor series expansion of $u'(u, r)$ in the neighborhood of $u = 0$ and $r = r_i$.

Expand to first order in $(r - r_i)$ and second order in u:

$$u'(u, r) \simeq u'(0, r_i) + u \cdot \left.\frac{\partial u'}{\partial u}\right|_{0,r_i} + \frac{1}{2}u^2 \cdot \left.\frac{\partial^2 u'}{\partial u^2}\right|_{0,r_i} + (r - r_i) \left.\frac{\partial u'}{\partial r}\right|_{0,r_i}$$

Evaluating equation (39), we find that the first term vanishes:

$$u'(u = 0, r = r_i) = 0.$$

From equation (40), we have

$$\left.\frac{\partial u'}{\partial u}\right|_{0,r_i} = \lambda(r_i) = 1.$$

Finally, rescale u such that

$$\left.\frac{1}{2}\frac{\partial^2 u'}{\partial u^2}\right|_{0,r_i} = 1$$
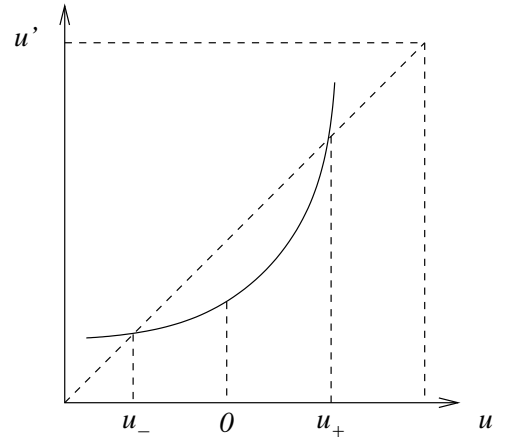
and set

$$\varepsilon \propto (r - r_i).$$
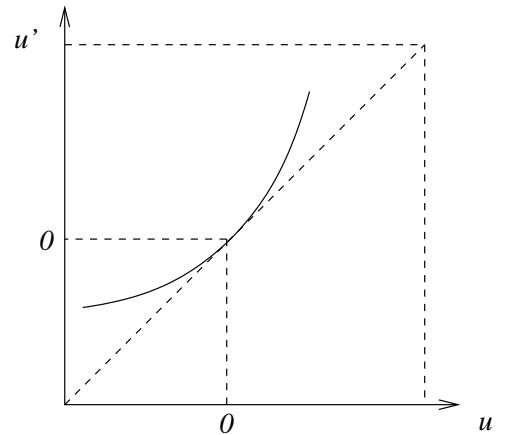
The model now reads

$$u' = u + \varepsilon + u^2,$$

where ε is now the control parameter.

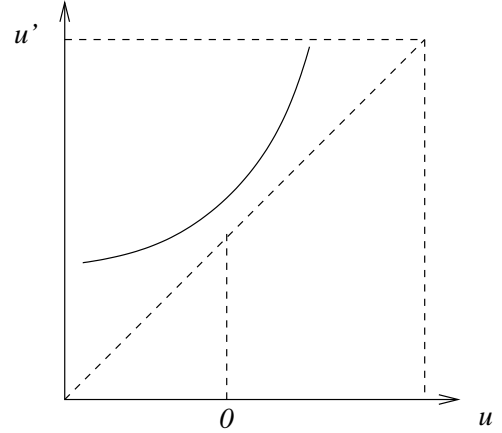Graphically, we have the following system:

- $\varepsilon < 0$, i.e. $r < r_i$.

- u_- is stable fixed point.

- u_+ is unstable.

- $\varepsilon = 0$, i.e. $r = r_i$.

- u' is tangent to indentity map.

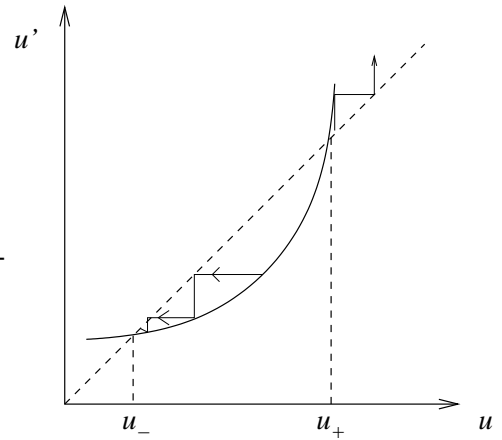- $u_- = u_+ = 0$ is marginally stable.

175

- $\varepsilon > 0$, i.e. $r > r_i$.

- no fixed points.
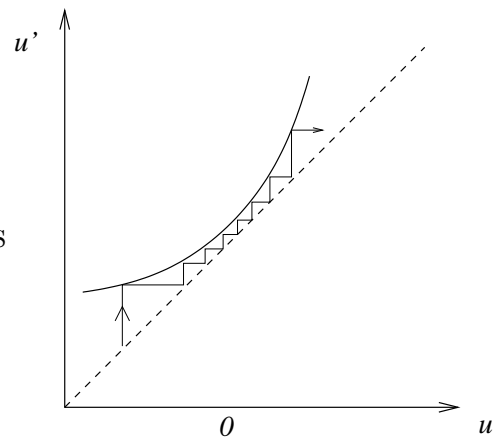
For $\varepsilon < 0$, the iterations look like

- u_- is an attractor for initial conditions $u < u_+$.

- For initial conditions $u > u_+$, the iterations diverge.

The situation changes for $\varepsilon > 0$, i.e. $r > r_i$:

- No fixed points.

- Iterations beginning at $u < 0$ drift towards $u > 0$.

The fixed points of $u'(u)$ represent stable oscillations of the continuous flow.

Thus for $u \simeq 0$, the drift for $\varepsilon > 0$ corresponds to a flow qualitatively similar to the stable oscillations near $u = 0$ for $\varepsilon < 0$.

However, when $\varepsilon > 0$, there is no fixed point, and thus no periodic solution.

The iterations eventually run away and become unstable—this is the *intermittent* burst of noise.

How does the laminar phase begin again, or "relaminarize"?

Qualitatively, the picture can look like
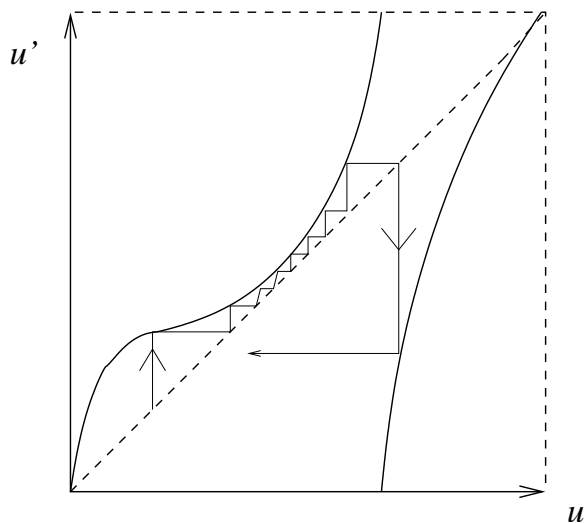
Note that the precise timing of the turbulent burst is unpredictable.

The discontinuity is *not* inconsistent with the presumed continuity of the underlying equations of motion—this is a map, not a flow.

Moreover the Lorenz map itself contains a discontinuity, corresponding to the location of the unstable fixed point.

17.3   Average duration of laminar phase

What can we say about the average duration of the laminar phases?

Writing our theoretical model as a map indexed by k, we have

$$u_{k+1} = u_k + \varepsilon + u_k^2.$$

For $u_{k+1} \simeq u_k$, we can instead write the differential equation

$$\frac{\mathrm{d}u}{\mathrm{d}k} = \varepsilon + u^2.$$

The general solution of this o.d.e. is

$$u(k) = \varepsilon^{1/2} \tan\left[\varepsilon^{1/2}(k - k_0)\right].$$

Take $k_0 = 0$, the step at which iterations traverse the narrowest part of the channel.

We thus have

$$u(k) = \varepsilon^{1/2} \tan\left(\varepsilon^{1/2}k\right).$$

We see that $u(k)$ diverges when

$$\varepsilon^{1/2}k = \pm\frac{\pi}{2} \quad \text{or} \quad k = \pm\frac{\pi}{2}\varepsilon^{-1/2}.$$

The divergence signifies a turbulent burst.

When $k \sim \varepsilon^{-1/2}$, $u_{k+1} - u_k$ is no longer small, and the differential approximation of the difference equation is no longer valid.

Thus: if $\tau =$ time ($\propto$ number of iterations) needed to traverse the channel, then

$$\tau \propto \varepsilon^{-1/2} \quad \text{or} \quad \tau \propto (r - r_i)^{-1/2}. \tag{41}$$

Thus the laminar phase lasts increasingly long as the threshold $r = r_i$ is approached from above.

17.4 Lyaponov number

We can also predict a scaling law for the Lyaponov number.

Near the fixed point ($u \simeq 0$, $\varepsilon > 0$), the increment δu_{k+1} due to an increment u_k is, to first order,

$$\delta u_{k+1} \simeq \lambda_1 \delta u_k$$

where λ_1 is eigenvalue that passes through $(+1)$.

After N iterations,

$$\delta u_N \simeq \lambda_N \lambda_{N-1} \lambda_{N-2} \cdots \lambda_1 \delta u_1.$$

Suppose $N \simeq$ the duration of the laminar phase. Then

$$\lambda_N > 1 \quad \text{and} \quad \lambda_{N-1} \simeq \lambda_{N-2} \simeq \cdots \simeq \lambda_1 \simeq 1.$$

The Lyapunov number Λ is

$$\Lambda = \frac{1}{N} \prod_i \lambda_i \simeq \frac{\lambda_N}{N} \propto \frac{1}{N} \propto \frac{1}{\tau} \propto \sqrt{\varepsilon}.$$

where the last relation used equation (41). (Recall that $\ln \Lambda =$ Lyaponov *exponent*.)

Results from the Lorenz model verify this prediction. The "intermittent channel" of the Lorenz map is seen in

BPV, Figure IX.14

and the associated $\varepsilon^{1/2}$ scaling of the Lyaponov number is seen in

BPV, Figure IX.15

Behavior qualitatively similar to that predicted by our model has been observed in the B-Z reaction:

BPV, Figure IX.16–17

17.5 Quasiperiodicity

Finally, we make a few remarks about the third universal route to chaos, known as *quasiperiodicity.*

Recall that there are 3 generic ways in which a limit cycle on a Poincaré map may become unstable: An eigenvalue λ of the Floquet matrix (the Jacobian of the map) crosses the unit circle at

- $+1$ (as in the example of intermittency above);

- -1 (as we saw in the introduction to period doubling); and

- $\lambda = \alpha \pm i\beta$, $|\lambda| > 1$. This corresponds to the transition via *quasiperiodicity.*

As we have seen, the latter case results in the addition of a second oscillation.

This is a *Hopf bifurcation*: the transformation of a limit cycle to a quasiperiodic flow, or a torus T^2.

The route to chaos via quasiperiodicity describes how a torus T^2 (i.e., a quasiperiodic flow) can become a strange attractor.

17.5.1 An historical note

In 1944, the Russian physicist Landau proposed a theory for the transition from laminar flow to turbulence as the Reynolds number is increased.

Briefly, he envisioned the following sequence of events as Re increases beyond Re_c:

- Laminar flow (constant velocity) becomes periodic with frequency f_1 by a Hopf bifurcation.

- Period flow→quasiperiodic flow; i.e., another Hopf bifurcation. The second frequency f_2 is incommensurate with f_1.

- More incommensurate frequencies $f_3, f_4, \ldots, f_r$ appear in succession (due to more Hopf bifurcations).

- For r large, the spectrum appears continuous and the flow (on a torus T^r) is aperiodic (i.e., turbulent).

Recall that we have learned previously that, for dissipative flows,

$$\text{dimension of phase space} > \text{attractor dimension.}$$

Thus a consequence of Landau's theory is that a system must have many degrees of freedom to become chaotic.

We now know, however, from the work of Lorenz, that

- 3 degrees of freedom suffice to give rise to a chaotic flow; and

- the chaos occurs on a strange attractor, which is distinct from a torus (since trajectories diverge on the strange attractor).

17.5.2   Ruelle-Takens theory

Lorenz's observations were deduced theoretically by Ruelle and Takens in 1971.

The Ruelle-Takens theory is the *quasiperiodic* route to chaos. As a control parameter is varied, the following sequence of events can occur:

- Laminar flow $\rightarrow$ oscillation with frequency f_1.

- A second Hopf bifurcation adds a second (incommensurate) frequency f_2.

- A third Hopf bifurcation adds a third frequency f_3.

- The torus T^3 can become unstable and be replaced by a strange attractor.

The transition is demonstrated beautifully in terms of changing power spectra in the Rayleigh-Bénard experiment described by

Libchaber et al., Figure 15

Libchaber, A., Fauve, S. and C. Laroche.1983. Two-parameter study of the routes to chaos. Physica D. 7: 73-84.

Note that the Rayleigh number of the two spectra varies by less than 1%.

Such a transition can also be seen in Poincaré sections, such as the Rayleigh-Bénard experiment of

BPV, Figures VII.20, VII.21